

Genetic analysis of MAMP-triggered immunity in Arabidopsis

Inaugural-Dissertation

zur

Erlangung des Doktorgrades

der Mathematisch-Naturwissenschaftlichen Fakultät

der Universität zu Köln

vorgelegt von

Nico Tintor

aus Novi Sad

Köln, Dezember 2011

Die vorliegende Arbeit wurde am Max-Planck-Institut für
Pflanzenzüchtungsforschung in Köln in der Abteilung Molekulare
Phytopathologie (Direktor: Prof. Dr. P. Schulze-Lefert) angefertigt.

Berichterstatter:	Prof. Dr. Paul Schulze-Lefert Prof. Dr. Ute Höcker Dr. Cyril Zipfel
Prüfungsvorsitzender:	Prof. Dr. Ulf-Ingo Flügge
Tag der Disputation:	26.01.2012

Table of Contents

Table of Contents	V
Publications	VII
Abbreviations	IX
Summary	XI
Zusammenfassung	XIII
1. Introducon	1
1.1 MAMP-triggered immunity	2
1.2 Effector-triggered immunity	3
1.3 MTI as a basis for ETI, SAR and nonhost resistance	5
1.4 Damage-associated molecular patterns (DAMPs)	6
1.5 Perception of bacterial flagellin and Elongation Factor-Tu in Arabidopsis	7
1.6 Signaling through FLS2 and EFR	7
1.6.1 FLS2 and EFR immune complexes	7
1.6.2 FLS2 and EFR signaling outputs	9
1.6.3 Subcellular localization and trafficking of FLS2	10
1.7 ER quality control for membrane proteins	10
1.8 Phytohormone signaling	12
1.8.1 Ethylene signaling	13
2. Results	19
2.1 Receptor quality control in the endoplasmic reticulum for plant innate immunity	19
2.1.1 MAMP perception leads to the repression of sucrose-induced anthocyanin accumulation in Arabidopsis seedlings	19
2.1.2 Identification of a <i>psl2</i> mutant in a genetic screen for Arabidopsis mutants that allow sucrose-induced anthocyanin accumulation in the presence of MAMPs	21
2.1.3 PSL2 is required for stable accumulation of functional EFR but not FLS2	24
2.1.4 Identification of PSL2 reveals an essential function of UGGT for stable accumulation of EFR	26
2.1.5 Interallelic complementation between <i>psl2</i> alleles	29
2.1.6 PSL1/CRT3 and PSL2/UGGT act in concert for EFR function	32
2.2 <i>psl25</i> plants show varied defects in EFR signaling outputs and carry a mutation in ER Glucosidase I	35
2.2.1 Identification of <i>psl25</i> mutants in a forward-genetic screen for Arabidopsis elf18-insensitive mutants	35
2.2.2 <i>psl25</i> carries a mutation in Arabidopsis GLUCOSIDASE I	37
2.2.3 PSL25 is required for generation of functional EFR	37
2.2.4 EFR outputs are differentially impaired in <i>psl25</i> plants	39

2.3	Ethylene signaling regulates pre- and post-recognition steps in MAMP-triggered immunity	43
2.3.1	Isolation of an Arabidopsis <i>ps/36</i> mutant that is impaired in responses to elf18 and flg22	43
2.3.2	Both FLS2- and EFR-triggered outputs are altered in <i>ps/36</i> plants	43
2.3.4	Ethylene perception and signalling is required for MAMP-triggered suppression of anthocyanin accumulation	45
2.3.5	EIN2 is required for FLS2 transcript accumulation	49
2.3.6	EFR signalling is impaired in <i>ein2</i> alleles despite WT-like EFR accumulation	49
2.3.7	Genetic requirements for MAMP-triggered anthocyanin suppression	52
2.3.8	Flg22- and elf18-induced transcriptional reprogramming of defense-related genes is diminished in <i>ein2</i> plants	55
2.3.9	Genome-wide analysis of elf18-induced transcriptional reprogramming in <i>ein2</i> plants	60
2.3.10	<i>ein2</i> plants retain elf18-triggered immunity towards virulent <i>Pseudomonas syringae</i>	66
3.	Discussion	
3.1	ER quality control for plant innate immunity	67
3.2	Ethylene signaling regulates pre- and post-recognition steps in MAMP-triggered immunity	71
4.	Materials and Methods	77
	Materials	77
	Buffers	77
	Media	80
	Methods	81
	Molecular biological methods	84
	Biochemical methods	90
	References	91
	Acknowledgements	98
	Erklärung	100

Publications

Serrano M, Kanehara K, Torres M, Yamada K, **Tintor N**, Kombrink E, Schulze-Lefert P, Saijo Y (2011) Repression of sucrose/ultraviolet-B light-induced flavonoid accumulation in microbe-associated molecular pattern-triggered immunity in Arabidopsis. *Plant Physiol.* 2012 Jan;158(1):408-22.

Christensen A, Svensson K, Thelin L, Zhang W, **Tintor N**, Prins D, Funke N, Michalak M, Schulze-Lefert P, Saijo Y, Sommarin M, Widell S, Persson S (2010) Higher Plant Calreticulins Have Acquired Specialized Functions. *PLoS One* 2010 Jun 28 5(6) e11342.

Lu X, **Tintor N**, Mentzel T, Kombrink E, Boller T, Robatzek S, Schulze-Lefert P, Saijo Y (2009) Uncoupling of sustained MAMP receptor signaling from early outputs in an Arabidopsis endoplasmic reticulum glucosidase II allele. *Proc Natl Acad Sci USA* 2009 Dec 29 106(52) 22522-7.

Saijo Y, **Tintor N**, Lu X, Rauf P, Pajerowska-Mukhtar K, Häweker H, Dong X, Robatzek S, Schulze-Lefert P (2009) Receptor quality control in the endoplasmic reticulum for plant innate immunity. *EMBO J.* 2009 Nov 4 28(21) 3439-49.

Abbreviations

ACC	1-aminocyclopropane-1-carboxylic acid
ACO	ACC oxidase
ACS	ACC synthase
BAK1	BRI1 ASSOCIATED KINASE1
BRI1	BRASSINOSTEROID INSENSITIVE1
CDPK	calcium-dependent protein kinases
CNX	calnexin
CRT	calreticulin
CRT3	calreticulin 3
CSP	cold-shock protein
CTR1	CONSTITUTIVE TRIPLE RESPONSE1
DAMP	damage-associated molecular patterns
EF-TU	Elongation Factor-TU
EIN2	ETHYLENE INSENSITIVE2
EIN3	ETHYLENE INSENSITIVE3
EIN3-LIKE1	ETHYLENE INSENSITIVE3-LIKE1
EFR	EF-TU RECEPTOR
EPF1	EPIDERMAL PATTERNING FACTOR 1
ER	endoplasmic reticulum
ERAD	ER-associated degradation
ERQC	ER quality control
ET	ethylene
ETI	effector-triggered immunity
ETR1	ETHYLENE RECEPTOR1
FLS2	FLAGELLIN SENSING2
<i>gcs</i>	glucosidase
HR	hypersensitive response
JA	jasmonic acid
<i>knf</i>	knopf
LPS	lipopolysaccharide
LRR	leucine-rich-repeat
MAMP	microbe-associated molecular patterns
MTI	MAMP-triggered immunity
MKK	MITOGEN ACTIVATED PROTEIN KINASE KINASE
MPK	MITOGEN ACTIVATED PROTEIN KINASE
MEKK1	MITOGEN ACTIVATED PROTEIN KINASE KINASE KINASE
NB	Nucleotide binding

NO	nitric oxide
OST	oligosaccharyltransferase
PAD4	PHYTOALEXIN DEFICIENT4
PAMP	pathogen associated molecular patterns
PGN	peptidoglycan
PMR4	POWDERY MILDEW RESISTANT4
PRR	pattern recognition receptor
<i>Pst</i> DC3000	<i>Pseudomonas syringae</i> pathovar <i>tomato</i> DC3000
RLK	receptor-like kinases
ROS	reactive oxidative species
SAR	systemic acquired resistance
SA	salicylic acid
UGGT	UDP-glucose:glycoprotein glucosyltransferase

Summary

In their natural environment, plants live in a close association with a large variety of microorganisms. A number of these microorganisms can be detrimental to plants and are considered as potential pathogens. In order to ward off these pathogens, plants have developed a highly effective and dynamic immune system.

As a first line of defense, plants recognize the presence of microbes through the perception of molecular structures typical of a microbial class, termed microbe-associated molecular patterns (MAMPs). In Arabidopsis, the Leu-rich repeat receptor-like kinases FLS2 and EFR recognize the bacterial MAMPs flagellin and EF-Tu (and their bioactive epitopes flg22 and elf18), respectively. Perception of these MAMPs triggers defense responses that restrict microbial invasion and growth. However, the molecular basis of MAMP-triggered immunity (MTI) is still largely unknown. As MTI functionally links to and provides an evolutionary basis for different branches of plant immunity, it is instrumental for the understanding of plant-microbe interactions.

The work presented here aimed at the identification of molecular components of MTI. A forward-genetic screen revealed *priority in sweet life (psl)* mutants that show de-repressed anthocyanin accumulation in the presence of elf18 or flg22. PSL2 was identified as the single-copy Arabidopsis UDP-glucose:glycoprotein glucosyltransferase (UGGT), whereas PSL25 most likely identifies the Arabidopsis endoplasmic reticulum (ER) Glucosidase I. These are components of an ER protein quality control (ERQC) pathway that ensures proper folding and maturation of membrane-resident and secreted proteins. These and other ERQC components are required for the generation of functional EFR.

PSL36 was identified as a novel allele of *EIN2 (ETHYLENE INSENSITIVE2)*, a central regulator of the ethylene(ET) pathway. Loss of EIN2 function results in pronounced defects in FLS2 and EFR signaling outputs. Whereas ET signaling is crucial for *FLS2* expression, EFR steady-state levels are unaltered in *ein2* plants. These data point to a role for ET in post-recognition signaling by EFR. The identification of a set of EFR-triggered genes that depend on ET-signaling for their full activation reveals possible mechanisms of signal integration during MTI.

Zusammenfassung

Pflanzen leben in der Natur in einer engen Verbindung mit einer großen Vielfalt an Mikroorganismen. Viele dieser Mikroorganismen können die Pflanzen schädigen und werden daher als potentielle Pathogene betrachtet. Um diese Pathogene abzuwehren, haben die Pflanzen ein hoch effizientes und dynamisches Immunsystem entwickelt.

Als die erste Abwehrlinie erkennen Pflanzen Mikroben anhand von molekularen Strukturen die spezifisch für Mikroben sind, sogenannte, Mikroben-assoziierte molekulare Muster (MAMM). In Arabidopsis erkennen die Rezeptor-Kinasen FLS2 und EFR die MAMMs flagellin und EF-Tu (beziehungsweise ihre bioaktiven Epitope flg22 und elf18). Erkennung dieser MAMMs löst eine Immunantwort aus, die das Eindringen und Ausbreitung der Mikroben einschränkt. Jedoch ist die molekulare Grundlage dieser MAMMs-induzierten Resistenz (MIR) größtenteils unbekannt. Da MIR mit weiteren Ebenen des pflanzlichen Immunsystems eng verknüpft ist und ihre evolutionäre Grundlage stellt, ist die Erforschung des MIR entscheidend für das Verständnis des Zusammenlebens von Pflanzen und Mikroben.

Die hier vorgestellte Arbeit hatte das Ziel molekulare Komponenten des MIR zu identifizieren. Eine genetische Sichtung identifizierte die „priority in sweet life (psl)“ Mutanten, die eine Aufhebung der Anthocyanin-Unterdrückung durch elf18 oder flg22 zeigen. PSL2 wurde als Arabidopsis UDP-glucose:glycoprotein glucosyltransferase (UGGT) identifiziert, und PSL25 identifiziert höchst wahrscheinlich die im Endoplasmatischen Retikulum lokalisierte Glucosidase I. Diese sind Komponenten des ER Protein Qualitätskontroll-Mechanismus (ERQK), die die korrekte Faltung und Reifung von sekretierten und Membran-gebundenen Proteinen sichert. Diese und andere ERQK Komponenten werden für die Generierung eines funktionalen EFR benötigt.

PSL36 wurde als ein neuer Allel von EIN2 (ETHYLENE INSENSITIVE2) identifiziert, das ein zentraler Regulator des Ethylen(ET) Signalweges ist. Ein disfunktionaler EIN2 resultiert in gestörten Antworten von FLS2 und EFR. ET spielt eine entscheidende Rolle für die Expression von FLS2, EFR Akkumulation ist jedoch unverändert in *ein2* Mutanten. Dies deutet auf eine Rolle von ET für die Signalfunktion von EFR hin. Wir identifizierten eine Reihe von EFR-induzierten Genen, die einen funktionierenden ET-Signalweg für ihre Aktivierung benötigen. Dies könnte zur Entdeckung von wichtigen Signalmechanismen des MIR führen.

1. Introduction

In the nature, plants exist in close association with a large variety of microbes. Some of these microbes can propagate on certain host plants and cause disease symptoms, thus they are considered as pathogens. Based on their lifestyle and infection strategies, these pathogenic microbes can be classified as necrotrophs or biotrophs (Dangl and Jones 2001, Glazebrook 2005). Necrotrophs first kill plant cells and subsequently feed on the dead material. Biotrophs keep their hosts alive and retrieve nutrients from living cells. However, many pathogens display an intermediate lifestyle and are referred to as hemibiotrophs (Dangl and Jones 2001, Glazebrook 2005).

In order to prevent colonization by microbes, plants developed an effective immune system. As a consequence, most plant species are resistant to most microbes. This phenomenon is called nonhost resistance and describes the resistance of a plant species against all strains of a non-adapted pathogen (Nurnberger and Lipka 2005). In contrast to vertebrates, plants lack specialized immune cells and rely on the innate immunity of each cell. This implies a tight coordination of defense responses with other physiological processes in plant cells.

The plant immune system largely relies on two classes of immune sensors that recognize two types of microbial signatures. The first class of immune receptors recognizes conserved molecules that are present in most microbes but absent in plants, and induces a defense response that limits pathogen growth (Segonzac and Zipfel 2011). Adapted pathogens however developed virulence strategies to suppress this basal defense and can thus proliferate in their host plants. Deployment of effector proteins into plant cell represents a major pathogenicity strategy (Block and Alfano 2011). The second class of plant immune receptors specifically recognizes the presence of these effectors and activates a more robust immune response that eventually terminates the pathogens growth

(Chisholm et al. 2006, Jones and Dangl 2006, Bent and Mackey 2007, Tsuda and Katagiri 2010).

Activation of defense responses confers enhanced immunity not only at the infection site, but also in distant tissues. It has been long noted that a primary infection renders plants more resistant to a secondary infection at distant leaves. This phenomenon was termed systemic acquired resistance (SAR) (Durrant and Dong 2004).

1.1 MAMP-triggered immunity

Microbe-associated molecular patterns (MAMPs, also called PAMPs for pathogen associated molecular patterns) are molecules that are conserved in many microbial species and normally not present in the plant body. Known MAMPs include the bacterial proteins flagellin, elongation factor-Tu (EF-Tu), Ax21 and cold shock protein, as well as constituents of the bacterial cell wall, such as lipopolysaccharides (LPS) and peptidoglycans (PGN). Other known MAMPs are fungal chitin and pep13 from oomycetes (Boller and Felix 2009, Nurnberger et al. 2004, Segonzac and Zipfel 2011). The molecules that are recognized as MAMPs typically exert an important function for the fitness of the microbes. Consequently, MAMPs tolerate little variation of their structure and are considered as slow-evolving (Jones and Dangl 2006). Nevertheless, MAMPs are not invariable and can be altered in order to prevent their recognition, as shown for flagellin from *Xanthomonas* strains (Sun et al. 2006).

MAMP-receptors (termed pattern recognition receptors, PRRs) identified to date in plants are restricted to membrane anchored proteins with a putative extracellular domain containing leucine-rich-repeats (LRRs) or LysM-motifs (Boller and Felix 2009, Zipfel 2008). Bacterial flagellin is perceived by the receptor-like kinase (RLK) FLAGELLIN SENSING 2 (FLS2) in most plant species. EF-Tu is recognized by the related RLK EF-TU RECEPTOR (EFR).

However, in contrast to flagellin, EF-Tu recognition has been noted only in *Brassicaceae*, showing differential phylogenetic distribution of PRRs.

Recognition of MAMPs leads to a state of enhanced cellular immunity that restricts the invasion and/or propagation of potential pathogenic microbes, termed MAMP-triggered immunity (MTI). Interestingly, MTI is active against a broad spectrum of pathogens with different lifestyles (Boller and Felix 2009). Activation of MTI by different PRRs triggers a stereotypical set of physiological responses that are detectable within seconds/minutes and hours/days. Early responses include rapid generation of reactive oxidative species (ROS spiking), activation of Mitogen-activated kinases (MAPKs), and Ca^{2+} influx, and are followed by a massive transcriptional reprogramming that typically results in accumulation of antimicrobial compounds and cell-wall reinforcements with callose (Nurnberger et al. 2004, Boller and Felix 2009, Nicaise et al. 2009). However, the contribution of the individual defense responses to the establishment of MTI is in the most cases still unclear.

1.2 Effector-triggered immunity

The importance of MTI is illustrated by the finding that pathogenic microbes often actively suppress or evade MTI in order to successfully infect plants (Gohre and Robatzek 2008, Block and Alfano 2011). Suppression of plant defense responses is mediated by the action of effector proteins (Chisholm et al. 2006, Block and Alfano 2011). Bacterial pathogens deliver effector proteins into plant cells by a needle-like structure called the type III secretion system (TTSS). Upon their delivery, TTSS effectors interact with and modify multiple defense components, thereby manipulating the host to the pathogens advantage. It has been shown that two unrelated bacterial TTSS effectors, AvrPto and AvrPtoB target the PRRs FLS2 and EFR and their interacting partner (Xiang et al. 2008, Gohre et al. 2008, Shan et al. 2008).

The recognition of effectors is mediated by another class of immune-receptors, called Resistance (R) proteins. R proteins are modular proteins,

consisting of domains, such as an LRR-domain, a nucleotide-binding (NB)-domain and an N-terminal coiled-coil (CC) or Toll/Interleukin-1 receptor (TIR) domain. Most R-proteins are intracellular proteins, however a subset of R-proteins have an extracellular domain (for example the Cf-family). The successful recognition of an effector by a matching R-protein triggers an immune response, termed effector-triggered immunity (ETI) (Jones and Dangl, 2006, Tsuda and Katagiri, 2010). In this case, the recognized effector is called an avirulence (Avr) protein. The recognition of effectors can be either direct through physical interaction between effector and R-protein, or indirect through sensing the effectors actions (the guard hypothesis; Dangl and Jones 2001). It is thought that co-evolution between host plants and pathogenic microorganisms results in the development of novel effectors, which in turn triggers the development of matching R proteins (Chisholm et al. 2006, Jones and Dangl 2006, Bent and Mackey 2007).

Defense responses induced during ETI show significant overlap with those that are activated during MTI (Nurnberger et al. 2004, Bent and Mackey 2007). However, the kinetics and amplitude of the induced responses often differ between MTI and ETI (Tsuda and Katagiri 2010). It is generally accepted that defense-responses induced by ETI are more robust than those activated during MTI. Furthermore, in contrast to MTI ETI is often associated with localized programmed cell death, termed the hypersensitive response (HR). However, recent reports demonstrate that the induction of HR is not essential for the activation of robust immunity during ETI (Slootweg et al. 2010, Heidrich et al. 2011). This raises the question, what actually stops pathogen growth in most cases?

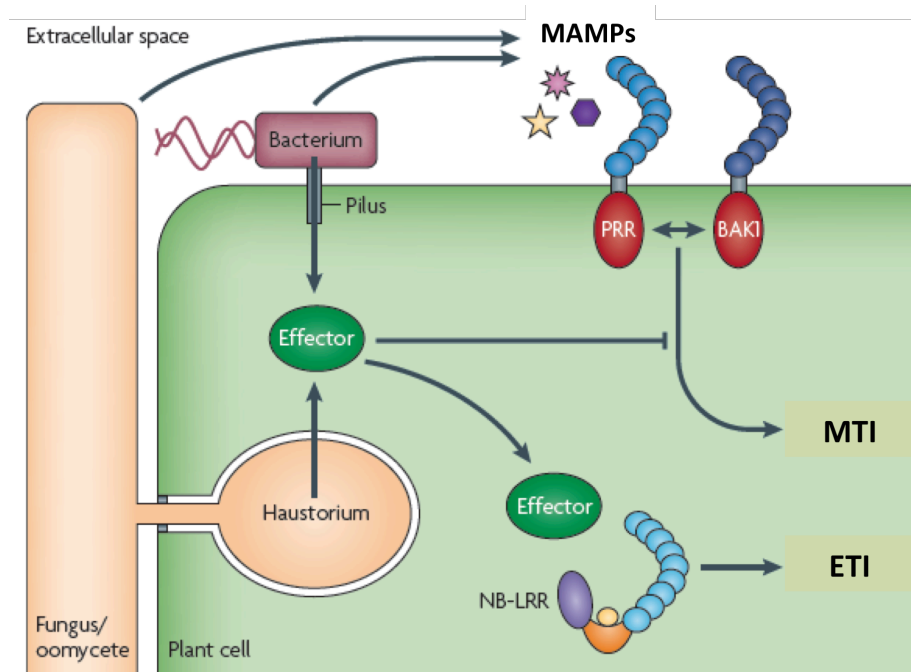


Figure 1. The conceptual framework of plant immunity connecting MAMP recognition, effector action and effector recognition. Modified from Dodds and Rathjen, Nature Reviews 2010

Plant PRRs recognize MAMPs and initiate MTI that is suppressed by effector proteins. R proteins, such as the here shown NB-LRR recognize the presence of the effector and induce ETI.

1.3 MTI as a basis for ETI, SAR and nonhost resistance

For long time the significance of MAMP recognition for overall plant disease resistance was doubtful. However, work on the flagellin perception system in *Arabidopsis* revealed several important features of MTI (Gomez-Gomez and Boller 2000). Most importantly, genetic evidence was obtained for the role of flagellin perception in limiting bacterial growth, by showing that loss of the flagellin receptor FLS2 increased susceptibility to adapted bacterial pathogens (Zipfel et al. 2004).

Later, it was shown that flagellin recognition also plays a role in limiting growth of non-adapted bacterial pathogens, thereby demonstrating a role for MTI in nonhost resistance (Li et al. 2007). This notion was further supported by the cloning of FLS2 as a major QTL for nonhost-resistance of Arabidopsis against the bean pathogen *Pseudomonas syringae* pathovar *phaseolicola* (Forsyth et al. 2010). Interestingly, SAR is induced also by exogenous application of MAMPs, suggesting that MTI activation is sufficient to enhance immunity in systemic tissues (Mishina et al. 2007). Furthermore, it was shown that transcriptome changes during MTI and ETI significantly overlap (Navarro et al. 2004). A possible direct link between ETI and MTI signaling was revealed in barley-powdery mildew interactions. Upon its activation, the R-protein MLA10 interacts with transcriptional repressors and thereby de-represses MAMP-responsive genes (Shen et al. 2007). In conclusion, MTI functionally links to other immune branches in plants, and might provide a basis for their activation. The more important it becomes to understand the mechanisms regulating MAMP perception and signaling.

1.4 Damage-associated molecular patterns (DAMPs)

As MAMPs are equally present in pathogenic and non-pathogenic microbes, it has been hypothesized that the innate immunity of vertebrates responds to MAMPs in the context of additional signals, the so called patterns of pathogenesis, in order to distinguish pathogenic microbes from commensal microorganisms (Vance et al. 2009).

Likewise, plants perceive in addition to non-self structures such as MAMPs also endogenous elicitors known as DAMPs (damage-associated molecular patterns). These endogenous elicitors are generated and/or released as a consequence of cellular damage caused by a pathogen attack, e.g. cell wall fragments (Boller and Felix 2009, Ferrari et al. 2007). Immuno-stimulatory peptides that are encoded in the plant genome and are activated in response to pathogens or wounding, e.g. systemin from tomato or PROPEP1 to 6 from Arabidopsis, might represent such DAMPs (Boller 2005, Ryan et al. 2007).

1.5 Perception of bacterial flagellin and Elongation Factor-Tu in Arabidopsis

The best characterized MAMP-perception systems in Arabidopsis are those that recognize the bacterial proteins flagellin and elongation factor-Tu (EF-Tu). The bioactive epitopes reside in the conserved N-termini of flagellin and Ef-TU, and are termed flg22 and elf18, respectively. Exogenous application of flg22 and elf18 is sufficient to trigger immune responses in Arabidopsis (Felix et al 1999, Kunze et al. 2004). Furthermore, pre-treatment with flg22 or elf18 renders plants more resistant to a subsequent challenge by pathogens, thus induces MTI (Zipfel et al. 2004, Kunze et al. 2004).

Flg22 and elf18 are perceived by the receptor-like kinases (RLKs) FLS2 and EFR, respectively (Gomez et al. 2000, Zipfel et al. 2006). FLS2 and EFR are highly related in their module structure, as both belong to the same subclade of the LRR-RLK family that consists of an N-terminal LRR domain, a single transmembrane domain and a C-terminal kinase domain. Importantly, perception of these MAMPs seems to be highly specific, as known flg22- and elf18-induced responses are entirely dependent on FLS2 and EFR, respectively. Not only FLS2 but also EFR seems to be critical for overall host immunity, since loss of this PRR in Arabidopsis *efr* mutants results in increased susceptibility to both adapted and non-adapted strains of bacteria (Zipfel et al. 2006, Nekrasov et al. 2009, Saijo et al. 2009).

1.6 Signaling through FLS2 and EFR

1.6.1 FLS2 and EFR immune complexes

MAMP-mediated activation of PRRs induces a series of cellular responses that are detectable within seconds/minutes and hours/days (Boller and Felix

2009, Nicaise et al. 2009). One of the first signaling events involves the LRR-RLK BAK1 that was initially identified for its role in brassinolide signaling (Nam et al. 2002). FLS2 and EFR form ligand-induced complexes with BAK1 and other closely related RLKs belonging to the SERK (SOMATIC-EMBRYOGENESIS RECEPTOR-LIKE KINASE) family (Chinchilla et al. 2007, Roux et al. 2011). This complex formation is detectable within seconds after MAMP application, indicating the existence of pre-formed, loose complexes (Schulze et al. 2010). Loss of BAK1 results in reduced sensitivity to flg22 and elf18 that is more pronounced in *bak1 serk1/bkk1* double mutants (Roux et al. 2011). These data demonstrate requirement of BAK1 for FLS2 and EFR signaling and indicate functional redundancy among SERK family members. Besides BAK1 and other SERKs, additional interactors of FLS2 and EFR have been identified. The membrane-localized cytoplasmic kinases BOTRYTIS-INDUCED KINASE1 (BIK1) and related PBLs (for PBS1-like) associate with FLS2 and EFR and are phosphorylated in a PRR-dependent manner (Lu et al. 2010, Zhang et al. 2010). Importantly, it was shown that the *bik1* and *pbs1* mutants are impaired in MAMP-responses and MTI (Lu et al. 2010, Zhang et al. 2010). Loss of single or multiple components of these PRR complexes, for example in *bak1* and *bik1* mutants, results in impaired cell death control. As the deregulated cell death in these mutants depends on SA and shows further similarities to an HR response, it is conceivable that the integrity of PRR complexes is monitored by R proteins that become activated when parts of these complexes are absent. Interestingly, *fls2* or *efr* mutants do not show such pleiotropic phenotypes. However, given that BAK1 regulates responses to multiple MAMPs, it might be more crucial for MTI and consequently guarded more stringently than individual PRRs.

Together, it seems that FLS2, EFR and probably other PRRs as well act as parts of multiprotein-complexes. However, the exact composition and dynamic changes of these immune-complexes upon elicitation remain to be addressed. Also, it is an intriguing question, how pre-recognition complexes are assembled.

1.6.2 FLS2 and EFR signaling outputs

Application of multiple MAMPs, for example flg22 and elf18 rapidly and transiently activates the MAPKs 3, 4 and 6. Flg22 activates at least two MAPK-cascades consisting of MKK4/5-MPK3/6 and MEKK1-MKK1/2-MPK4 (Asai et al. 2002, Suarez-Rodriguez et al. 2007, Qiu et al. 2008). However, functional redundancy between MPK3 and 6 and embryonic lethality of the *mpk3 mpk6* double-mutants hampered detailed characterization of their contribution to MAMP-responses. Generation of reactive oxidative species, the so-called ROS burst represents another early MAMP output. MAMP-induced ROS spiking is mediated by the NADPH oxidase RbohD and *rbohD* mutants are slightly but significantly more susceptible to weakly virulent bacteria, suggesting a role of this output for MTI (Zhang et al. 2007, Mersmann et al. 2010). Other early MAMP outputs are Ca²⁺ spiking, activation of ion fluxes across the plasma membrane and generation of nitric oxide (NO) (Boller and Felix 2009). Recent work reported distinct but overlapping roles of MAPKs and Calcium-dependent protein kinases (CDPKs) for flg22-induced transcriptional reprogramming (Boudsocq et al. 2010). These findings indicate a high level of complexity already at an early stage of MAMP-signaling. Cell-wall reinforcements by the β -glucan callose comprise a late response to MAMPs. MAMP-induced callose deposition is dependent on the callose-synthase PMR4 (Kim et al. 2005). However, *pmr4* mutants are not only defective in MAMP-induced callose deposition, but also show constitutively upregulated SA levels. However, *pmr4 pad4* double-mutants that are deficient in SA accumulation show slightly increased susceptibility to non-adapted *Pseudomonas syringae* pv *phaseolicola* when compared to the respective single mutants (Ham et al. 2007). This indicates a role of callose deposition in restricting growth of this bacterium.

Importantly, distinct MAMPs such as flg22 and elf18 induce very similar early outputs. For example the set of genes induced upon MAMP perception at early time points (30-60 minutes) is almost identical between flg22 and elf18 (Zipfel et al. 2006). This suggests the existence of common signaling pathways that integrate signaling from multiple MAMP-receptors.

However, it remains elusive how a single PRR can activate such a diverse array of outputs.

1.6.3 Subcellular localization and trafficking of FLS2

It is generally predicted that most plant PRRs would localize to the plasma membrane as they perceive likely extracellular structures. Indeed, FLS2 was localized to the PM in Arabidopsis (Robatzek et al. 2006). However, upon perception of its ligand, FLS2 re-localizes to mobile intracellular vesicles (Robatzek et al. 2006). Ligand-induced receptor internalization might represent a signaling mechanism and/or might contribute to signaling attenuation. Importantly, most early PRR signaling outputs are transiently activated. Recently, it was shown that FLS2 is targeted for proteasome-mediated degradation as a mechanism for signaling attenuation (Lu et al. 2011).

1.7 ER quality control for membrane proteins

Prolonged activation of defense responses interferes with other physiological processes in plants and results in growth retardation, repression of abiotic stress responses and/or cell death (Boller and Felix 2009, Shirasu 2009, Yasuda et al. 2008). Therefore, a stringent control of immune receptor abundance/quality can be presumed. Indeed, forward-genetic screens revealed the requirement of cytosolic chaperones for the accumulation of intracellular immune receptors of the NB-LRR class (Shirasu 2009). However, it is unknown whether, and if so, how such quality control serves for the generation and function of transmembrane MAMP receptors.

In eukaryotic cells, membrane proteins are translocated through the endoplasmic reticulum (ER) to their functional site. Correct folding of proteins is instrumental for their proper function, thus it is not surprising that several folding and quality control pathways co-operate in the ER (Aneli and Sitia

2008). One of the best studied ER quality control (ERQC) pathways is the calnexin(CNX)/calreticulin (CRT) cycle that mediates correct folding of N-glycosylated proteins (Helenius and Aebi 2004). CNX and CRT are two lectins that specifically interact with proteins that carry monoglucosylated glycans and facilitate their correct folding (Williams 2006). The pre-assembled glycan chain ($\text{Glc}_3\text{Man}_9\text{GlcNAc}_2$) incorporating three terminal glucose residues is attached to nascent polypeptides by the oligosaccharyltransferase (OST) complex. Subsequently, ER-resident glucosidase I and II trim two glucose residues and produce thereby the binding site for CRTs and CNXs. Glucosidase I removes the outermost glucose residue, whereas glucosidase II that is comprised of an α and β subunit removes the second and third glucose residue. Removal of the last glucose residue disrupts the binding between client protein and the lectins CRT and CNX. Properly folded proteins are then released from the ER and can be transported to their functional site.

However, proteins that still exhibit folding defects are recognized by UDP-glucose:glycoprotein glucosyltransferase (UGGT) that acts as a folding sensor in the ER. This enzyme specifically catalyzes glucosylation of glycans that are attached to misfolded proteins but not to native proteins (Parodi 2000). In this way it mediates re-glucosylation of client proteins and thereby re-creates the binding site for CRTs and CNXs. Thus, incompletely folded proteins are retained in the ER by the concerted actions of UGGT and CRT/CNX. The action of UGGT and glucosidase II can drive cycles of binding to and release from CRTs and CNXs until the client proteins is correctly folded or eliminated by ER-associated degradation (ERAD).

In Arabidopsis, knowledge about this branch of ERQC is much more limited. Several *uggt* alleles were identified as allele-specific suppressors of a mutant version of the LRR-RLK brassinosteroid receptor BRI1 (Jin et al. 2007). Interestingly, this aberrant BRI1-9 receptor is retained in the ER in WT plants due to its misfolding, but *uggt* mutants allow its escape from the ERQC and localization to the plasma membrane despite its misfolding, where the partially misfolded but signaling competent receptor can exert some of its native functions. Furthermore, it was shown that CRT3 (one of the

Arabidopsis calreticulin homologs) and BIP are required for ER-retention of BRI1-9 (Jin et al. 2009). These results provide further evidence for UGGTs and CRTs function in ERQC of membrane proteins. However, it remains questionable whether WT BRI is a client of the UGGT/CRT chaperone system, since *uggt* and *crt3* show in contrast to *bri* a WT-like morphology.

Also several mutants of glucosidase I and glucosidase II homologs have been characterized in Arabidopsis. Mutations in glucosidase I (designated *knf* and *gcs1*) show lethality during seed development, revealing essential function of N-glycan trimming for embryo development (Boisson et al. 2001). The defects in these glucosidase I mutants were mostly attributed to dramatically reduced cellulose content, resulting in aberrant anisotropic growth (Gillmor 2002). Interestingly, these reports claim that most cellular functions were intact in *knf* and *gcs* mutants, suggesting that glucosidase I function is required only for a limited number of client proteins. However, the client protein involved in cellulose synthesis remains unknown. Interestingly, a hypomorphic glucosidase I allele retains viability and thus provides a tool to address glucosidase I functions in mature plants (Furumizu et al. 2008). These *knf101* plants are slightly smaller than WT and show defects in epidermal patterning, resulting in increased stomata density and root hair number. Genetic analysis suggest the involvement of glucosidase I in the same stomata patterning pathway as *EPIDERMAL PATTERNING FACTOR 1 (EPF1)*, but the exact client substrate has not been identified.

1.8 Phytohormone signaling

The phytohormones salicylic acid (SA), jasmonic acid (JA) and ethylene (ET) are pivotal regulators of plant defense responses against pathogenic microbes (Glazebrook 2005, Pieterse et al. 2009). A cross-talk between these hormone signaling pathways allows the plant to fine-tune the induction of defense responses against different pathogens. Mainly antagonistic

interactions have been reported for SA and JA, whereas JA and ET often act synergistically (Glazebrook 2005, Pieterse et al. 2009). Although the role of SA in resistance against biotrophs and JA in defense against necrotrophs has been demonstrated in many plant-pathogen interactions, the situation is far more complex and plenty of exceptions to this rule exist (Glazebrook 2005, Pieterse et al. 2009).

Pathogen-induced SA is mainly derived from chorismate by the isochorismate synthase SID2 (SA INDUCTION DEFICIENT 2) (Wildermuth et al. 2002). SA-induced redox changes are perceived by NPR1 (NONEXPRESSOR OF PATHOGENESIS-RELATED GENES1) and this leads to translocation of NPR1 to the nucleus where it regulates the expression of a multitude of genes. Importantly, not all SA-induced responses are mediated by NPR1 and conversely, NPR1 also regulates SA-independent processes (Pieterse and Van Loon 2004, Dong 2004). The lipase-like proteins EDS1 (ENHANCED DISEASE SUSCEPTIBILITY1) and PAD4 (PHYTOALEXIN-DEFICIENT4) are important regulators of SA-dependent and SA-independent immune responses (Wiermer et al. 2005).

SA-levels are induced by application of flg22 in Arabidopsis, and *sid2* mutants show partial reduction of flg22-triggered immunity to *Pseudomonas syringae* (Tsuda et al. 2008).

The bioactive JA-isoleucine conjugate is synthesized by JAR1 (JASMONATE RESISTANT1). Perception of JA-Ile by the F-box COI1 (CORONATINE INSENSITIVE1) containing E3 ubiquitin ligase complex results in the degradation of JAZ (JASMONATE ZIM DOMAIN) transcriptional repressors and thereby triggers JA responses (Chico et al. 2008).

1.8.1 Ethylene signaling

The gaseous phytohormone ethylene (ET) regulates a variety of stress responses and developmental processes in plants. Among others, ET is involved in fruit ripening, senescence, germination, cell elongation, cell fate determination, wound response and pathogen defense (Wang et al. 2002, Van

Loon et al. 2006). To ensure proper control of these processes, ET biosynthesis and responsiveness are tightly regulated.

ET is synthesized from methionine through several enzyme catalyzed steps (Wang et al. 2002). The rate-limiting step of ethylene synthesis is the conversion of S-adenosyl-methionine to 1-aminocyclopropane-1-carboxylic acid (ACC) by ACC synthase (ACS). The subsequent conversion of ACC to ET is mediated by ACC oxidase (ACO). Arabidopsis encodes nine characterized ACS isoforms that are regulated by complex transcriptional and post-translational mechanisms. It has been proposed that the different ACS isoforms are differentially regulated and thus contribute to the multitude of ET responses (Wang et al. 2002, Tsuchisaka and Theologis 2004). A common principle seems to be a low steady-state ACS level that can be rapidly increased by post-translational stabilization, for example through phosphorylation on certain residues (Wang et al. 2002, Tatsuki and Mori 2001). Interestingly, it was demonstrated that MPK3 and 6 target and phosphorylate ACS6, resulting in its stabilization and fast ET generation (Liu et al. 2004, Yoo et al. 2008).

ET is perceived by a small family of 5 ET-receptors that show structural similarity with bacterial two-component histidine kinases (Stepanova and Alonso 2009, Yoo et al. 2009). Genetic studies demonstrate that the receptors act as negative regulators of ET responses. ET binding to its receptor induces an inactive conformation thereof and thus allows activation of downstream responses. CTR1, a Raf-like protein kinase physically associates with the ET-receptors ETR1 and ETR2 and negatively regulates ethylene responses, as demonstrated by the constitutive ET response phenotype of *ctr1*. EIN2 is a positive regulator of ET signaling that acts genetically downstream of CTR1 (Alonso et al. 1999). Mutations in *EIN2* result in strong ET insensitivity, thus EIN2 play essential roles in most ET-regulated processes. Nonetheless, its biochemical function is still unknown. EIN2 is comprised from an N-terminal domain showing similarity to NRAMP metal ion transporter and a C-terminal globular domain.

Recent work localized EIN2 at the ER-membrane where it interacts with ET-receptors (Bisson et al. 2009). It seems that the C-terminal domain carries the ET-response inducing function, as overexpression of this domain leads to constitutive ET-responses (Alonso et al. 1999). ET perception and signaling mediates stabilization and nuclear accumulation of the transcription factors EIN3 and EIN3-LIKE1 and further homologs (An et al. 2010). Here, transcription factor cascades induce the activation of ET-responsive genes and thus ET outputs (Solano et al. 1998).

Ethylene generation increases in plants upon perception of pathogen attack and is associated with the activation of defense responses (Broekaert et al. 2006). However, it seems that ET differentially contributes to defense against pathogens with different lifestyles. Generally, ET is important for resistance against necrotrophs, like *Alternaria brassicicola* and *Botrytis cinerea*, and has no effect on disease development by biotrophs (Glazebrook 2005, Van Loon 2006). However, there seem to be exceptions from this general rule.

ET influences the interaction of Arabidopsis with the hemibiotrophic bacteria *Pseudomonas syringae* in complex ways. When virulent *Pseudomonas syringae* pathovar *tomato* DC3000 (*Pst* DC3000) were infiltrated into the leaf tissues, *ein2* plants showed less symptoms but supported bacteria growth to similar levels as wild-type plants (Bent et al. 1992). This indicated a role for ET in development of yellow senescence-like symptoms, but not in controlling bacteria proliferation. A recent report shows enhanced resistance of *ein3 eil1* and *ein2* plants to *Pst*. DC3000 and explains this finding by constitutive elevation of SA levels and responses in these plants (Chen et al. 2009). In contrast, *etr1* and *ein2* plants allow enhanced growth of virulent *Pst* DC3000 and weakly virulent *Pst* DC3000 Δ AvrPto AvrPtoB, when the bacteria were applied by spray inoculation (Mersmann et al. 2010, Pieterse et al. 1998). Furthermore, *ein2* seedlings are defective in flg22-induced activation of several defense genes, callose deposition and accumulation of glucosinolate-related metabolites, resulting in enhanced susceptibility to *Pst* DC3000 (Clay et al. 2009).

Recently, it was shown that *FLS2* transcript and protein levels are strongly reduced in ET-pathway mutants, e.g. in *ein2*, *etr1* and *ein3 eil1* (Boutrot et al. 2010, Mersmann et al. 2010). Furthermore, binding of EIN3 to the *FLS2* promoter suggests direct ET-regulated transcriptional activation of this gene. These findings might explain reduced flg22-responsiveness of ET-signaling mutants. However, ET increases rapidly upon flg22 perception, and it remains elusive, whether, and if so, how this MAMP-induced ET contributes to MAMP-signaling.

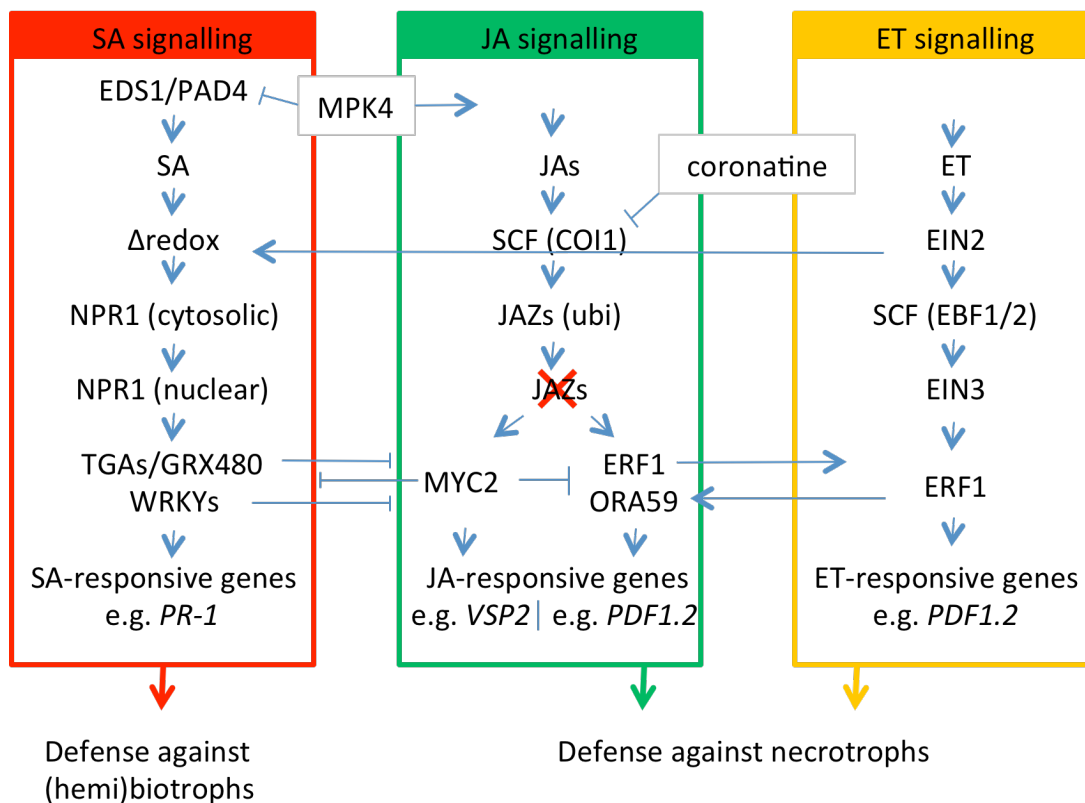


Figure 2. Phytohormone crosstalk during defense responses (modified from Pieterse et al. 2010). Negative interactions between the SA and JA pathways, and positive interactions between the JA and ET pathways are prevalent.

MTI activation by bacterial MAMPs such as flagellin involves the generation of SA and ET (Felix et al. 1999, Tsuda et al. 2008). Furthermore, it was shown that JA levels increase in response to pep13 treatment in potato (Halim et al. 2009). Thus, SA, ET, and JA signaling can be activated during MTI (Tsuda and Katagiri, 2010). However, single mutations in the ET and SA pathways only moderately affect MTI in Arabidopsis (Zipfel et al 2004, Boutrot et al 2010, Tsuda et al 2008). In contrast, quadruple mutants that are deficient in signaling mediated by SA, ET, JA and PHYTOALEXIN DEFICIENT4 (PAD4), show 80% reduced flg22- and elf18-triggered immunity (Tsuda et al. 2009). More importantly, measurement of the immunity levels in all combinatorial mutants indicate positive contributions of the SA, ET, JA and PAD4 pathways to flg22- and elf18-triggered immunity. On the other hand, numerous reports indicate antagonistic relationships between these phytohormone pathways (Glazebrook 2005). However, the underlying mechanisms that integrate these immune pathways for MTI activation that would often antagonize each other remain elusive.

2. Results

2.1 Receptor quality control in the endoplasmic reticulum for plant innate immunity

2.1.1 MAMP perception leads to the repression of sucrose-induced anthocyanin accumulation in Arabidopsis seedlings

Earlier studies indicate a crosstalk between MAMP perception and abiotic stress-induced flavonoid accumulation in plants (Lo and Nicholson, 1998; McLusky et al, 1999). Anthocyanins represent a major class of flavonoids that are induced upon sucrose stress (Solfanelli et al. 2005; Teng et al. 2005). We subjected Arabidopsis seedlings to sucrose stress by growing them in an MS medium, containing 100 mM sucrose, at which anthocyanin accumulation has been described to be saturated (Solfanelli et al. 2005). After 2-3 day exposure to the sucrose stress, anthocyanin accumulation becomes visible typically as purple and dark green pigmentation of cotyledons and hypocotyls (Figure 1A). However, simultaneous application of the bacterial MAMPs flg22 or elf18 with the sucrose stress represses anthocyanin accumulation (Figure 1A). This flg22 and elf18-triggered repression of anthocyanin accumulation occurs via the cognate MAMP-receptors FLS2 and EFR, respectively, as demonstrated by the lack of this response in the *fls2* and *efr* mutants (Figure 1A). Our conclusions were largely confirmed by photometric quantification of anthocyanin contents (Figure 1B). Importantly, already sub-optimal MAMP doses (10 nM) led to significant suppression of anthocyanin

Results

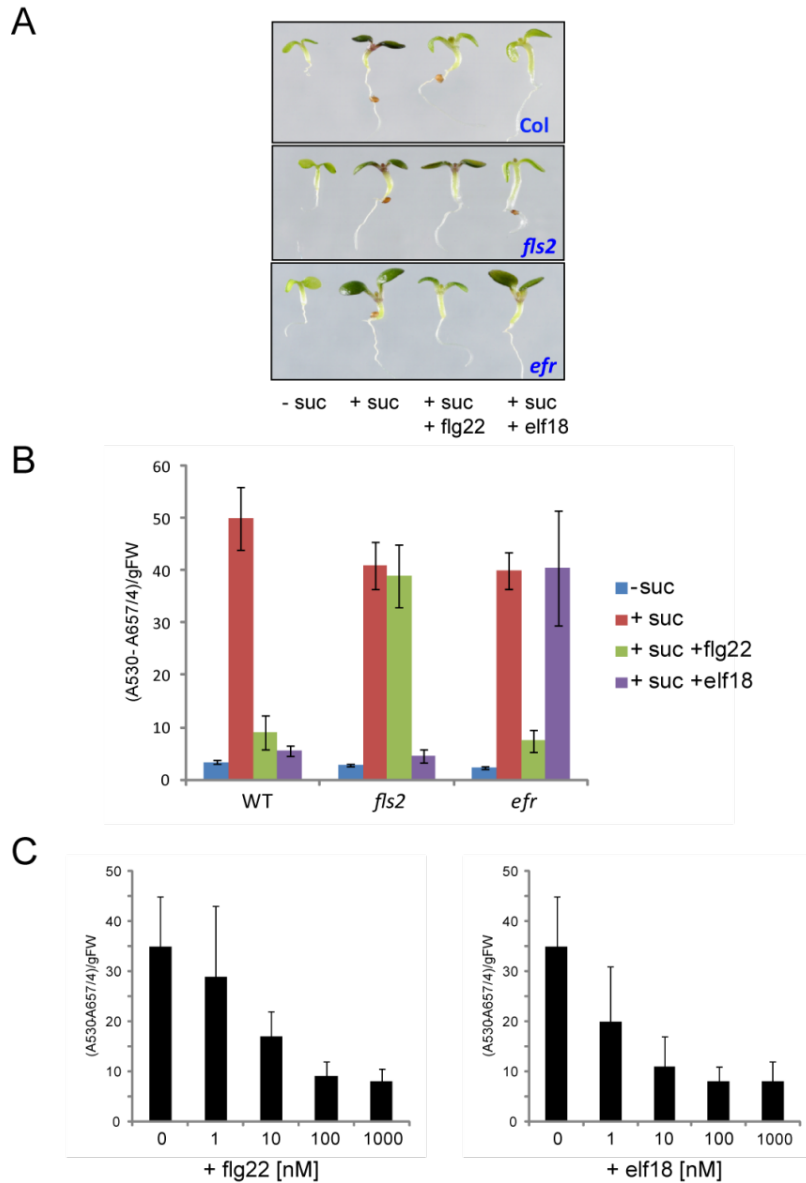


Figure 1. The bacterial MAMPs repress sucrose-induced anthocyanin accumulation.

(A) Arabidopsis WT (Col), *fls2* and *efr* seedlings grown in absence (-suc) or presence (+suc) of sucrose and 0,5 μ M flg22 or elf18.

(B) Anthocyanin content of seedlings grown in absence (- suc) or presence (+ suc) of sucrose and 0,5 μ M flg22 or elf18.

(C) Anthocyanin content of Col seedlings grown in the presence of 100 mM sucrose and the indicated concentrations of flg22 or elf18.

The image shown in Figure 1A was obtained by Dr. Yusuke Saijo.

accumulation, arguing against the possibility that high MAMP doses exert phytotoxic effects and thereby prevent anthocyanin accumulation (Figure 1C). Moreover, the results suggest a hierarchical relationship in which MAMP-signaling overrides sucrose signaling irrespective their relative input levels. In sum, we define suppression of sucrose-induced anthocyanin accumulation as a characteristic MAMP signaling output that occurs in a MAMP dose-dependent manner and requires the earlier defined MAMP-receptors.

2.1.2 Identification of a *psl2* mutant in a genetic screen for Arabidopsis mutants that allow sucrose-induced anthocyanin accumulation in the presence of MAMPs

In order to identify the molecular components of MTI, we initiated genetic screens for MAMP-insensitive plants in Arabidopsis. The above described MAMP-induced suppression of anthocyanin accumulation led to the development of a fast screening method, based on macroscopic inspection of seedling colors. We have screened > 60 000 ethylmethanesulfonate-mutagenized M2 seedlings for plants that are defective in this MAMP signaling output. This led to the identification of > 50 '*priority in sweet life*' (*psl*) mutants that show de-repression of anthocyanin accumulation in the presence of elf18, but retain flg22-dependent repression, including *psl2* (Figure 2A and B). All the *psl* plants identified to date do not constitutively produce anthocyanins at high levels (Figure 2B). We identified more than 5 complementation groups including novel *efr* alleles and non-EFR *psl2* alleles. The results indicate the existence of separate genetic requirements between FLS2 and EFR functions. This was unexpected, as these PRRs are highly related in the overall module structure and function, and seem to activate shared signalling pathways (Zipfel et al, 2006).

Results

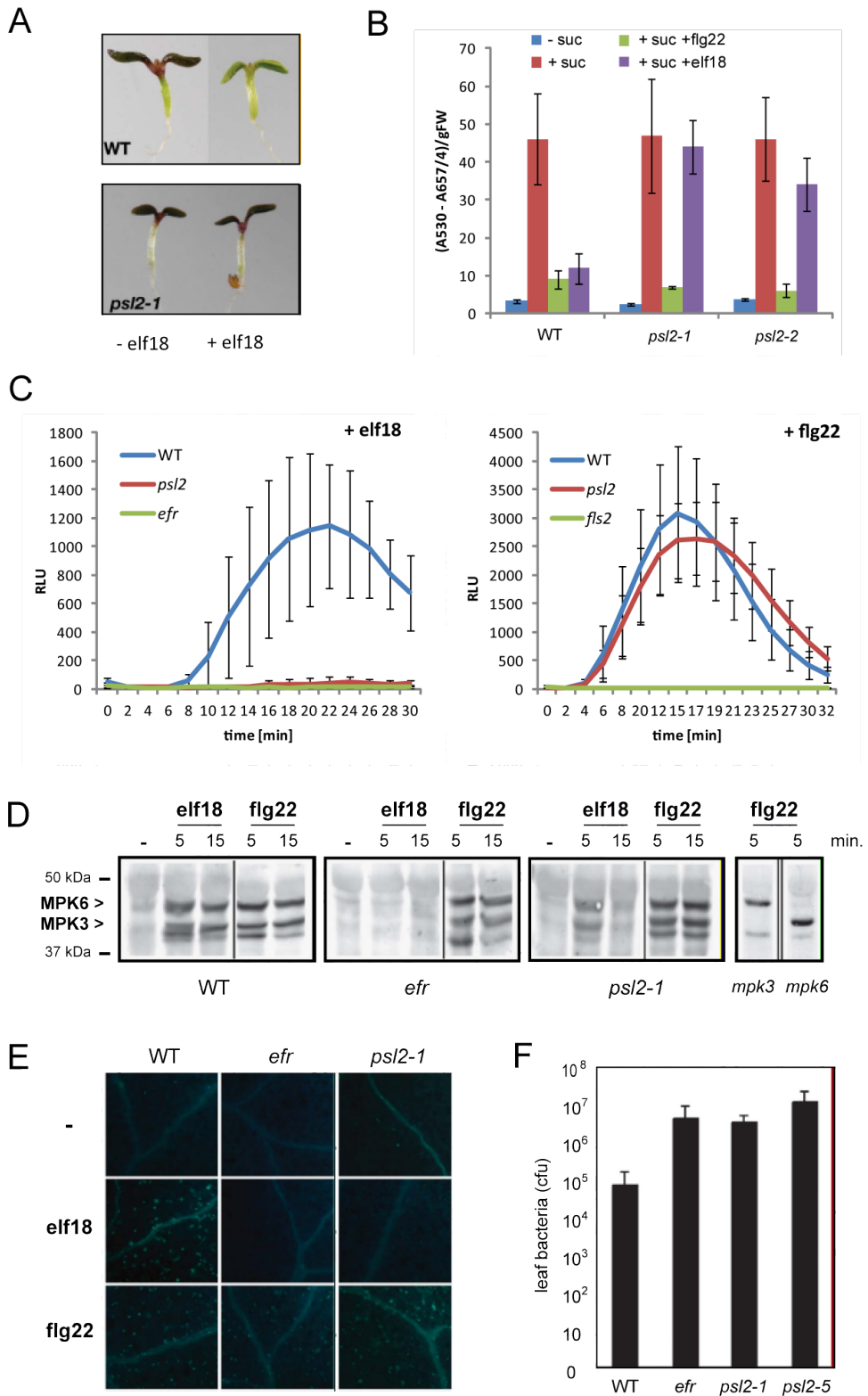


Figure 2. Arabidopsis non-EFR *psl2* mutant is specifically impaired in EFR-triggered immune responses

- (A) Arabidopsis WT (*gl1*) and *psl2-1* seedlings were grown in presence of 100 mM sucrose with (+ elf18) or without (- elf18) 0,5µM elf18.
- (B) Anthocyanin content of Arabidopsis WT (*gl1*), *psl2-1* and *psl2-2* seedlings grown in the absence (-suc) or presence (+suc) of sucrose and 0,5 µM flg22 or elf18.
- (C) ROS generation in leaf discs of WT, *psl2-1* and *efr* or *fls2* plants triggered by 100 nM elf18 or flg22.
- (D) Immunoblot analysis of MAPK activation in WT, *efr*, *psl2-1*, *mpk3* and *mpk6* seedlings upon treatment with water (-), 1 µM elf18 or flg22 for the indicated times. An anti-activ MAPK antibody was used. Positions of molecular weight marker are indicated on the left.
- (E) Callose deposition in WT, *efr* and *psl2-1* seedlings upon treatment with water (-), 1 µM elf18 or flg22. Shown are cotyledons after staining with Aniline blue.
- (F) *Pst* DC3000 bacterial growth in leaves of 4-week-old WT, *efr*, *psl2-1* and *psl2-5* plants 3 days after spray inoculation with bacteria at 10⁹ cfu/ml.

Next, we assayed *psl2* plants for characteristic MAMP signaling outputs. Perception of elf18 and flg22 induces a rapid and transient oxidative burst, which is dependent on the NADPH oxidase AtRbohD (Zhang et al. 2007) in Arabidopsis. However, elf18-induced ROS spiking was undetectable in *psl2* plants (Figure 2C). Furthermore, *psl2* seedlings showed strongly reduced activation of MAPK 3 and 6 in response to elf18 (Figure 2D). In order to test a late MAMP output, we monitored PMR4/GSL5-dependent callose deposition (Kim et al, 2005). Elf18-induced callose deposition was essentially non-detectable in *psl2* seedlings, as revealed by Aniline blue staining (Figure 2E). Thus, *psl2* plants showed elf18-insensitivity in four characteristic MAMP outputs that are detected within minutes (such as ROS-spiking and MAPK activation) and hours/days (callose deposition and anthocyanin suppression), respectively. However, *psl2* plants retain WT-like responsiveness to flg22 in all these assays (Figure 2A–E). This suggests that *psl2* is specifically impaired in EFR mediated signalling upstream of the general machineries that execute those responses.

In order to ensure the functional significance of these observed defects in MAMP signalling, we have tested host immunity against phytopathogens in the *psl2* plants. Earlier studies rather suspected a role of EFR in conferring immunity to the virulent phytopathogenic bacterium *Pseudomonas syringae* pathovar *tomato* DC3000 (*Pst*. DC3000), as the elf18 epitope derived from these bacteria less efficiently induce physiological responses in *Arabidopsis* than *E.coli* derived elf18 (Kunze et al. 2004). However, it is not known how these epitopes are generated and recognized during the pathogen infection process, thus the responses to exogenous elf18 application might not mimic all aspects of EFR-recognition specificity or EFR-induced immunity. Indeed, it has been described that loss of EFR increases the growth of a less virulent strain of *Pst* in leaves, suggesting that EFR contributes to the recognition of the bacteria (Nekrasov et al. 2009). Under our conditions, the *efr* mutants reproducibly showed increased susceptibility to virulent *Pst* DC3000. Of note, we used high doses of bacteria inoculum and kept the plants under high humidity during the infection procedure. Thus, differences in experimental conditions may explain the conflicting published data (Saijo et al. 2009, Nekrasov et al. 2009, Haeweker et al. 2010). Consistent with the observed deficiency in the elf18-induced events examined, *psl2* plants exhibit robust super- susceptibility when challenged with virulent *Pst*, to comparable levels to *efr* plants (Figure 2F). This supports functional requirements of PSL2 for MTI. Taken together, our genetic evidence identifies *PSL2* as a non-receptor component specifically required for EFR mediated immunity.

2.1.3 PSL2 is required for stable accumulation of functional EFR but not FLS2

As *psl2* plants showed vast defects in all tested responses to elf18, we examined possible alterations at the level of the receptor. We have generated specific antibodies against the C-terminal 109 amino acids of EFR and

Results

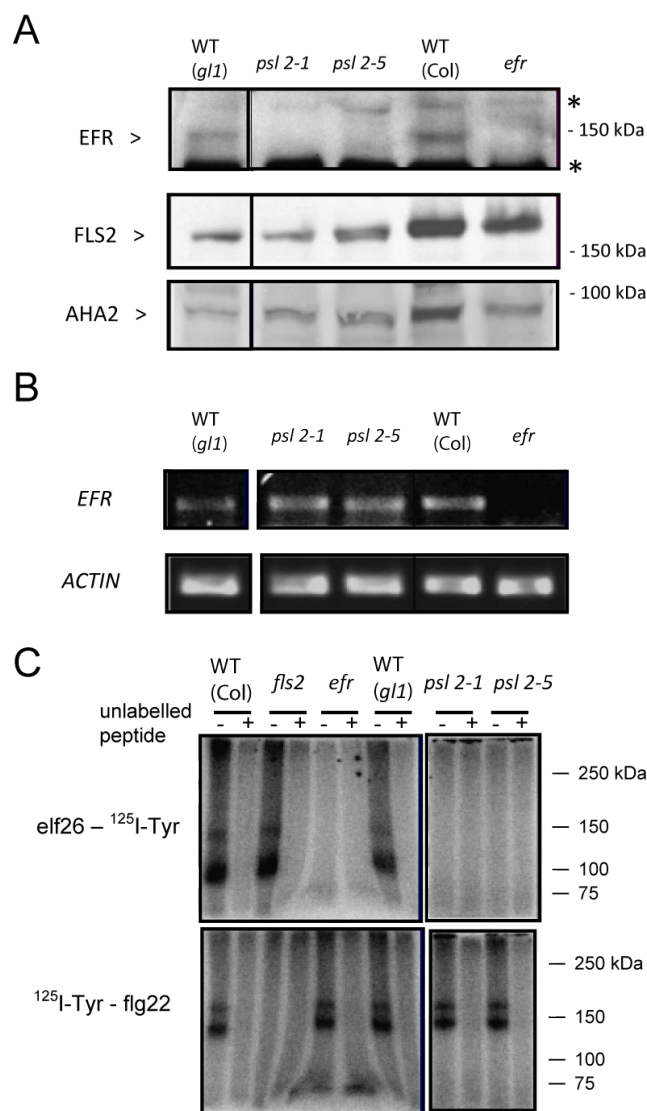


Figure 3. PSL2 is required for stable accumulation of functional EFR.

(A) Immunoblot analysis of the microsomal membrane fraction derived from 4-week-old non-elicited plants with the following antibodies: anti-EFR (top panel), anti-FLS2 (middle panel) and anti-H⁺ATPase2 (AHA2) (bottom panel). Asterisks indicate cross-reacting bands. Positions of molecular weight markers are shown on the right.

(B) Analysis of *EFR* expression by semi-quantitative RT-PCR for the samples used in (A)

(C) *In vitro* chemical cross-linking of extracts from 2-week-old seedlings with the radio-labelled *elf26* or *flg22* probes. Plant extracts were incubated in the absence (-) or presence (+) of 10 μM unlabelled competitor peptides *elf18* or *flg22*, respectively.

The immunoblot data in (A) was obtained by Dr. Yusuke Saijo, the expression data in (B) by Dr. Xunli Lu and ligand-binding data in (C) by Dr Silke Robatzek.

monitored the endogenous EFR protein by immunoblot analysis. An EFR-specific band was detected in the microsomal membrane fraction, derived from leaves of non-elicited WT plants (Figure 3A). Its apparent size is approximately 145 kDa which is larger than the predicted size of 113 kDa. Consistent with this finding, previous studies demonstrate specific binding of radiolabelled elf26 ligand (analogous to elf18) to an approx. 150 kDa protein in the cell-free extracts from *Arabidopsis* seedlings (Kunze et al. 2004). These data indicate extensive post-translational modifications of the EFR protein leading to the increase of the apparent molecular size. Our immunoblot data revealed that the steady-state levels of EFR are strongly reduced in *psl2* plants. However, EFR transcript levels are retained in *psl2* like the WT plants, indicating that the mutant is impaired at a post-transcriptional step in the receptor biogenesis (Figure 3B). Interestingly, FLS2 levels are retained to WT-like levels in *psl2* plants, further supporting a specific role of PSL2 for the EFR, but not FLS2 pathway (Figure 3A). Consistent with the observed decrease in EFR abundance, EFR-dependent elf26 binding, but not FLS2-dependent flg22 binding, is greatly diminished in the *psl2* mutants (Figure 3C). Together, we conclude that PSL2 is required for stable accumulation of functional EFR.

2.1.4 Identification of *PSL2* reveals an essential function of UGGT for stable accumulation of EFR

In order to identify the *PSL2* gene, *psl2-1* (in the Col-5 background carrying *gl1* mutation), was crossed to *Landsberg erecta* (Ler-0). The F1 progeny derived from this cross showed WT-like elf18 responsiveness, indicating a monogenic recessive nature of the *psl2-1* mutation. This was further confirmed by analyzing the F2 generation that segregated in a 3:1 ratio between WT-like and *psl2*-like individuals. Positional cloning indicated the genomic localization of *PSL2* in a 48 kb interval at the lower arm of chromosome 1 (Figure 4A). Sequence analysis

Results

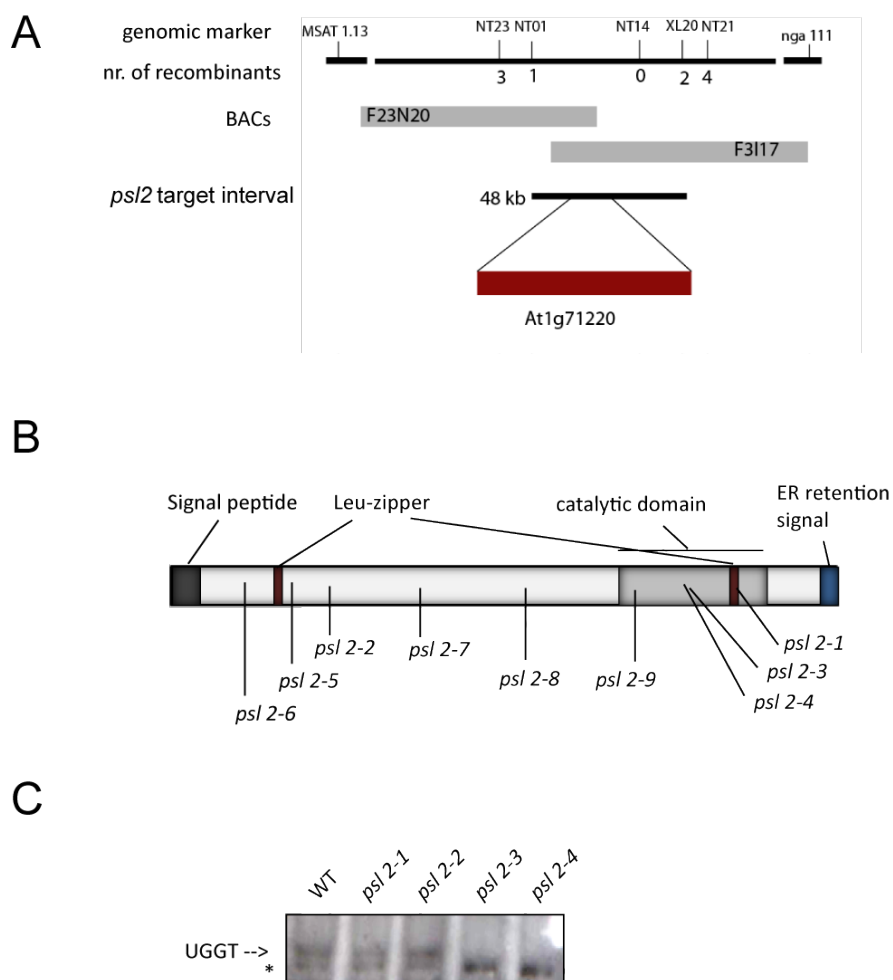


Figure 4. *PSL2* encodes for an Arabidopsis UGGT

(A) Genetic mapping of *PSL2*. *PSL2* was mapped to a 48 kb region at the bottom of chromosome 1 between markers NT01 and XL20. Molecular markers and numbers of recombination for each marker are shown above and below the line, respectively. The *PSL2* target interval is indicated. The position of At1g71220 that encodes for UGGT is indicated.

(B) Schematic representation of the structure of UGGT. UGGT is characterized by an N-terminal signal peptide, C-terminal ER retention signal, two Leu Zipper motifs and a catalytic domain. Positions of changes in aa in the isolated alleles for *psl2* mutants are shown at the bottom.

(C) Immunoblot analysis of total protein extracts from non-elicited 2-week-old seedlings with anti-UGGT antibodies. A cross-reacting band is indicated with an asterisk.

identified a single-nucleotide mutation within *At1g71220*, resulting in a predicted amino acid exchange from aspartic acid to asparagine. We confirmed that *PSL2* identifies *At1g71220* through recovery of multiple *psl2* alleles among previously uncharacterized *psl* mutants, that all show single-nucleotide mutations in *At1g71220* (Figure 4B).

At1g71220 encodes a protein of 1613 amino acids, with an N-terminal signal peptide that is required for the entry to the secretory pathway, and the C-terminal ER-retention signal, indicative of an ER luminal protein (Figure 4B). The protein shows sequence homology with UDP-glucose:glycoprotein glucosyltransferase (UGGT) from yeast,

Drosophila and several vertebrates. Like these UGGTs, the Arabidopsis UGGT consists from a large N-terminal domain that shows less sequence conservation and is thought to recognize folding defects of client proteins, and a highly conserved C-terminal domain carrying the catalytic site (Parodi et al. 2000).

In the Arabidopsis genome only one copy of the gene encoding UGGT is annotated. However, *psl2* plants show no obvious effects on plant growth and development under our growth conditions, consistent with the earlier described *uggt* alleles in Arabidopsis (Jin et al. 2007). This is in sharp contrast to the *uggt* knockout mice that are embryonically lethal, which hampers further in-depth studies in a whole organism context (Anelli and Sitia, 2008).

Table 1. Summary of putative *ps2* alleles

A list of isolated *psl* mutants that show an SNP in the *UGGT* gene is shown, including the predicted effects on the protein sequence.

allele name	predicted effects on UGGT
<i>psl2-1</i>	D1497N
<i>psl2-2</i>	E306K
<i>psl2-3</i>	R1409K W1443stop
<i>psl2-4</i>	W1443stop
<i>psl2-5</i>	truncated protein of ca 330aa
<i>psl2-6</i>	G199E
<i>psl2-7</i>	G531E
<i>psl2-8</i>	Q693stop
<i>psl2-9</i>	W1381stop

2.1.5 Interallelic complementation between *psl2* alleles

Our screen for elf18 hyposensitive plants identified nine *psl* mutants that show single-nucleotide mutations in the *UGGT* gene (Fig 4, Table 1). The *psl2-1* mutation occurs at an aspartic acid in the putative catalytic domain that is conserved in all known UGGT homologs. Both *psl2-3* and *psl2-4* mutations affect the C-terminal part as well. The *psl2-5* mutation resides in the 6th splice acceptor site and is predicted to induce a frame-shift, thereby producing a truncated protein of only 330 amino acids. The *psl2-2* mutation occurs in the N-terminal region, substituting a less conserved glutamic acid with lysine.

Next, UGGT steady-state accumulation was monitored in some of the *psl2* mutants by immunoblot analysis. Total protein extracts from non-elicited seedlings were probed with anti-UGGT antibodies raised against a recombinant

UGGT fragment (aa 325 to 882). Immunoblot data indicate that *psl2-1* and *psl2-2* accumulate UGGT at the WT-like levels, whereas full-length UGGT was not detected in *psl2-3* and *psl2-4* seedling extracts (Figure 4C). These data indicate that the single amino acid changes in *psl2-1* and *psl2-2* do not affect steady-state accumulation but another feature of UGGT function. It is interesting to note that previous work on mammalian UGGTs defined the aspartic acid altered in *psl2-1* as an essential residue for the enzymatic activity (Tessier et al. 2000). This suggests that PSL2-1 has a defect in its enzymatic activity.

Interestingly, a cross between *psl2-1* and *psl2-2* yielded F1 plants that show complementation of the *psl* phenotype, as typically seen in those between recessive mutations in distinct loci. However, an independent map-based cloning attempt located the *psl2-2* mutation to the same chromosomal region as *psl2-1*, and subsequent DNA sequencing analysis revealed a SNP in the PSL2 locus in the mutant (g1754a and g1756a). This indicates that it defines another *psl2* allele. Taken together, these data point to interallelic complementation between *psl2-1* and *psl2-2*. Importantly, the *psl2-1* and *psl2-2* mutations locate in the C-terminal and N-terminal domains, respectively, and allow WT-like accumulation of UGGT (Fig.4C).

Following this interesting finding, we extensively tested a series of the F1 progenies generated by crossing between different *psl2* alleles for their elf18 responsiveness (summarized in Table 2). F1 plants derived from at least two independent crosses were subjected to elf18-induced anthocyanin repression and ROS spiking assays. Interestingly, the F1 hybrids between *psl2-2* and *psl2-4* also restore elf18-responsiveness in both assays (Figure 5A and B). However, progenies from crosses between *psl2-1* and the putative null allele *psl2-5* retained the elf18-insensitive phenotype of the parental lines. Similarly, F1 seedlings derived from crosses of *psl2-1* with *psl2-3* showed elf18 insensitivity. The data indicate that *psl2* mutants in the C-terminal and N-terminal domain of

Results

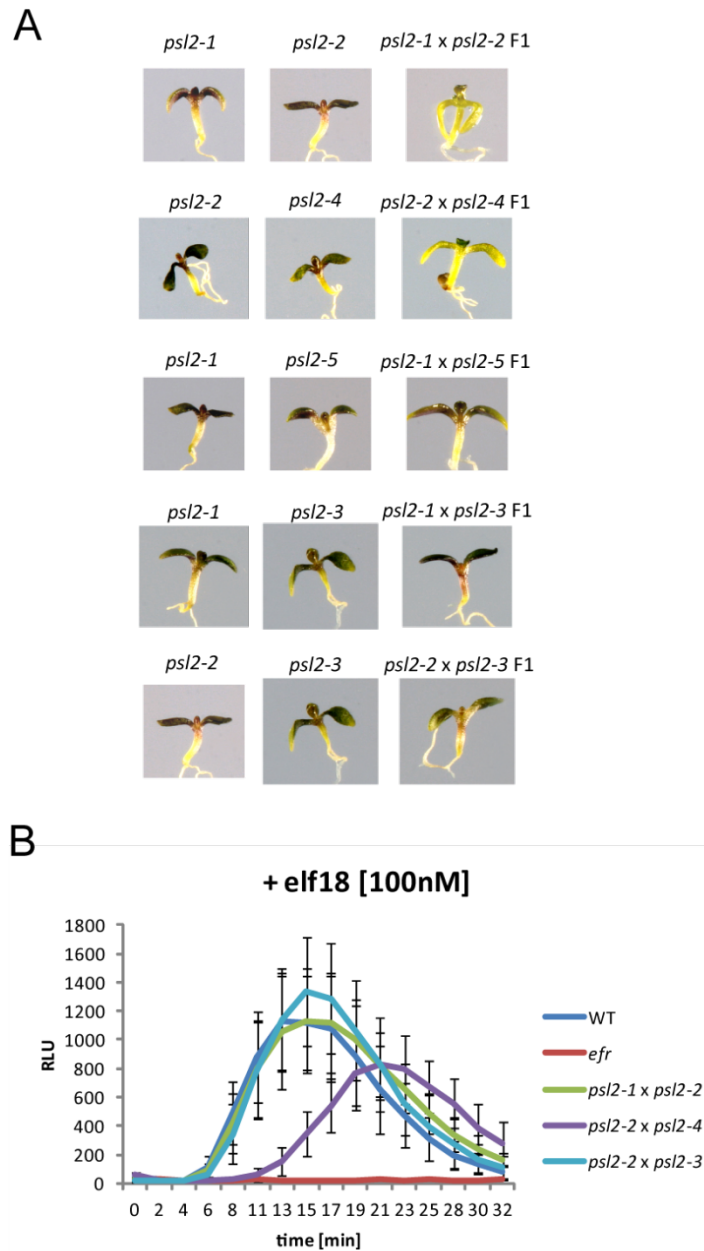


Figure 5. Inter-allelic complementation between *psl2* alleles

(A) *psl2* mutant alleles were crossed with each other in different combinations and seedlings of parents and progeny were grown in the presence 100 mM sucrose and 0,5 μ M elf18. Shown are representative seedlings for each genotype.

(B) ROS generation triggered with 100 nM in leaf discs of the depicted plants at 100 nM elf18.

UGGT could complement each other, whereas mutants carrying a putative null allele or those carrying a point substitution in the same domains are not able to show such inter-allelic complementation of the *psl2* phenotype. Interestingly, combining *psl2-2* and *psl2-3* alleles lead to complementation of a subset of elf18-triggered outputs. Their F1 plants restored WT-like ROS spiking in response to elf18, whereas they remain to be impaired in anthocyanin repression. Such uncoupling of early ROS spiking and late-phase anthocyanin suppression has been observed in the EFR pathway in several non-UGGT *psl* plants (Lu et al. 2009).

Table 2. Summary of *psl2* allelic crosses

(+) indicates WT-like response, (-) indicates *psl2*-like response.

F1 plants	anthocyanin suppression	ROS spiking
<i>psl2-1</i> x <i>psl2-2</i>	+	+
<i>psl2-2</i> x <i>psl2-4</i>	+	+
<i>psl2-2</i> x <i>psl2-3</i>	-	+
<i>psl2-1</i> x <i>psl2-5</i>	-	-
<i>psl2-1</i> x <i>psl2-3</i>	-	-
<i>psl2-1</i> x <i>psl2-6</i>	-	-
<i>psl2-3</i> x <i>psl2-6</i>	-	-
<i>psl2-4</i> x <i>psl2-6</i>	-	-

2.1.6 PSL1/CRT3 and PSL2/UGGT act in concert for EFR function

The *psl1* and *psl2* mutants were identified in our genetic screen for elf18 insensitive plants. Map-based cloning revealed that *PSL1* encodes one of the three calreticulins (CRTs) in Arabidopsis, designated CRT3 (Saijo et al. 2009). In yeast and animal cells it has been well documented that UGGT and CRT work in concert as part of the ERQC machinery (Anelli and Sitia 2008). In order to verify

functional interactions between UGGT and CRT3, we analyzed a series of *psl1* *psl2* double mutants. In contrast to *psl2* alleles that were fully insensitive to elf18 in all tested assays, weak *psl1* alleles were partially and differentially impaired in elf18-induced responses (Saijo et al. 2009). For example, *psl1-3* retains ROS spiking and MAPK activation to WT-like levels. However, this residual elf18 responsiveness is fully abolished in the *psl2-1 psl1-3* double mutants (not shown). Likewise, we could not detect increased de-repression of anthocyanin levels in the *psl1-4 psl2-1* double mutants that combine two severely dysfunctional alleles (Figure 6). These data support a model in which UGGT and CRT3 work in concert for EFR function, presumably through the generation of functional EFR.

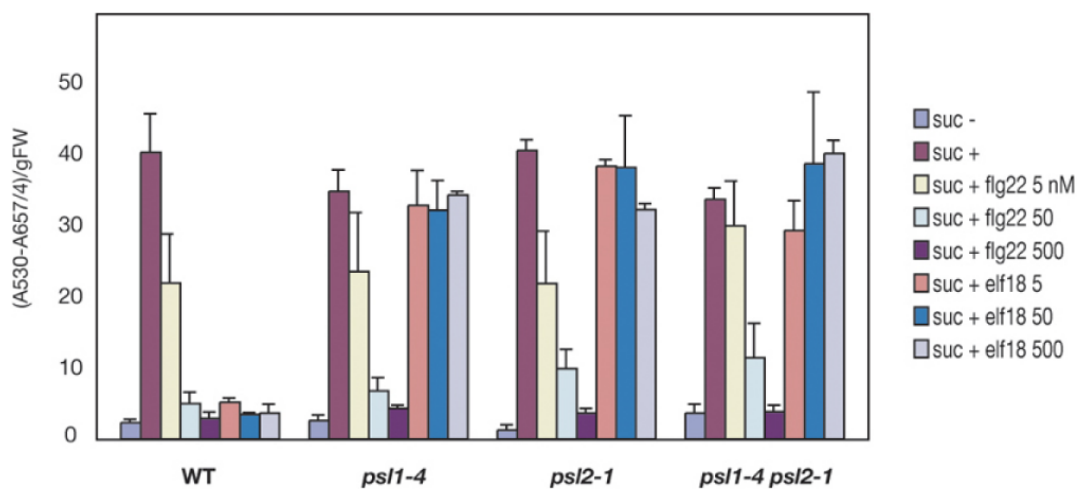


Figure 6. *psl1 psl2* double mutants show no additive effects in anthocyanin accumulation as compared to the parental lines.

Anthocyanin content of WT (Col), *psl1-4*, *psl2-1* and *psl1-4 psl2-1* seedlings, when grown in absence (-suc) or presence (+suc) of 100 mM sucrose and the indicated concentrations of flg22 or elf18.

2.2 *ps/25* plants show varied defects in EFR signaling outputs and carry a mutation in ER Glucosidase I

2.2.1 Identification of *ps/25* mutants in a forward-genetic screen for *Arabidopsis* elf18-insensitive mutants

We identified the *ps/25* mutant in the above described screens for MAMP-insensitive plants. *ps/25* seedlings show strongly de-repressed anthocyanin accumulation in the presence of elf18, whereas flg22-mediated anthocyanin suppression is only slightly affected (Figure 7 A and B).

We noticed that *ps/25* seedlings hyper-accumulate anthocyanins in response to exogenous sucrose (Figure 7B). This was not observed in *ps/2* and previously described *ps/* mutants (Saijo et al. 2009, Lu et al. 2009). Furthermore, *ps/25* seedlings showed several morphological alterations when compared to WT seedlings. Especially, the root growth of *ps/25* seedlings was strongly inhibited in the presence of high sucrose concentrations in the absence of MAMP application (Figure 7A). When grown on MS media containing lower concentrations of sucrose (25 mM), the difference between WT and *ps/25* roots were much less pronounced (data not shown). Root growth inhibition in *ps/25* plants was independent of MAMP treatment (Figure 7A). Importantly, the short root phenotype and elf18-insensitivity co-segregated in F2 progenies from a cross between *ps/25* and *Landsberg erecta* (*Ler*) plants, indicating that the same mutation is responsible for both phenotypes.

Results

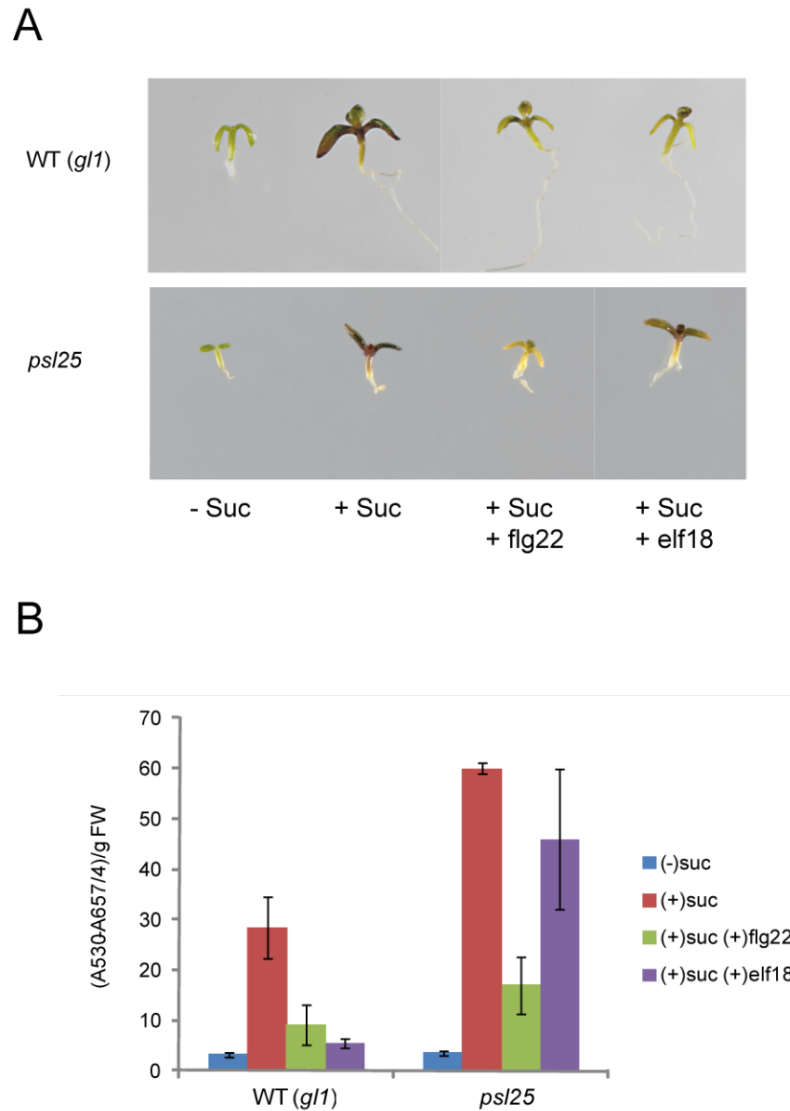


Figure 7. *psl25* seedlings show de-repressed anthocyanin accumulation in the presence of elf18.

(A) Arabidopsis WT (*gl1*) and *psl25* seedlings were grown in the absence (-Suc) or presence of 100 mM sucrose (+Suc) and 0,5 μ M flg22 or elf18.

(B) Anthocyanin content of seedlings treated as in (A).

2.2.2 *psl25* carries a mutation in Arabidopsis *GLUCOSIDASE I*

To identify the *PSL25* gene by map-based cloning, a mapping population was generated by crossing *psl25* (Col background) with Ler plants. The F2 progenies segregated in an approximate 3:1 ratio for the WT:*psl* phenotype, indicating the monogenetic recessive nature of the mutation. Low-resolution mapping was conducted using a previously described set of SSLP markers (Lukowicz et al. 2000). The *psl25* phenotype co-segregated with the Col-polymorphism of a SSLP marker on the lower arm of chromosome 1. Further analysis of the F2 plants showing a recombination event in this genomic region pointed to a 1500 kb interval as genomic location for *PSL25* (Figure 8A). This region contains a gene encoding the only predicted Arabidopsis homolog of eukaryotic ER-resident glucosidase I (*G I*). Since several previously characterized *psl*-mutants were identified as components of the ER-resident protein quality control machinery, we presumed that the *G I* gene would identify *PSL25*. Sequence analysis of the *G I* locus in *psl25* plants revealed a point-mutation resulting in an amino acid substitution (glycine to glutamic acid).

2.2.3 *PSL25* is required for generation of functional EFR

In order to analyze possible alterations at the level of the receptor, we tested EFR ligand binding activity in *psl25* and WT seedlings. Incubation of plant extracts with radiolabelled elf26 (equivalent to elf18) revealed strongly reduced ligand binding activity in *psl25* plants (Figure 9). These data indicate that EFR generation or folding is impaired in *psl25* plants.

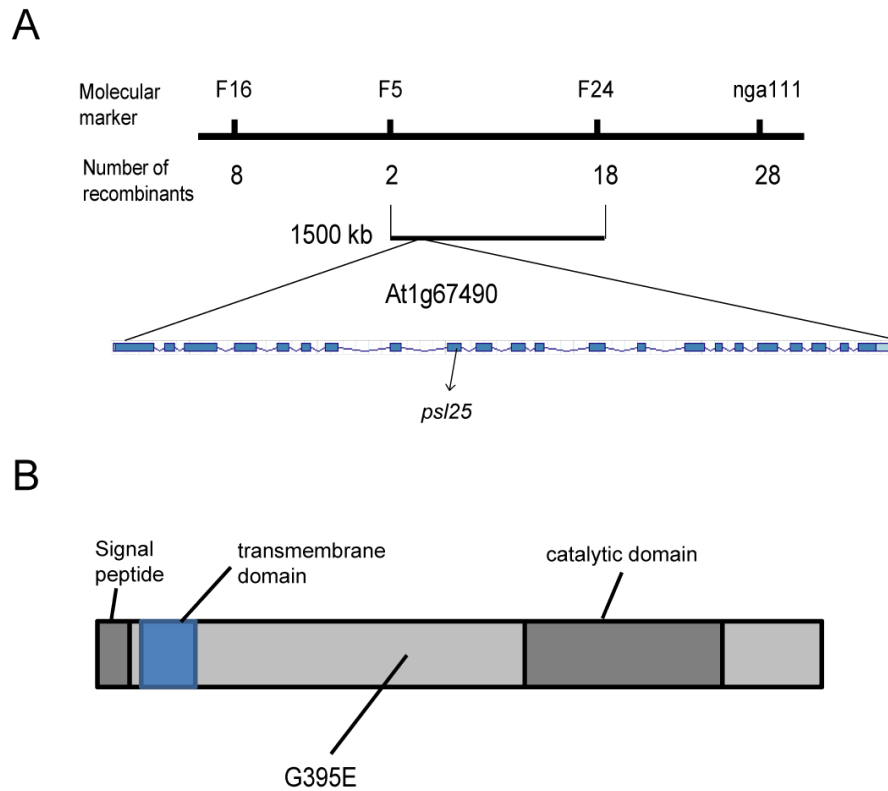


Figure 8. Genetic mapping of *PSL25*.

(A) *PSL25* was mapped to a 1500 kb region at the bottom of chromosome 1 between the markers F5 and F24. Molecular markers and numbers of recombination for each marker are shown above and below the line, respectively. The position of At1g67490 that encodes for GLUCOSIDASE I is indicated.

(B) Schematic representation of the structure of GLUCOSIDASE I, characterized by an N-terminal signal peptide, a single transmembrane domain and a predicted catalytic domain is shown. The position of changes in aa in *psl25* mutants is shown.

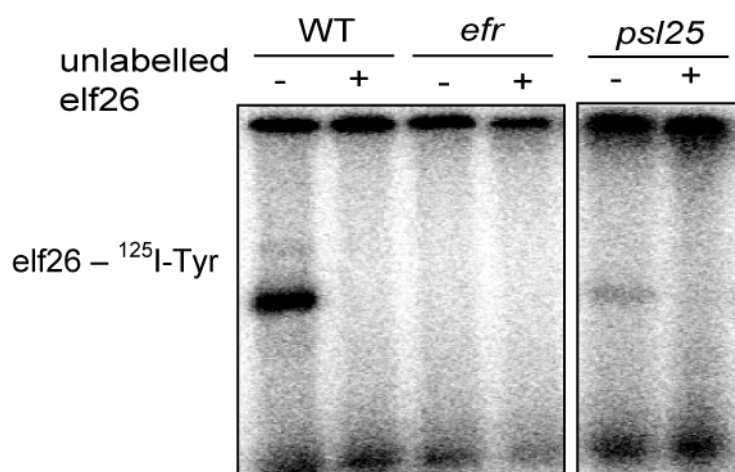


Figure 9. PSL25 is required for ligand-binding activity of EFR.

In vitro chemical cross-linking of extracts from 2-week-old seedlings with the radio-labeled elf26 probe in the absence (-) or presence (+) of 10 μ M unlabeled competitor peptide elf18.

2.2.4 EFR outputs are differentially impaired in *psl25* plants

Next, we tested characteristic MAMP signaling outputs in *psl25* plants. ROS spiking in response to elf18 was undetectable in *psl25* leaves, whereas flg22-triggered ROS spiking was not significantly impaired (Figure 10B). Interestingly, *psl25* seedlings showed nearly WT-like activation of MPK3 and 6 upon elf18 and flg22 perception (Figure 10A). Thus, MAPK activation can occur in the absence of ROS spiking in the EFR pathway. Conversely, nearly WT-like MAPK-activation is not sufficient to trigger ROS spiking in *psl25* plants. These results indicate that EFR triggers MAPK activation and ROS spiking through separate signaling pathways.

In order to verify the functional significance of the observed defects in EFR signaling outputs, we challenged *ps/25* plants with virulent *Pseudomonas syringae* DC3000. Consistently with previous data, *efr* plants showed higher susceptibility to this pathogen under our conditions in which we use a high dosage of the bacteria for spray inoculation and keep the plants under high humidity throughout the infection procedure. Interestingly, *ps/25* were also hyper-susceptible to *Pst* DC3000, to a slightly higher level than *efr* (Figure 10D). This implies that G I activity is required for an EFR-independent function of immune branch as well.

Results

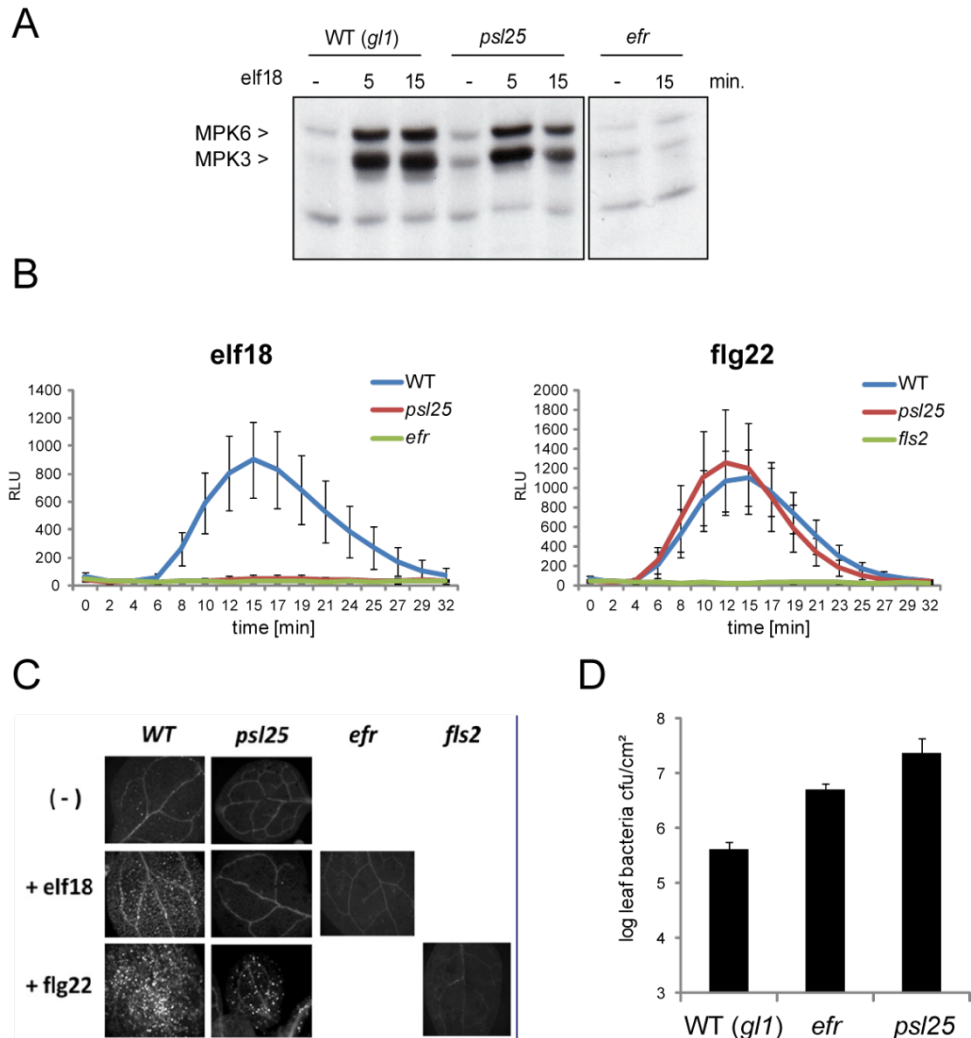


Figure 10. *psl25* plants are impaired in a subset of EFR-triggered responses.

(A) Immunoblot analysis of MAPK activation in WT (*gl1*), *psl25* and *efr* seedlings upon treatment with water (-) or 1 μ M elf18 for the indicated times. An anti-active MAPK antibody was used. Positions of molecular weight markers are indicated on the left.

(B) ROS generation in leaf discs of WT (*gl1*), *psl25*, *efr* and *fls2* plants triggered by 100 nM elf18 or flg22.

(C) Callose deposition in cotyledons of WT (*gl1*), *psl25*, *efr* and *fls2* seedlings triggered by water (-), 1 μ M elf18 or flg22.

(D) Pst DC3000 bacterial growth in leaves of 4-week-old WT (*gl1*), *efr* and *psl25* plants 3 days after spray inoculation with bacteria 10^9 cfu/ml.

2.3 Ethylene signaling regulates pre- and post-recognition steps in MAMP-triggered immunity

2.3.1 Isolation of an *Arabidopsis ps/36* mutant that is impaired in responses to elf18 and flg22

As described in chapter 1, our forward-genetic screen has led to the identification of a collection of *priority in sweet life (psl)* mutants that de-repress anthocyanin accumulation in the presence of elf18, retain WT-like responsiveness to flg22 (Saijo et al. 2009, Lu et al. 2009). We initially isolated *ps/36* mutants as an elf18 hyposensitive *psl* mutant. In the presence of low doses of elf18, *ps/36* seedlings show moderate de-repression of anthocyanin accumulation (Figure 11B and C). Interestingly, *ps/36* plants show more pronounced anthocyanin de-repression in the presence of flg22 (Figure 11B). However, when treated with as high as 1 μ M of flg22, *ps/36* seedlings show a detectable reduction of anthocyanin content, indicating residual flg22 responsiveness retained in the mutant (Figure 11D). Of the *psl* mutants identified to date, the *ps/36* allele is unique for the hyposensitivity to both flg22 and elf18.

2.3.2 Both FLS2- and EFR-triggered outputs are altered in *ps/36* plants

We next tested whether *ps/36* plants are altered in different FLS2- and EFR-triggered signalling outputs. ROS spiking in response to flg22 and elf18 is reduced, albeit detectable in *ps/36* plants (Figure 12A). In contrast, *ps/36* plants retain WT-like activation of the MAP-kinases MPK3 and MPK6 in response to

Results

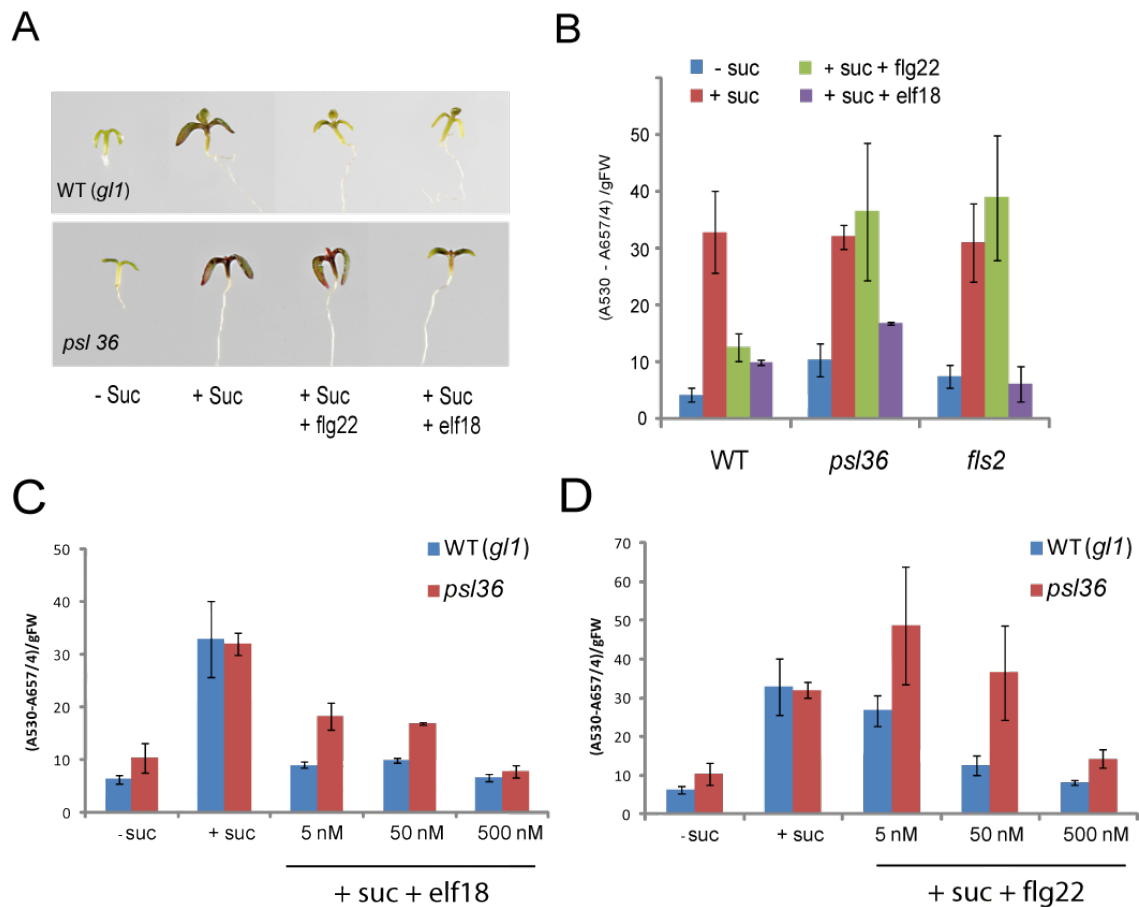


Figure 11. *psl36* seedlings are impaired in flg22- and elf18-triggered anthocyanin suppression.

- (A)** WT (*gl1*) or *psl36* seedlings grown in the absence (-Suc) or presence of 100 mM sucrose (+Suc) without or with 50 nM flg22 (+flg22) or 50 nM elf18 (+elf18).
- (B)** Anthocyanin content of WT (*gl1*), *psl36* and *fls2* seedlings grown as described in (A) for 2d.
- (C)** Anthocyanin content of WT (*gl1*) and *psl36* seedlings grown in the absence (-Suc) or presence of 100 mM sucrose (+Suc) without or with the indicated concentrations of elf18 (+Suc +elf18).
- (D)** Anthocyanin content of WT (*gl1*) and *psl36* seedlings grown in the absence (-Suc) or presence of 100 mM sucrose (+Suc) without or with the indicated concentrations of elf18 (+Suc +elf18).

flg22 and elf18 (Figure 12B). Furthermore, both flg22- and elf18-triggered callose deposition is reduced in *psl36* seedlings (Figure 12C). Together, *psl36* plants are impaired in early ROS spiking and late callose deposition upon both flg22 and elf18 application, despite WT-like MAPK-activation. This suggests that a role of PSL36 is prominent for the former two outputs as well as anthocyanin repression, but is dispensable for MAPK activation in both PRR pathways. Our data also point to a separation of signalling pathways emanating from FLS2 to these outputs, in good accordance with our earlier described uncoupling in the EFR pathway (Saijo et al. 2009, Lu et al. 2009).

To test possible effects of the observed alterations in MAMP-signalling on plant immunity, we challenged *psl36* plants with the virulent bacterium *Pseudomonas syringae* pv *tomato* (*Pst*) DC3000 in a spray inoculation assay. Consistent with the above defects in PRR-triggered immune responses, *psl36* plants allow enhanced growth of the bacteria (Figure 12D).

2.3.4 Ethylene perception and signalling is required for MAMP-triggered suppression of anthocyanin accumulation

We identified the *PSL36* gene by map-based cloning. Our mapping positioned the *PSL36* locus within 1.2 Mb in the upper arm of chromosome 5 (Figure 13A). Among the loci in this chromosomal region, we focused on *EIN2* that encodes a major regulator of responses to the phytohormone ethylene (ET), since a role of ET has been described for FLS2 function (Boutrot et al. 2010, Mersmann et al. 2010). Indeed, our sequencing analysis of the *EIN2* locus found a point substitution (g3915a; Figure 13A) in the *EIN2* ORF sequence in the *psl36* mutant. This mutation causes a precocious stop-codon, thereby presumably resulting in a truncation of the EIN2 protein (Figure 13B).

Results

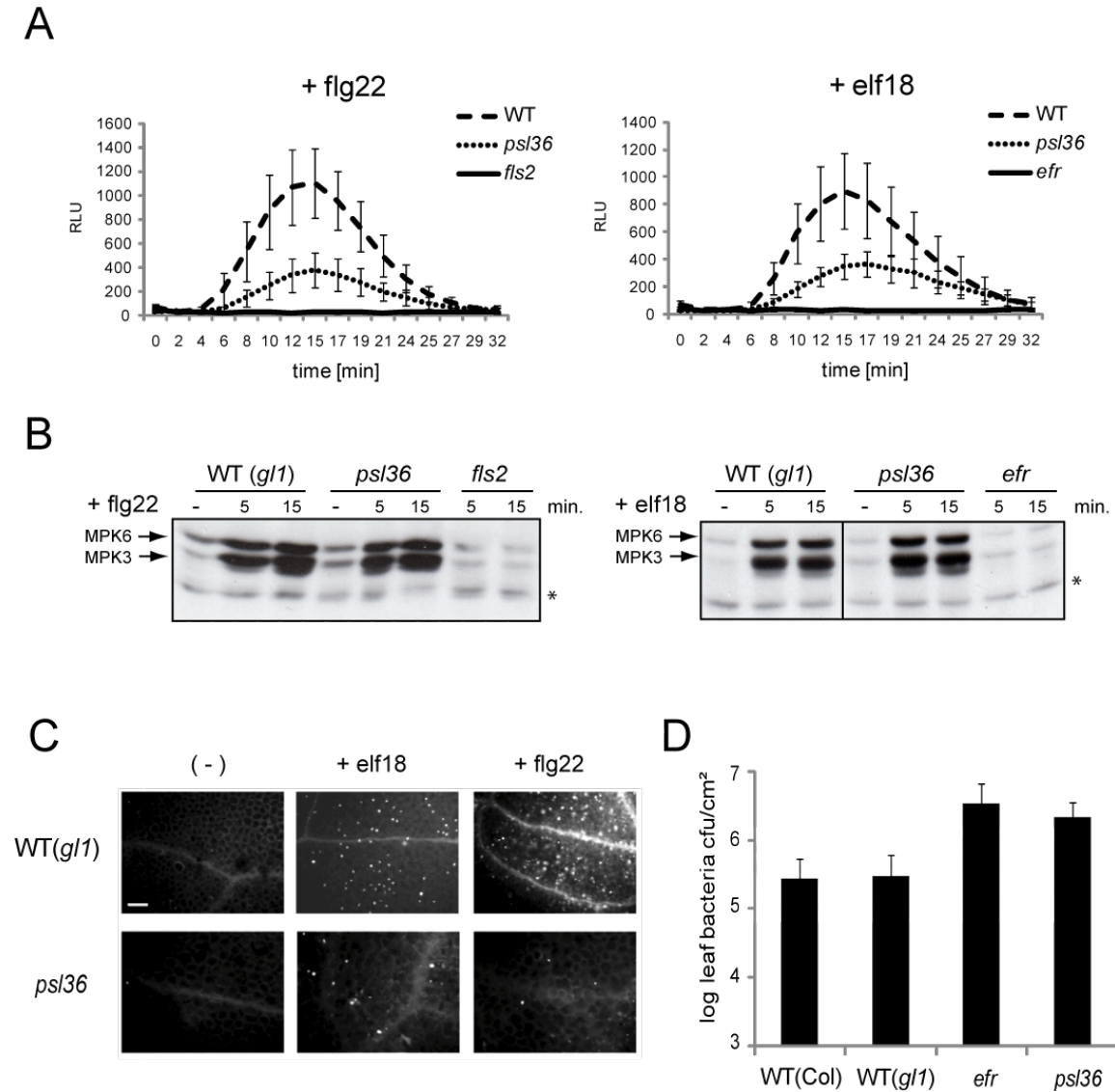


Figure 12. *psl 36* plants show altered responses to both *flg22* and *elf18* and allow enhanced growth of virulent *Pseudomonas syringae* pv *tomato* DC3000.

(A) ROS spiking triggered in leaf disks of WT (*gl1*), *psl36*, *efr* and *fls2* plants treated with 100 nM *flg22* or 100 nM *elf18*.

(B) Immunoblot analysis of MAPK activation in WT (*gl1*), *psl36*, *fls2* and *efr* seedlings upon application of water (-), 1 μ M *flg22* or *elf18* for the indicated times. An anti-active MAPK antibody was used. Positions of MPK6 and MPK3 are indicated. A cross-reacting band is indicated with an asterisk and serves as loading control.

(C) Callose deposition in WT (*gl1*) and *psl36* seedlings treated with water (-), 1 μ M *flg22* or 1 μ M *elf18* for 16h.

(D) *Pst* DC3000 bacterial growth in leaves of 4-week-old WT (Col and *gl1*), *efr* and *psl36* plants 4 days after spray inoculation with bacteria at 10^9 cfu/ml.

We then verified co-segregation of the mutation in the *EIN2* gene with the defect in flg22-triggered anthocyanin suppression in the F2 population derived from crossing between *psl36* and Col-0 plants (Table 3). These results indicate that *PSL36* identifies *EIN2*.

In the presence of 1-aminocyclopropane-1-carboxylate (ACC), a precursor of ethylene, WT seedlings show a characteristic ET-induced morphological response, called the triple response (Alonso et al. 1999). We found that *psl36* seedlings are insensitive to ACC application as well as *ein2-1* plants (Figure 13C). This verifies that the mutation identified in the *EIN2* locus of *psl36* plants defines a loss-of-function allele of *EIN2*.

We verified that *ein2-1*, carrying a stop codon at aa 590 in the EIN2 protein, also shows the aforementioned *psl36*-like anthocyanin de-repression phenotype (Fig 14A). We thus conclude that *PSL36* identifies *EIN2*.

Next, to assess a role of ET in the EFR and FLS2 pathways, we assayed earlier described ET perception and signalling mutants for elf18- and flg22-triggered anthocyanin-repression. We found that *etr1-1*, a dominant-negative ET-receptor mutant allele shows de-repressed anthocyanin accumulation in the presence of flg22 (Figure 13D). In contrast, *ein3* mutants that affect an important TF in ET-signalling show no clear discernable effects in this flg22 output, probably due to functional redundancy with EIN3-LIKE (EIL) proteins, as reported for many ET-responses (Chao et al. 1997). Together, these data define ET-signalling as an essential component for flg22-triggered suppression of sucrose-induced anthocyanin accumulation, consistent with earlier studies describing a role of ET in the FLS2 pathway (Clay et al. 2009, Boutrot et al. 2010, Mersmann et al. 2010).

Results

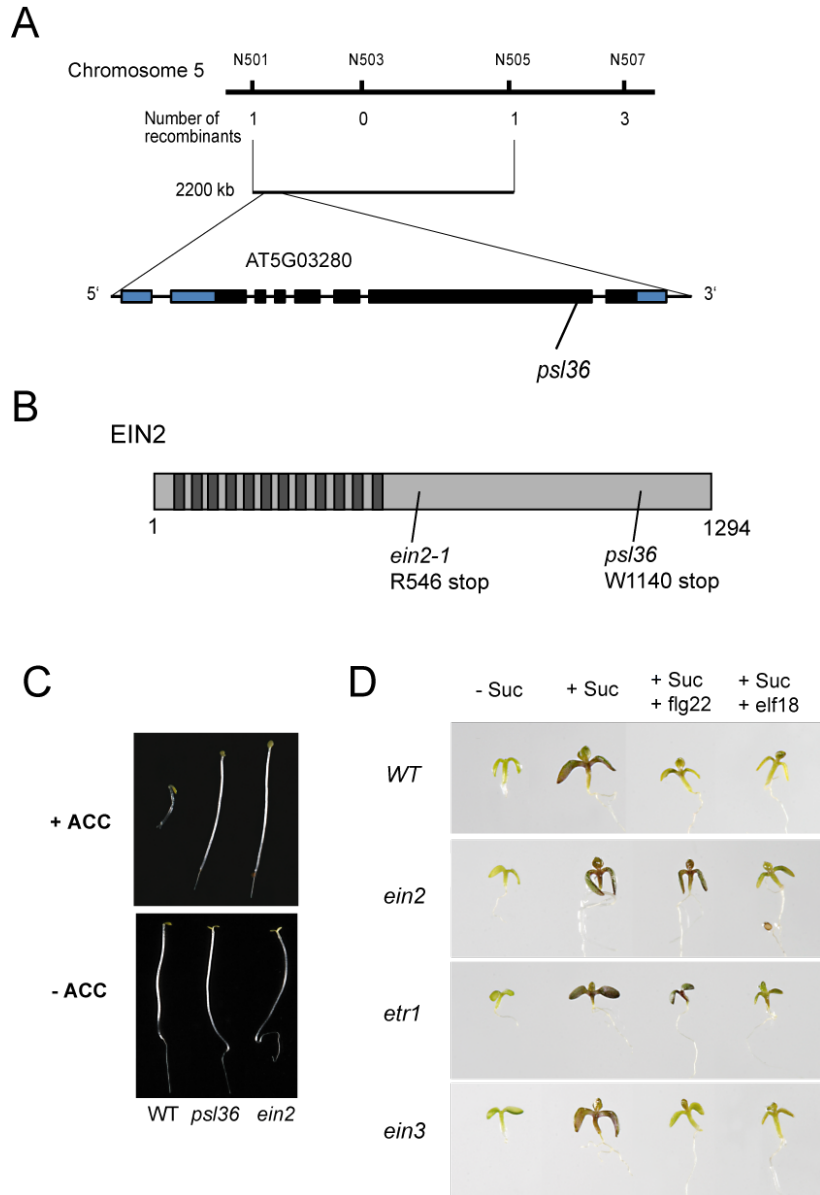


Figure 13. Identification of *PSL36* as a novel *EIN2* allele.

(A) Genetic mapping of *PSL36*. The *PSL36* locus was mapped between markers N501 and N505 at the top of chromosome 5. Sequence analysis revealed a point mutation (g3915a) in the 6th exon of the *EIN2* gene.

(B) Schematic description of the structure of the EIN2 protein (1294 aa residues). The predicted 12 transmembrane helices are indicated by dark boxes. Positions of changes in aa in the *ein2-1* and *psl36* alleles are shown at the bottom.

(C) Etiolated WT, *psl36* and *ein2-1* seedlings grown in the presence or absence of 10 μ M ACC (1-aminocyclopropane-1- carboxylate) for 4 days.

(D) WT (Col), *ein2-1*, *etr1-1* and *ein3-1* seedlings grown in the absence (-) or presence (+) of 100 mM sucrose and 0,5 μ M flg22 or elf18.

Table 3. Co-segregation test of the *psl* phenotype and the corresponding mutant genotype in F2 plants of the *psl36* x Col cross

Cross	Phenotype	No. of plants tested	Genotype		
			+/+	+/-	-/-
<i>psl36</i> x Col-0	<i>psl</i>	30	0	0	30
	WT	32	18	14	0

2.3.5 EIN2 is required for FLS2 transcript accumulation

The observed alterations in flg22 responses prompted us to examine potential changes in FLS2 protein levels in *ein2* plants. Immunoblot analysis of total protein extracts derived from non-elicited *psl36* and *ein2-1* plants revealed a great decrease in FLS2 accumulation (Figure 14A). In accordance with reduced FLS2 levels, also *FLS2* transcripts accumulated to much lesser degree in *ein2* seedlings (Figure 14B). These results are in good agreement with earlier findings of a role of ethylene signalling for *FLS2* expression (Boutrot et al. 2010, Mersmann et al. 2010).

2.3.6 EFR signalling is impaired in *ein2* alleles despite WT-like EFR accumulation

Besides altered flg22-responsiveness, we observed pronounced defects in EFR outputs in *ein2-1* and *psl36* plants (Figure 11, 12 and 18). Thus, we examined if ET signalling is also required for EFR transcript/protein accumulation as described for FLS2. Interestingly, both EFR transcript and protein levels are not significantly altered in *ein2-1* and *psl36* plants (Figure 15A and B). These data

point to a role of ET in post-recognition signalling by EFR. Consistent with the differential regulation of the two PRR genes by ET, the *FLS2* promoter is predicted to contain 9 potential EIN3/EIL1 binding sites, and indeed has been shown to be bound by EIN3 (Boutrot et al. 2010). On the other hand, only two such motifs are present in the EFR promoter. This might explain the differential contribution of ET for transcriptional control of the two PRR genes.

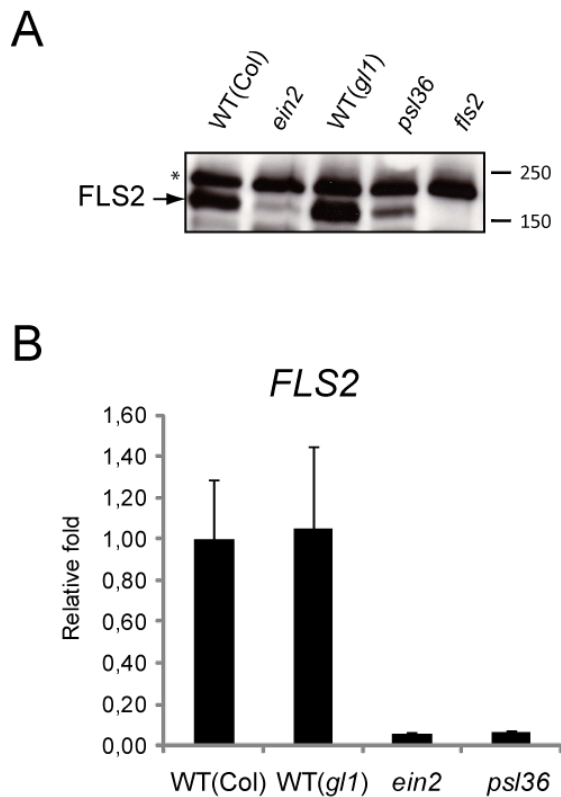


Figure 14. *FLS2* protein and transcript levels are strongly reduced in *ein2* plants.

(A) Immunoblot analysis of total protein extracts from 2-week-old non-elicited WT (Col-0, *gl1*), *ein2-1*, *psl36* and *fls2* seedlings with anti-*FLS2* antibodies. Non-specific bands (*) were used as loading controls. Positions of molecular weight markers are indicated on the right. Immunoblot data were obtained in collaboration with Dr. Kazue Kanehara.

(B) Quantitative real-time PCR analysis for *FLS2* expression in 12-days-old non-elicited WT (Col-0, *gl1*), *ein2-1* and *psl36* seedlings. *ACTIN2* gene was used for normalization.

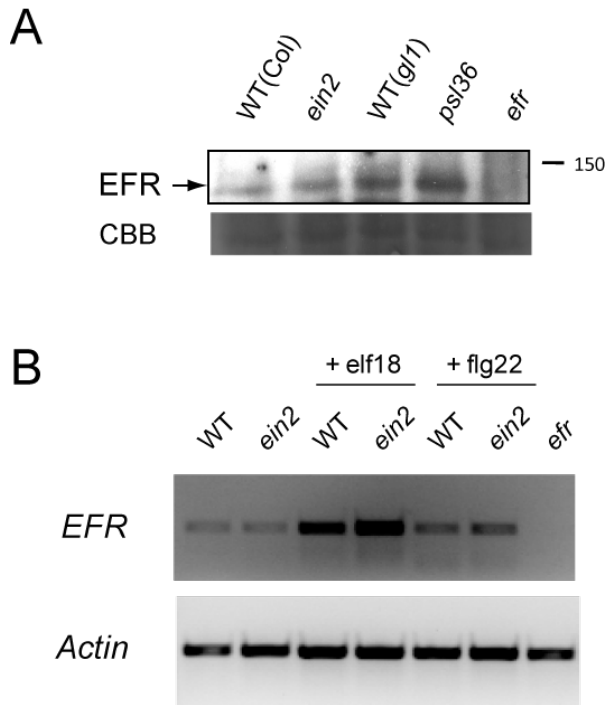


Figure 15. *EFR* protein and transcript levels are WT-like in *ein2* plants.

(A) Immunoblot analysis of total protein extracts from 2-week-old non-elicited WT (Col-0, *gl1*), *ein2-1*, *psl36* and *efr* plants with anti-*EFR* antibodies. A Coomassie blue-stained blot is presented as loading control. Positions of molecular weight markers are indicated on the right. Immunoblot data were obtained in collaboration with Dr. Kazue Kanehara.

(B) Semi-quantitative RT-PCR analysis for *EFR* expression in 12-days-old WT (Col-0), *ein2-1* and *efr* seedlings, treated with water, 1 μ M elf18 or 1 μ M flg22 for 24 hours. The *ACTIN2* gene was used as control for equal loading.

2.3.7 Genetic requirements for MAMP-triggered anthocyanin suppression

Our finding that *ein2* seedlings de-repress anthocyanin accumulation in the presence of flg22 and elf18 prompted us to test the involvement of other defense components in this MAMP response. Single mutants interfering with the JA (*coi1* and *jar1*) and SA (*sid2*, *eds5*, *pad4*, *npr1*, *NahG*) pathways, as well as two weak mutants of the ET-pathway did not show clear discernable effects on flg22- or elf18 mediated suppression of anthocyanin accumulation (Figure 16A). We obtain the same result with the *eds1* and *ndr1* seedlings. *Rar1 sgt1* double mutants show slightly enhanced anthocyanin levels in the presence of both MAMPs.

The *dde2 ein2 pad4 sid2* quadruple mutants are defective in JA, ET, SA and PAD4 signalling sectors (Tsuda et al. 2009). We monitored anthocyanin levels in the quadruple and the depicted triple mutant combinations in the presence of flg22 or elf18. The quadruple mutant and all triple mutants carrying the *ein2* mutation were defective in flg22-induced anthocyanin suppression, whereas EIN2 is sufficient to restore WT-like flg22-responsiveness in the *dde2 pad4 sid2* triple mutants in this assay (Figure 16B). At the concentrations of as high as 1 μ M elf18, the quadruple and all triple mutants show WT-like anthocyanin suppression, demonstrating that a high dose of elf18 overcomes the aforementioned EIN2 requirement for EFR (Figure 16B). Thus we conclude that of the four components tested EIN2 predominantly contributes to FLS2-triggered anthocyanin suppression, but that all the four components tested are dispensable for EFR-triggered anthocyanin suppression in the presence of high doses of the ligand. This points to the existence of a fifth element that compensates the loss of the above four branches in the EFR pathway, of which the engagement requires high doses of elf18.

Results

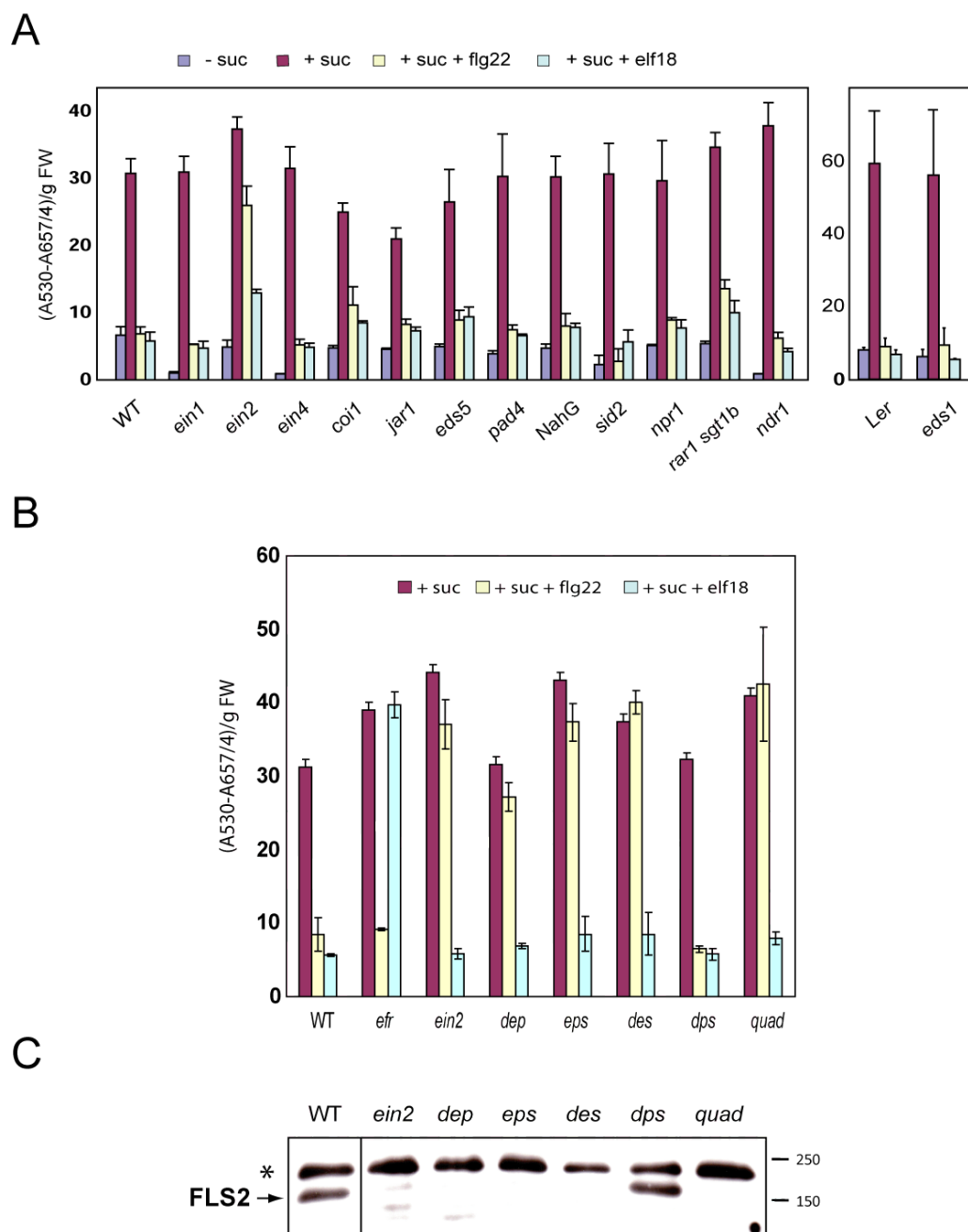


Figure 16. Genetic requirements for MAMP-triggered suppression of anthocyanin accumulation.

(A) Anthocyanin content of WT (Col), *ein1*, *ein2*, *ein4*, *coi1*, *jar1*, *eds5*, *pad4*, *NahG*, *sid2*, *rar1 sgt1b*, *ndr1*, WT (Ler) and *eds1* seedlings grown in absence (-suc) or presence (+suc) of 100 mM sucrose and 0,5 μ M flg22 or 0,5 μ M elf18.

(B) Anthocyanin content of the following seedlings: Wt (Col), *efr*, *ein2*, *dep* = *dde2 ein2 pad4*, *eps* = *ein2 pad4 sid2*, *des* = *dde2 ein2 sid2*, *dps* = *dde2 pad4 sid2*, *quad* = *dde2 ein2 pad4 sid2* grown in the presence of 100 mM sucrose (+suc) and 1 μ M flg22 (+suc +flg22) or 1 μ M elf18 (+suc +elf18). These data were obtained by Dr. Kazue Kanehara.

(C) Immunoblot analysis of total protein extracts from 2-week-old non-elicited seedlings with anti-FLS2 antibodies. A non-specific band (*) is shown as loading control. Positions of molecular weight markers are indicated on the right. These data were obtained by Dr. Kazue Kanehara.

Previous work revealed ET-mediated regulation of *FLS2* expression and corroborated a close link between reduced *FLS2* levels and reduced flg22 responsiveness in ET-signalling mutants. Thus, we determined *FLS2* steady-state protein levels in non-elicited seedlings by immunoblot analysis. Consistent with the flg22 insensitive phenotype, *FLS2* levels were strongly reduced in all lines carrying the *ein2* mutation, but WT-like in the *dde2 pad4 sid2* triple mutants (Figure 16C). Thus, ET predominantly serves to maintain *FLS2* levels independently of SA, JA and PAD4 functions, consistent with the earlier described role of EIN3 in transcriptional regulation of the *FLS2* gene via direct binding to the *FLS2* promoter (Boutrot et al. 2010). Furthermore, these data suggest that a reduction in *FLS2* steady-state levels causes anthocyanin de-repression in *ein2* mutants, as suspected in earlier studies (Boutrot et al. 2010).

In order to test this idea, we generated *ein2* plants that express an *FLS2*-fusion protein with C-terminal tag under the control of the constitutively active CaMV 35S-promoter, which would be active in an EIN2 independent manner. It was previously shown that C-terminal GFP fusions to *FLS2* retain functionality (Robatzek et al. 2006). Interestingly, all 12 independent transgenic lines tested allowed flg22-mediated anthocyanin repression, thereby demonstrating that the CaMV 35S promoter-driven *FLS2* expression overcomes the aforementioned requirement for an intact ET-signalling for *FLS2* expression (Figure 17, shown are representative seedlings from two independent transgenic lines). This

strongly suggests that a major contribution of ET to FLS2-triggered anthocyanin suppression occurs at the level of *FLS2* transcription.

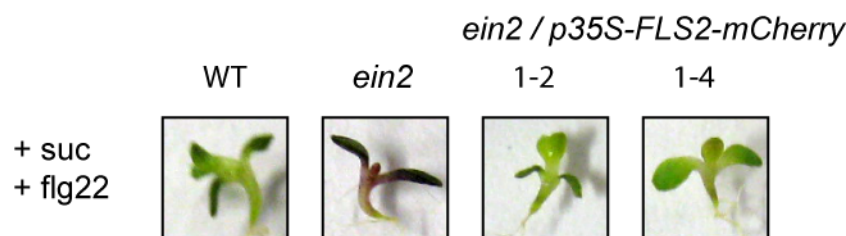


Figure 17. Constitutive expression of *FLS2* restores flg22-responsiveness in *ein2* plants.

Representative images from WT, *ein2-1* and two *ein2-1* seedlings carrying the *35S::FLS2-mCHERRY* transgene are shown. Seedlings were grown in the presence of 100 mM sucrose and 0,5 μ M flg22. The two shown *ein2-1/35S::FLS2-mCHERRY* transgenic seedlings are derived from two independent transformation event. Analysis of twelve independent transgenic lines led to the same conclusion. The experiment was repeated twice.

2.3.8 Flg22- and elf18-induced transcriptional reprogramming of defense-related genes is diminished in *ein2* plants

MAMP perception triggers massive transcriptome reprogramming that is thought to contribute to the host plant immunity against potentially infectious microbes. Our earlier studies point to the importance of sustained rather than initial or transient transcriptional reprogramming as a critical step for robust MTI activation (Lu et al. 2009). Thus, we tested if *ein2* plants show alterations in defense gene expression in response to these MAMPs. *ERF1* is an early ET responsive gene encoding an AP2-domain containing transcription factor that regulates many ET-responses (Solano et al. 1998). MYB51 is a transcription factor that has been shown to regulate many glucosinolate biosynthesis-related genes (Gigolashvili et al. 2007). Both genes are rapidly upregulated by elf18

Results

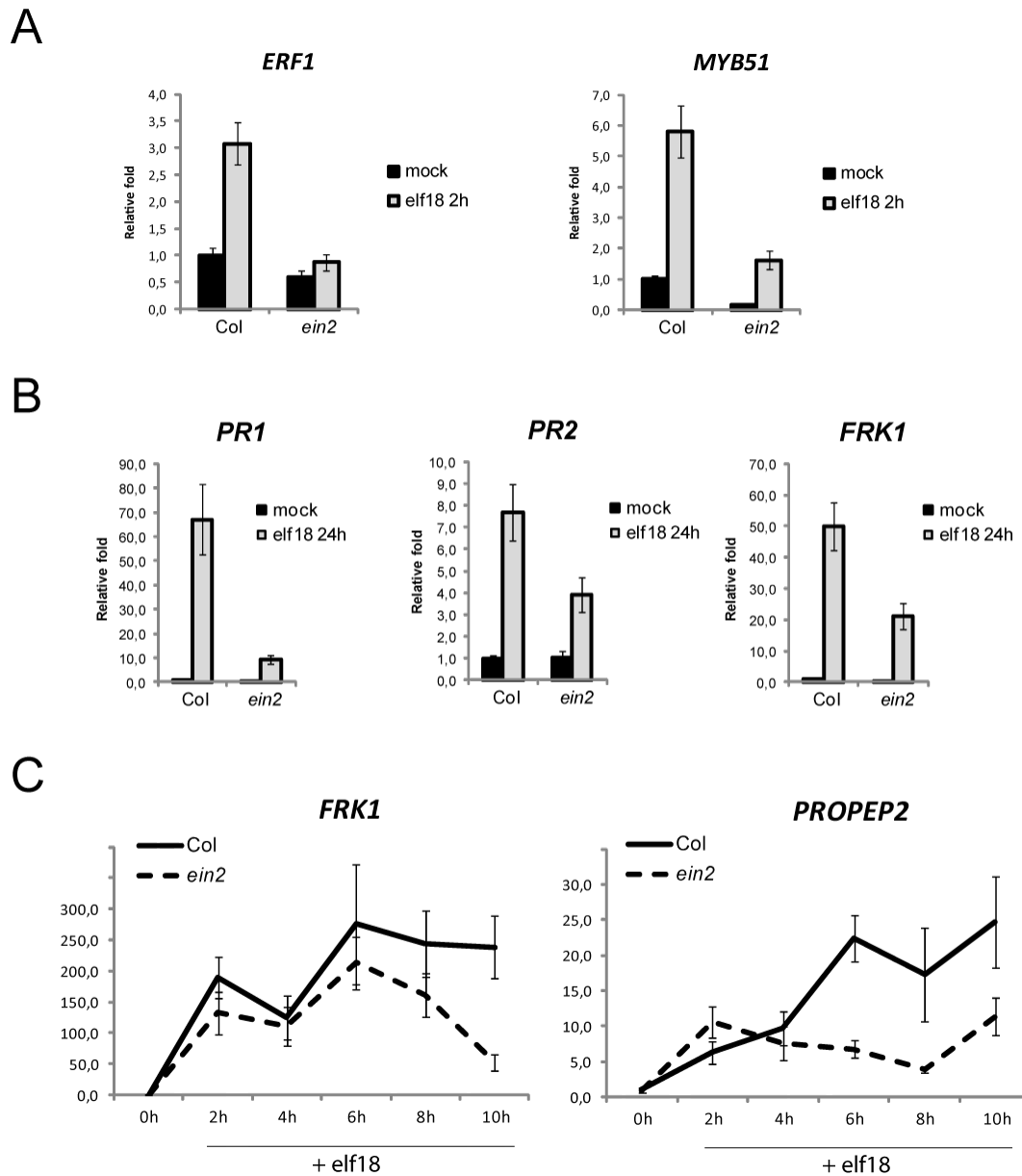


Figure 18. Elf18-induced activation of defense-related genes is diminished in *ein2* seedlings.

(A) *ERF1* and *MYB51* expression in 2-week-old Col and *ein2* seedlings upon treatment with water (mock) or 1 μ M elf18 for 2h. Gene expression was measured by quantitative RT-PCR (qPCR) analysis, normalized to At4g26410 (reference gene) expression and plotted relative to mock-treated Col expression level. A representative data set with mean \pm SD of three experimental replicates is shown. We obtained a similar conclusion in two independent experiments.

(B) *PR1*, *PR2* and *FRK1* expression in 2-week-old Col and *ein2* seedlings upon treatment with water (mock) or 1 μ M elf18 for 24h. Transcript level was measured by qPCR and analyzed as in (A). The experiment was repeated at least three times, with similar results.

(C) Expression of *FRK1* and *PROPEP2* over time in 2-week-old Col and *ein2* seedlings upon treatment with 1 μ M elf18. Gene expression was measured by qPCR and analyzed as in (A). The expression levels are plotted relative to Col at 0h. The experiment was repeated twice, with similar results.

treatment in WT plants. However, *ein2* seedlings are strongly impaired in this elf18-response (Figure 18A). This indicates the requirement of EIN2 and likely an intact ET-signaling for elf18-triggered induction of these genes.

As mentioned above, our recent findings suggest that sustained activation of defense-related genes represents a critical step for effective MTI (Lu et al. 2009). We measured transcript accumulation of three well characterized defense-marker genes, *PR1*, *PR2* and *FRK1*, at 24 hours after MAMP treatment. Remarkably, *ein2* plants showed significantly reduced *PR1*, *PR2* and *FRK1* transcript levels as compared to WT (Figure 18B). In order to test possible involvement of EIN2 in early and late-phase activation of defense genes, we traced their activation kinetics over time upon MAMP application. *PROPEP2* encodes a putative precursor for an endogenous elicitor that is activated upon MAMP-treatment. WT and *ein2* plants were similar in elf18-induced activation of *PROPEP2* and *FRK1* at the early time points tested. However, sustained activation of these genes was impaired in *ein2* plants (Figure 18C). These data indicate a role for EIN2 (and thus ET signalling) in initial and sustained activation of the tested defense-related genes.

Results

Next we compared between elf18- and flg22-triggered defense gene inductions in WT and *ein2* plants. Of note, the effects of *ein2* mutation on sustained activation of *PR1*, *FRK1* and *PROPEP2* are similar between the FLS2 and EFR pathways, despite their marked differences in the ET dependence for the expression and accumulation of the cognate receptors (Figure 19).

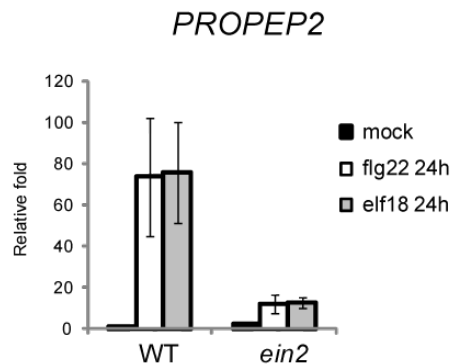
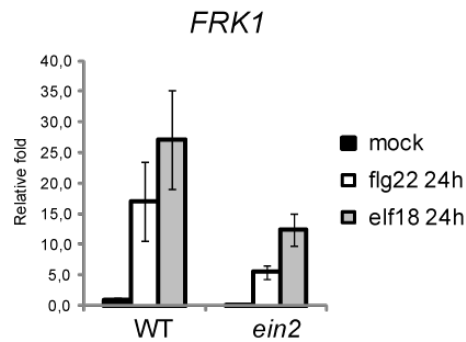
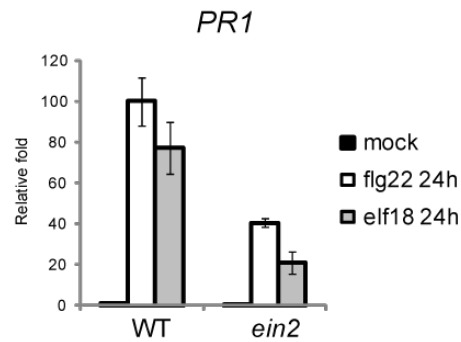


Figure 19. *ein2* plants show similar defects in flg22- and elf18-induced activation of defense genes.

Expression of PR1, FRK1 and PROPEP2 in 2-week-old Col and *ein2* seedlings upon treatment with water (mock), 1 μ M flg22 or elf18 for 24h. Gene expression was measured by qPCR and analyzed as described for Fig. 18 (A). The experiment was repeated at least three times, with similar conclusion.

Importantly, the *ein3 eil1* double-mutant that lacks two master regulators of ET responsive genes, show diminished defense gene activation in response to elf18, demonstrating that not only EIN2 but also other components of ET signalling are required for transcriptional reprogramming during MTI activation (Figure 20).

We verified that the *fls2* and *efr* mutants were fully insensitive to flg22 and elf18, respectively, for *PROPEP2* expression. Furthermore, *psl36* showed hyposensitivity to flg22 and elf18 as well as *ein2-1*, at least in *PROPEP2* activation (not shown).

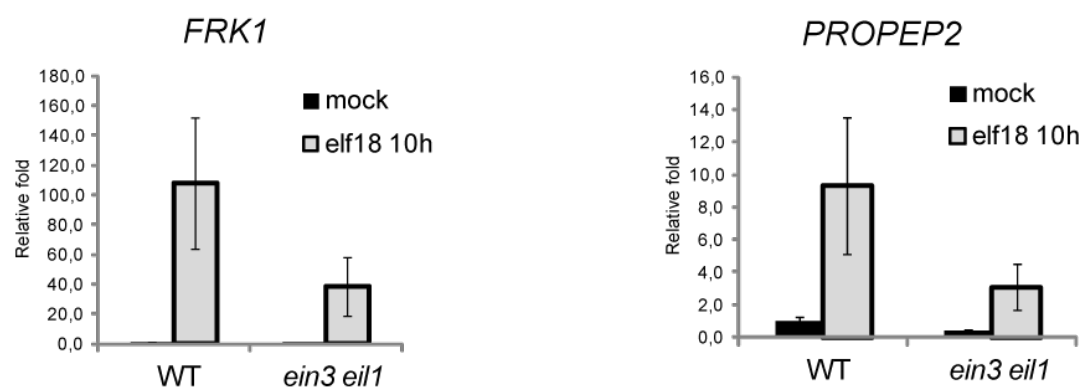


Figure 20. The transcription factors EIN3 and EIL1 are required for elf18-induced defense gene activation.

Expression of *FRK1* and *PROPEP2* in 2-week-old Col and *ein3 eil1* seedlings upon treatment with water (mock) and 1 μ M elf18 for 10h. Transcript levels were measured by qPCR and analyzed as described for Fig. 18 (A). The experiment was performed two times with similar results.

2.3.9 Genome-wide analysis of elf18-induced transcriptional reprogramming in *ein2* plants

Our findings point to a role for ET signalling in elf18-triggered transcriptional reprogramming, especially at late time points. To identify elf18-induced cellular processes that are controlled by ET signalling, we obtained genome-wide profiles for elf18-mediated transcriptome reprogramming by using ATH1 microarray chips. Approximately 2-week-old Col-0, *ein2-1* and *efr* seedlings grown in sterile liquid media were treated with elf18 for 0 and 10h. We used *efr* samples as a negative control. We identified genes that were at least twofold upregulated in Col, when compared to both untreated Col and elf18-treated *efr* samples. In order to identify ET-dependent genes, we focussed on genes of which EFR-triggered activation is more than two fold greater in Col than in *ein2* seedlings. The obtained microarray profiles with these criteria revealed 57 genes that are activated by EFR in an EIN2-dependent manner (Table 4). Importantly, *PR1* and *PR2* genes were among these, confirming our previous gene expression results obtained by quantitative RT-PCR (Figure 18B). However, several genes that show EIN2 dependent induction upon elf18 application in qPCR experiments (Figures 18, 19, 20), such as *PROPEP2* and *FRK1*, did not show a more than two fold reduction in EFR-triggered induction in *ein2* plants in the above microarray experiments. This might be due to lower sensitivity of microarrays in comparison to qPCR experiments.

Next, we cross-referenced our microarray profiles with publicly available gene expression profiles, with a focus on the elf18-induced ET-dependent genes. Surprisingly, these genes have been described to be poorly responsive to exogenous application of ET or the ET precursor ACC (Figure 21). This was confirmed by our qPCR experiments that detected no significant ACC-triggered activation of the elf18-responsive genes tested (data not shown). In conclusion, although this group of genes depend on EIN2 for full activation by elf18, ET or ACC application alone is insufficient for their induction.

Results

Table 4. List of genes that are activated by EFR in an EIN2-dependent manner

GeneID	Ratio fold induction in Col vs. fold induction in <i>ein2</i> *	TAIR annotation
AT4G28420	6,40	aminotransferase, putative; similar to SUPERROOT1, indole-glucosinolate biosynthesis proces
AT1G12940	6,19	ATNRT2.5 (NITRATE TRANSPORTER2.5); nitrate transporter
AT4G37990	5,62	ELI3-2 (ELICITOR-ACTIVATED GENE 3)
AT3G57240	5,23	BG3 (BETA-1,3-GLUCANASE 3); hydrolase, hydrolyzing O-glycosyl compounds
AT4G38410	4,83	dehydrin, putative
AT1G21320	4,66	VQ motif-containing protein
AT1G66090	3,94	disease resistance protein (TIR-NBS class), putative
AT1G14550	3,63	anionic peroxidase, putative
AT1G17020	3,50	SRG1 (SENESCENCE-RELATED GENE 1); oxidoreductase
AT5G39520	3,44	unknown protein
AT5G48175	3,16	similar to PYK10 (phosphate starvation-response 3.1)
AT4G13420	3,14	HAK5 (High affinity K ⁺ transporter 5); potassium ion transporter
AT2G17040	3,13	ANAC036 (Arabidopsis NAC domain containing protein 36); transcription factor
AT1G02940	3,04	ATGSTF5 (Arabidopsis thaliana Glutathione S-transferase 5 (class phi))
AT2G02990	3,02	RNS1 (RIBONUCLEASE 1); endoribonuclease
AT3G61390	2,84	U-box domain-containing protein
AT3G07380	2,84	unknown protein
AT2G27390	2,80	proline-rich family protein
AT1G49570	2,76	peroxidase, putative
AT1G73120	2,75	unknown protein
AT1G76470	2,67	cinnamoyl-CoA reductase
AT4G17670	2,65	senescence-associated protein-related
AT3G44350	2,60	ANAC061 (Arabidopsis NAC domain containing protein 61); transcription factor
AT2G30660	2,60	3-hydroxyisobutyryl-coenzyme A hydrolase, putative / CoA-thioester hydrolase, putative
AT4G17030	2,57	ATEXLB1 (ARABIDOPSIS THALIANA EXPANSIN-LIKE B1)
AT2G14610	2,57	PR1 (PATHOGENESIS-RELATED GENE 1)
AT1G22210	2,55	trehalose-6-phosphate phosphatase, putative
AT4G04500	2,53	protein kinase family protein
AT3G22231	2,51	PCC1 (PATHOGEN AND CIRCADIAN CONTROLLED 1); defense-related peptide
AT5G17760	2,43	AAA-type ATPase family protein
AT4G39950	2,42	CYP79B2 (cytochrome P450, family 79, subfamily B, polypeptide 2)
AT4G14400	2,42	ACD6 (ACCELERATED CELL DEATH 6)
AT5G61010	2,39	ATEX070E2 (EXOCYST SUBUNIT EXO70 FAMILY PROTEIN E2)
AT3G01970	2,35	WRKY45; transcription factor
AT5G22500	2,35	acyl CoA reductase, putative / male-sterility protein, putative
AT4G34210	2,30	ASK11 (ARABIDOPSIS SKP1-LIKE 11); ubiquitin-protein ligase
AT2G43510	2,23	ATT1 (ARABIDOPSIS THALIANA TRYPSIN INHIBITOR PROTEIN 1)
AT4G37370	2,20	CYP81D8 (cytochrome P450, family 81, subfamily D, polypeptide 8)
AT5G11210	2,19	ATGLR2.5 (Arabidopsis thaliana glutamate receptor 2.5)
AT1G16130	2,17	WAKL2 (WALL ASSOCIATED KINASE-LIKE 2)
AT3G57260	2,17	BGL2 (PATHOGENESIS-RELATED PROTEIN 2); glucan 1,3-beta-glucosidase/ hydrolase
AT2G18660	2,16	AtPNP-A; plant natriuretic peptide
AT1G44130	2,13	nucellin protein, putative
AT1G71140	2,12	MATE efflux family protein
AT5G43580	2,12	serine-type endopeptidase inhibitor
AT1G74080	2,09	MYB122 (myb domain protein 122); DNA binding / transcription factor
AT5G48400	2,08	ATGLR1.2 (Arabidopsis thaliana glutamate receptor 1.2)
AT3G54950	2,08	PLA IIIA/PLP7 (Patatin-like protein 7)
AT1G19250	2,08	FMO1 (FLAVIN-DEPENDENT MONOOXYGENASE 1)
AT1G13590	2,08	ATPSK1 (PHYTOSULFOKINE 1 PRECURSOR)
AT2G45570	2,07	CYP76C2 (cytochrome P450, family 76, subfamily C, polypeptide 2)
AT3G60420	2,06	unknown protein
AT5G13320	2,05	PBS3 (AVRPPHB SUSCEPTIBLE 3)
AT1G19230	2,04	respiratory burst oxidase protein E (RbohE) / NADPH oxidase
AT4G11280	2,02	ACS6 (1-AMINOCYCLOPROPANE-1-CARBOXYLIC ACID (ACC) SYNTHASE 6)
AT2G39350	2,02	ABC transporter family protein
AT4G19750	2,00	glycosyl hydrolase family 18 protein

*** Explanation to Table 4:**

Shown is the ratio between fold-induction in Col upon elf18 treatment and fold-induction in *ein2* upon elf18 treatment for the listed genes. Fold induction refers to the relative difference in transcript abundance before treatment and after 10h of elf18 treatment.

Interestingly, many of these EFR-activated, ET-dependent genes are associated with SA-mediated signalling and are reported as SA-responsive (Fig 21). We wondered if elf18-triggered SA accumulation or signalling is impaired in *ein2* mutants. The apparent over-representation of SA-responsive genes suggests a possible link between the two immune branches. To test this idea, we also profiled a group of genes that are induced by elf18 at comparable levels between WT and *ein2* seedlings. These genes are thus considered as ET-independent EFR-triggered genes. Notably, many SA-responsive genes are also present in this group, suggesting that the activation of the SA-responsive genes by EFR occurs in an ET-independent manner as well. Together, we infer from these data that EFR-triggered activation of SA-mediated immunity is in part, albeit not entirely, dependent on ET. The ET-independent activation of SA-dependent genes during EFR-triggered immunity makes it unlikely that ET contributes to SA biogenesis and/or accumulation but rather suggests that ET modulates part of SA signalling branches.

Results

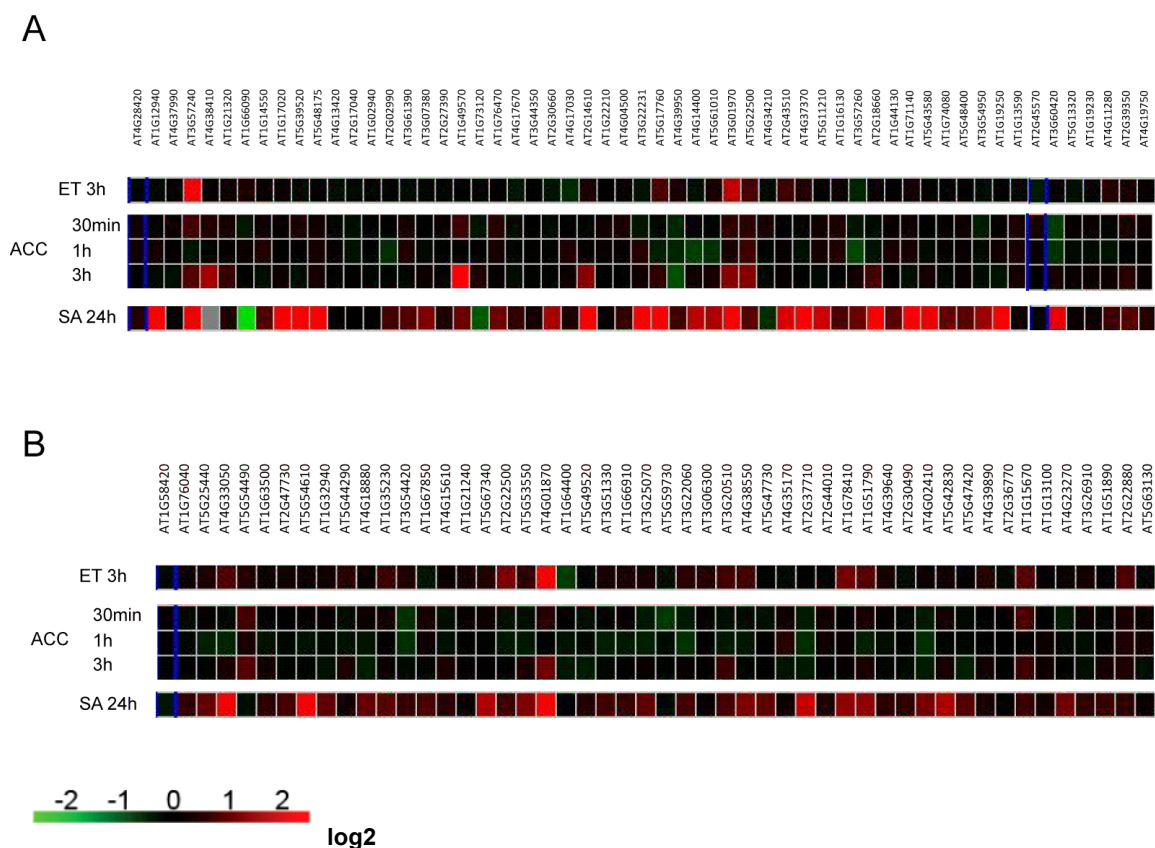


Figure 21. Expression profile of genes that are EFR-activated in a putatively ET-dependent (A) or ET-independent (B) manner.

(A) Shown are expression profiles for *elf18*-induced genes that are at least 2-fold stronger activated in Col than in *ein2* (ET-dependent activation; gene list is shown in table 4) upon treatment with ET, AAC and SA.

(B) Expression profile for *elf18*-induced genes that show no significant difference between Col and *ein2* (ET-independent activation; gene list is shown in suppl. table 1) in response to ET, ACC and SA. Due to space limitation only a subset of putatively ET-independent genes is shown.

The values were taken from publicly available microarray datasets, published in the Genevestigator databank.

Next, we examined gene ontology terms for the selected ET-dependent EFR-activated genes. Interestingly, it seems that genes classified to extracellular compartments are significantly enriched among these ET-dependent genes, when compared to all elf18-activated genes or to the entire Arabidopsis genome (Table 5).

Table 5. Gene Ontology terms

GO term frequencies were obtained by the program GO finder. ** and * indicate statistically significant enrichment compared to Arabidopsis genome.

Gene Ontology Term	Frequency among EFR-induced, ET-dep. genes	Frequency among all EFR-activated genes	Frequency in the whole genome
Extracellular region	15,8 % **	2,7 % *	1,5 %

Consistently with a possible role of ET-signalling in modulating extracellular signalling processes, we found numerous potential signalling peptides among our genes of interest. Notably, plant-derived short peptides were reported to act as signalling molecules during defense responses (Meier et al. 2008).

Importantly, we revealed *PROPEP2*, one of such short-peptide encoding genes as ET-dependent (Figure 18, 19 and 20). It was previously reported that *PROPEP2* contains an immuno-stimulatory epitope, termed Pep2 of which application activates defense-related genes in Arabidopsis (Huffaker et al. 2007). Based on the ET-dependent induction of the *PROPEP2* gene, we hypothesized that the putative endogenous elicitor Pep2 acts downstream of ET as one mechanism to ensure sustained defense-gene activation during MTI. If Pep2 triggered signalling acts downstream of EIN2 in such a signal amplification system, we would expect to see that Pep2 application activates (at least a subset of) ET-dependent EFR-target genes in *ein2* plants. To test this idea, we analyzed pep2-mediated defense gene induction in WT and *ein2* seedlings.

Pep2-mediated activation of *PR1* was indistinguishable between WT and *ein2* plants (Figure 22). These data are consistent with the hypothesis that pep2 acts downstream of EIN2 in the EFR pathway, at least for *PR1* induction.

In order to test the connection between EFR, ET and Pep2 signaling in a greater detail, we tested how the aforementioned EFR-activated, ET-dependent genes respond to pep2 application. To this end, we analyzed gene expression profiles of seedlings treated with pep2 for 2h (unpublished data). Of the 57 genes that are activated by EFR in an ET-dependent manner, 25 genes are induced more than twofold upon pep2 treatment (data not shown). Of these, eight genes seem to be activated in an ET-independent manner, as their induction upon Pep2 was essentially indistinguishable between WT and *ein2* seedlings, whereas nine genes show significant ET-dependence for their activation by Pep2. These results disfavour a simple model in which Pep2 acts downstream of ET in the EFR pathway. Rather, they point to the existence of a complex interaction between the Pep2 and ET pathways.

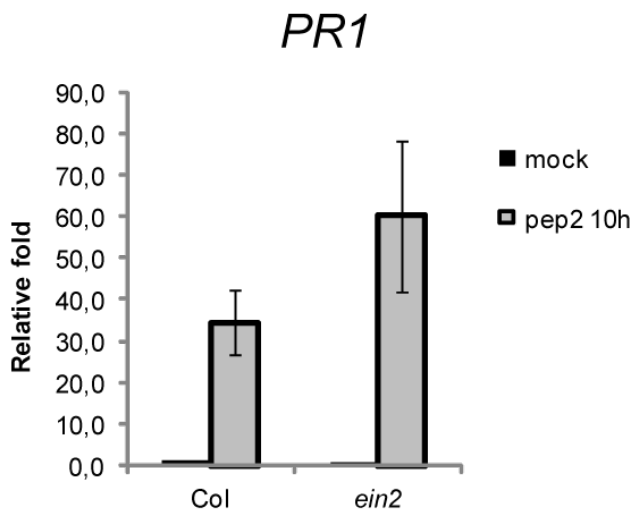


Figure 22. Pep2 treatment can trigger *PR1* activation in *ein2* plants.

Expression of *PR1* in 2-week-old Col and *ein2* seedlings upon treatment with water (mock) or 1 μ M pep2 for 10h. Transcript levels were measured by qPCR and analyzed as described for Fig 18 (A).

2.3.10 *ein2* plants retain elf18-triggered immunity towards virulent *Pseudomonas syringae*

The pronounced defects of *ein2* plants in elf18-triggered transcriptome reprogramming prompted us to test possible impairment of EFR-triggered immunity in these mutant plants. It has been previously shown that plant pretreatment with elf18 reduces the propagation of *Pst* DC3000 (Kunze et al. 2004). EFR-triggered immunity is defined as the decrease in bacterial growth in elf18-pretreated leaves as compared to water-pretreated mock leaves. Previous reports show detectable reduction of FLS2-triggered immunity in *ein2* plants, whereas EFR-triggered immunity is essentially WT-like in *ein2* plants (Tsuda et al. 2009). Under our conditions WT and *ein2* plants show a clear reduction of bacterial growth in elf18-pretreated leaves as compared to mock leaves (Figure 23). Thus, despite a defect in several EFR-triggered outputs in *ein2* plants, EFR-triggered immunity is largely retained in *ein2* plants at least under our conditions.

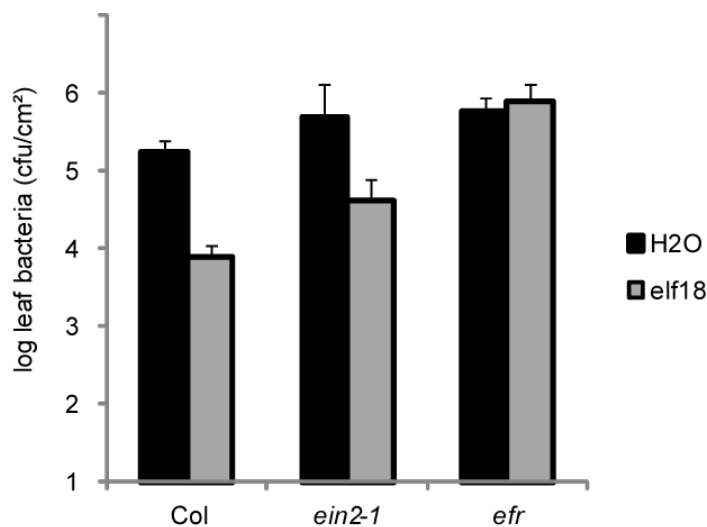


Figure 23. *ein2* plants retain WT-like elf18-triggered immunity to *Pst*.

Leaves from 4-week-old WT (Col), *ein2-1* and *efr* plants were infiltrated with water (mock) or 1 μ M elf18 and 24h later infiltrated with *Pst* DC3000 at 2.5×10^4 cfu. Bacterial growth was measured at 3 days after infection. SDs from biological replicates within one experiment are shown.

3. Discussion

3.1 ER quality control for plant innate immunity

Besides the here reported identification of PSL2 as UGGT and likely identification of PSL25 as G I, several other ERQC components were shown to play a role in EFR function. Steady-state accumulation of EFR is greatly reduced in strongly dysfunctional alleles of CRT3, GLUCOSIDASE II β subunit and STT3a that is part of the oligosaccharyl-transferase complex (Saijo et al. 2009, Lu et al. 2009, Li et al. 2009, Nekrasov et al. 2009). Additionally, mutations in glucosidase II α -subunit result in reduced ligand binding activity of EFR and impaired responses to elf18 (Lu et al. 2009). Furthermore it was shown that mutations in *ERD2b* that is homologues to ER-retention receptors interfere with stable accumulation of CRT3 and thus result in reduced EFR levels and elf18 responsiveness (Li et al. 2009). Intensive research on yeast and animal cells revealed the so-called CRT/CNX-cycle that involves STT3-dependent N-glycosylation, the ER-chaperones CNX and CRT, ER-resident glucosidase I and glucosidase II and UGGT. Thus, these components work together in a specific ERQC branch that seems to be evolutionary conserved in plants and animals. In addition, another ERQC mechanism involving SDF2 (STROMAL DERIVED FACTOR2), the Hsp40 ERdj3B and likely the Hsp70 BiP is required for accumulation of EFR (Nekrasov et al. 2009).

The demonstration of reduced EFR levels in these ERQC mutants strongly points to EFR as a client protein of this folding machinery. Consistently, it was shown that EFR is N-glycosylated *in vivo* and at least a sub-pool of EFR accumulates in endomembrane compartments where it could interact with

ERQC components (Saijo et al. 2009, Häweker et al. 2010). Furthermore, pharmacological inhibition of ERAD restored EFR accumulation in *uggt* and *crt3* mutants, indicating that ERAD prevents stable accumulation of misfolded EFR in these mutants (Saijo et al. 2009).

Interestingly, *ps/2* and *ps/25*, as well as other identified ERQC mutants show insensitivity to *elf18*, but retain *flg22* responsiveness. Consistently, EFR levels are greatly reduced, whereas FLS2 levels are unaffected in these mutants. Together, these data reveal a critical role of these ERQC components for EFR, but not for FLS2 biogenesis. This is surprising, as the two PRRs are highly similar in overall structure and thus in the biochemical mode of action, and seem to share downstream signaling components (Boller and Felix 2009). However, FLS2 seems to be widely conserved among plant families, even in dicots and monocots, whereas *elf18* responsiveness seems to be restricted to the Brassicaceae (Boller and Felix 2009). Thus, EFR might represent an evolutionarily young PRR that strictly relies on the identified ERQC components for its folding and maturation. On the other hand, the evolutionarily conserved FLS2 might have evolved its folding capacity even in the absence of these ERQC components. This might be achieved by the engagement of redundant ERQC branches in FLS2 biogenesis. It will be interesting to elucidate differences in EFR and FLS2 structure that could account for the differential requirement of ERQC components. It is unlikely that different expression levels of the two PRRs explain their differential dependence on the identified ERQC components, as *EFR* expression under the control of the *FLS2* regulatory sequences still requires presence of SDF2 for stable accumulation of the receptor (Nekrasov et al. 2009).

Interestingly, distinct EFR signaling outputs are differentially, rather than uniformly, impaired in *ps/25* plants. We observed partial and differential impairment of EFR outputs in weakly dysfunctional *crt3* and *glla* alleles as well, despite WT-like EFR accumulation. At present it is unclear whether EFR levels

are reduced in *ps/25* plants. The impaired EFR outputs in *crt3* and *glla* correlated with a reduction in receptor ligand-binding activity. Consistently, *ps/25* plants show such a reduction in EFR ligand-binding activity. Thus, improper folding of the LRR domain that likely mediates ligand binding results in selective impairment of EFR-triggered outputs. It is possible that the observed reduced ligand-binding activity in these mutants is a consequence of altered stability, maturation, subcellular partitioning of the receptor and/or combinations thereof. This model predicts an intimate relationship between ERQC of the LRR domain, sub-cellular actions of the receptor and receptor-triggered immune signaling. Future studies will be required to test this model and elucidate the underlying mechanisms.

Importantly, weakly dysfunctional ERQC mutants, such as *ps/25* can serve to dissect signaling outputs emanating from a single PRR. ROS spiking and callose deposition in response to *elf18* are undetectable in *ps/25* mutants, despite nearly WT-like activation of MAPKs 3 and 6. These results rather disfavor a model in which MAPKs act upstream of ROS spiking proposed based on the data obtained in the FLS2 pathway (Zhang et al. 2007). Alternatively, there might be differences between the EFR and FLS2 pathways concerning the sequential activation of these outputs. More importantly, our data disfavor a simple threshold model in which, e.g., more EFR signaling fluxes are required for ROS generation than MAPK activation, as rejected in weak alleles of *crt3* mutants (Saijo et al. 2009). Instead, it seems more likely that these diverse signaling outputs are separately activated by EFR. This suggests the existence of, at least in the case of EFR, parallel or multi-branched signaling pathways emanating from the receptor.

Intense research on yeast and animal cells identified molecular components and mechanisms of ERQC (Anelli and Sitia 2008, Helenius and Aebi 2004). However, this work was done almost exclusively on artificial, thus non-physiological client proteins. In Arabidopsis, a mutated version of the brassinolide receptor BRI1, designated BRI1-9 was identified as a client of UGGT and CRT3. However, WT BRI1 does not depend on the actions of UGGT and CRT3, because BR responsiveness seems to be retained in these two ERQC mutants (Jin et al. 2007 and 2009). Thus, EFR identifies the first native client of the UGGT-CRT3 branch of ERQC. The availability of a mutant collection that interferes with ERQC function to a varied degree might facilitate the identification of further client proteins. The existence of such a non-EFR client has been predicted since *uggt* and *stt3a* mutant plants show a defect in SA-mediated immunity in an EFR-independent manner (Saijo et al. 2009). Interestingly, *ps/25* mutants show some phenotypes that seem to be independent of EFR. Suppression of root growth and hyper-accumulation of anthocyanin in the presence of high exogenous sucrose might hint to enhanced sucrose or osmotic sensitivity of *ps/25* plants. Furthermore, previous characterization of a weakly dysfunctional G I allele revealed altered root growth and increased number of stomata in that mutant (Furumizu et al. 2008). It is interesting to note that *ps/25* plants show enhanced susceptibility to virulent *Pseudomonas* to a higher level than *efr*. As the bacteria were applied by spray inoculation onto the leaf surface and stomata provide a bacterial entry route into the leaf tissues (Melotto et al. 2006), it is conceivable that increased stomata number in *ps/25* would result in increased bacteria invasion and propagation. The generation and distribution of stomata is regulated by a complex pathway involving cell-cell communication through extracellular signaling peptides and their cell-surface LRR-receptors (Rowe and Bergmann 2010). Thus, several potential client proteins for G I mediated ERQC are present in this pathway.

3.2 Ethylene signaling regulates pre- and post-recognition steps in MAMP-triggered immunity

Induction of ET synthesis represents a hallmark of a multitude of defense responses (Broekaert et al 2006). However, to elucidate the role of ET during defense processes proved to be extremely difficult.

The isolation of a novel *ein2* allele (designated *ps/36*) that shows impaired responses to flg22 and elf18 implicates a role for ET in MAMP-signaling. We observe pronounced defects in flg22 induced responses in *ps/36* and previously described *ein2-1* plants, including ROS spiking, callose deposition, suppression of anthocyanin accumulation and activation of defense-related genes.

Consistently with recent publications, we find that steady-state expression of FLS2 is reduced in *ps/36* and *ein2-1* (Boutrot et al. 2010, Mersmann et al. 2010). It was suggested that reduced FLS2 levels explain the reduced flg22 responsiveness detected in ET-perception and -signaling mutants (Boutrot et al. 2010). However, to prove the causal relationship between lower FLS2 levels and impaired FLS2-outputs, ET-insensitive mutants that constitutively express *FLS2* need to be analyzed. We provide evidence that constitutive expression of *FLS2* by CMV-35S promoter in *ein2* plants restore flg22 sensitivity (Figure 17). However, we only tested one FLS2 output (suppression of sucrose-induced anthocyanin accumulation), and future research will be needed to test if ET-independent expression of *FLS2* could restore all flg22 responses in *ein2* plants. However, it is also possible that FLS2 accumulates to much higher levels in these plants, thereby overcoming a possible reduction of post-recognition signaling.

In contrast to ET-dependent expression of *FLS2*, *EFR* expression seems to be independent of ET-signaling, as demonstrated by WT-like *EFR* transcript and protein levels in *ein2-1* and *psl36* mutants (Figure 15). These data suggest distinct regulation of the two PRR genes by ET signaling. More importantly, *ein2* plants show significantly reduced *EFR* outputs despite WT-like steady-state *EFR* accumulation. Hence, *EFR* signaling defects in *ein2* plants seem to be a consequence of impaired post-recognition signaling of the receptor. Thus, analyzing *elf18*-responses in *ein2* mutants should provide insight into the role of ET in post-recognition signaling during MTI.

Our data suggest that ET modulates *EFR* signaling at multiple steps. We previously demonstrated that sustained *EFR* signaling is critical for establishment of robust MTI (Lu et al. 2009). Importantly, *ein2* seedlings are impaired in *elf18*-mediated activation of several defense genes tested (Figures 18-20). In order to substantiate this finding, we obtained genome-wide profiles for *elf18*-mediated transcriptome reprogramming in *ein2* mutants. This led to the identification of a set of genes that seem to depend on intact ET-signaling for their full activation (Table 4). Strikingly, the vast majority of these genes are not induced by ET or ACC treatment alone, suggesting that ET signaling activation is insufficient to activate these genes. Consequently, the full activation of this set of genes requires the presence of ET and another stimulus. This would indicate that ET acts as a modulator, rather than an integral component of signaling processes during *EFR*-triggered immunity.

A number of the identified ET-dependent genes are widely associated with SA-responses and signaling (e.g. *PR1* and *PR2*, *PBS3*, *FMO3*). Furthermore, roughly the half of these ET-dependent genes is activated by exogenously supplied SA (Figure 21). Thus, we speculate that ET signaling interacts with SA signaling during *EFR*-triggered immunity. This interaction might result in an elevated expression of SA-responsive genes. However, we note that many SA-responsive genes seem to be activated by *elf18* in an ET-independent manner

as well. This suggests that only a subset of SA-responses is influenced by ET-signaling. Among others, transcript levels of the SA biosynthetic enzyme SID2/ICS1 (Wildermuth et al. 2002) are not altered in *ein2* in our microarray experiments. Together, it seems unlikely that elf18-mediated SA accumulation is impaired in *ein2* seedlings.

The interactions between the ET and SA pathways seem to be very complex, as they can positively or negatively influence each other in a context-dependent manner (Wang et al. 2002, Pieterse et al. 2009, Dong 1998). Importantly, a substantial set of genes seems to be co-regulated by ET- and SA-dependent pathways during *Pseudomonas* infections on Arabidopsis (Glazebrook et al. 2003). Furthermore, in certain mutant backgrounds ET treatment potentiates SA-dependent *PR1* expression (in *edr1*, Frye et al. 2001) or the presence of EIN2 is necessary for SA accumulation (in *cpr6*, Clarke et al. 2001). On the other hand, several reports show antagonistic interactions between the SA and ET pathways (Chen et al. 2009). It is thus very likely, that the outcome of SA and ET interactions depends on the specific context. Our simplified experimental setup (with elf18 as single inducer) could probably highlight positive effects between ET and SA signaling.

ET signaling has been implicated in cellular damage response and induction of cell death, for example in response to ozone (Wang et al. 2002) or in the *acd5* mutants (Greenberg et al. 2000). Consistently, we notice many genes associated with cellular stress responses among our identified ET-dependent genes (e.g. two peroxidases, several genes involved in lignin biosynthetic processes and *WALL ASSOCIATED KINASE 2*, that was suggested as a putative sensor of cell wall integrity (Boller and Felix 2009)). In this context it is interesting to note that genes encoding the components acting in the extracellular compartments are significantly enriched among our identified ET-dependent genes.

Integration of MTI with cellular damage responses remains an important but underexplored aspect of plant immunity studies. So-called DAMPs might provide a functional link, as they are generated or activated during a pathogen attack, and exhibit defense-activating properties. However, DAMPs are still poorly defined. Plant-encoded peptides with elicitor-activity might represent DAMPs. Especially interesting are those that are transcriptionally upregulated during defense responses. Notably, we find numerous genes encoding peptides with or without secretion signal among the genes that are activated by EFR in an ET-dependent manner. Furthermore, we define *PROPEP2* as an ET-regulated gene and suggest that *pep2* can restore some, but not all *elf18* responses in *ein2* plants.

It is an interesting question, by which mechanisms ET signaling contributes to EFR-mediated transcriptional reprogramming. Our genetic data define the transcription factors EIN3 and EIL1 as mediators of *elf18*-induced defense gene activation (Figure 20). ERF1 and MYB51 are important transcriptional regulators of ET-responses and genes of the glucosinolate metabolism pathway, respectively. *Elf18*-induced transcriptional activation of both genes is strongly impaired in *ein2* plants (Figure 18A). It is tempting to speculate that these regulators are involved in *elf18*-induced gene expression changes, especially as *CYP79B2*, a known target of MYB51, is present among the ET-dependent genes. Genome-wide profiling of early *elf18*-induced transcriptome changes in *ein2* mutants is expected to identify the regulators of ET-signaling outputs.

In a previous work we showed the importance of sustained activation of EFR signaling for MTI, through the characterization of a weakly dysfunctional allele of ER glucosidase II (designated *radially swollen3*, *rsw3*) (Lu et al. 2009). *rsw3* plants retain WT-like activation of most tested *elf18* responses, including ROS spiking, MAPK activation, callose deposition and ET generation, but fail to confer *elf18*-triggered immunity to virulent *Pst* DC3000. This immune-compromised phenotype of *rsw3* correlated with a defect in sustained defense gene activation

and de-repressed anthocyanin accumulation. Interestingly, *ein2* plants are also compromised in elf18-mediated sustained activation of defense genes. However, genome-wide profiling of elf18-induced genes revealed substantial differences between *rsw3* and *ein2* (data not shown). Furthermore, anthocyanin suppression is only weakly affected in *ein2* seedlings, whereas *rsw3* seedling show strongly de-repressed anthocyanin levels (Lu et al. 2009). Conversely, *ein2* plants largely retain elf18-induced resistance, in contrast to *rsw3* plants. These findings clearly suggest that different aspects of EFR-signaling are affected in *rsw3* and *ein2* plants.

Despite significantly altered EFR-outputs in *ein2* plants, EFR-induced immunity to *Pst.* DC3000 remained largely intact (Figure 23). This can have several reasons. It is possible that the alterations in the elf18-responses are not sufficient to interfere with elf18-induced resistance. Alternatively, crosstalk with other defense-pathways might lead to activation of compensatory responses in *ein2* mutants, for example as reported for increased SA levels (Chen et al. 2009). Importantly, elf18-induced immunity was tested by pretreating plants with elf18, and subsequently infiltrating bacteria into the leaf tissue. However, as pointed out earlier, it seems that the contribution of ET signaling to resistance against *Pst.* is most prevalent when bacteria are applied onto the leaf surface. Furthermore, it seems that *ein2* seedlings show more pronounced defects in MAMP responses than adult plants. Consequently, the role of ET signaling in EFR-triggered immunity should be tested in seedlings in a pre-invasion manner. Modification of experimental procedures according to these criteria is currently ongoing.

4. Materials

BUFFERS

10X PCR buffer 100 mM Tris-HCl pH 8,4
500 mM KCl
20 mM MgCl₂

TAE buffer 400 mM Tris
10 mM EDTA
200 mM acetic acid
pH 8.5

RNA isolation kit

RNeasy Plant Kit (QIAGEN, Hilden, Germany)

DNA Isolation kit

SIGMA RED Extract-N-Amp plant PCR kit

Quick DNA isolation protocol

Buffer A: 100 mM NaOH
20% Tween 20

Buffer B: 100 mM Tris-HCl pH 2,0
2 mM EDTA

DNA Isolation by Edwards method

Edwards Buffer: 200 mM Tris-HCl pH 7,5
250 mM NaCl
25 mM EDTA
0,5% SDS

Protein lysis buffer 1

20 mM HEPES pH 7.5
13 % Sucrose
1 mM EDTA
1 mM DTT
1x complete protease inhibitor cocktail (Roche, Mannheim, Germany)

Protein lysis buffer 2 for MAPK assays

50 mM Tris pH 7.5
200 mM NaCl
1 mM EDTA
10 mM NaF
25 mM beta-glycerophosphate
2 mM sodium orthovanadate
10 % (w/v) glycerol
0.1 mM Tween 20
0.5 mM DTT
1 mM PMSF
1x complete protease inhibitor cocktail (Roche, Mannheim, Germany)

SDS-PAGE

2x loading buffer	125 mM Tris-HCl pH 6.8 5 % SDS 25 % Glycerol (v/v) 0,025 % Bromphenol blue (w/v) 0.2 M DTT
4 x separating gel buffer:	1,5 M Tris-HCl pH 8,8 0,4% SDS
4 x stacking gel buffer:	0,5 M Tris-HCl pH 6,8 0,4% SDS
Running buffer:	25 mM Tris pH 8.5 192 mM glycine 0.1% SDS
Coomassie staining solution:	40% Methanol 10% Acetic acid 0.1 % Coomassie Brilliant Blue
Coomassie destaining solution:	20% Methanol 10% Acetic acid

Western blot

Transfer Buffer	15 ml	1 M NaPO ₄
	5 ml	10% SDS
	800 ml	H ₂ O
	200 ml	Ethanol

Blocking Buffer (TBST + milk): 50 mM Tris-HCl
150 mM NaCl
0.01% Tween-20
5% milk powder

MEDIUM

MS-medium	1x MS medium	4.4 g/l Murashige & Skoog medium incl. Vitamins and MES-buffer DUCHEFA BIOCHEME # M0255.0050
------------------	--------------	--

For MS agar plates 0.8 % (w/v) plant agar (Duchefa, Haarlem, Netherlands)

was added to the above medium.

NYG broth medium	Bactopeptone	5 g/l
	Yeast extract	3 g/l
	Glycerol	20 ml/l
	pH 7.0	

For NYG agar plates (NGYA) 1.5 % (w/v) bacto agar (Becton, Franklin Lakes, USA) was added to the above broth.

Peptides

As elicitor-active surrogates the peptides flg22 and elf18 from flagellin and bacterial Elongation-Factor Tu (EF-Tu) were used. Peptides were synthesized by EZBiolab Inc. (Carmel, USA) with the following sequences: flg22 – QRLSTGSRINSAKDDAAGLQIA and elf18 – AcSKEKFERTKPHVNVGTIG. The peptides are described in Felix et al. (1999) and Kunze et al. (2004). For receptor-ligand binding experiments, radioactively labeled elf26 and flg22 were used, elicitor active surrogates of Elongation-Factor Tu and flagellin, respectively.

METHODS

Plant growth conditions/MAMP treatment

For the sucrose-MAMP crosstalk assays, seeds were surface-sterilized with 70% ethanol, imbibed for 1-3 days at 4°C and then grown under constant light in liquid media containing 0,5X MS medium for 3 days, and then for further 3 days with or without the addition of 100 mM sucrose and MAMPs at the indicated concentrations. For Western blot and gene expression analysis, seedlings were grown on agar plates containing 0,5X MS and 25 mM sucrose for 5-6 days under 12h light/12h dark conditions, then transferred to liquid media with 0,5X MS and 25 mM sucrose for additional 5-6 days. For MAPK assays, seedlings were grown on agar plates with 0,5X MS and 25 mM sucrose for 12-14 days under 12h light/12h dark conditions. Plants were grown on soil under 10h light/14h dark conditions for 4 to 5 weeks for ROS - and bacterial inoculation assays.

Isolation of *psl*-mutants

Ethane methyl sulfonate (EMS) mutagenized M2 seeds of Col-0 *glabrous1 (gl1)* were used for genetic screening under the conditions described above. flg22 and elf18 were applied at 0,5 μ M each concomitantly with sucrose-containing media. MAMP-insensitive mutant candidates were rescued by transferring to solid MS-medium plates. For the screening of the progeny M3 generation, flg22 and elf18 were applied separately at 0,5 μ M each.

MAMP-sucrose assay

Seeds were surface-sterilized with 70% ethanol, imbibed for 1-3 days at 4°C and then grown in 0,5 x MS liquid-medium in 48 well plates for 3 days. The medium was replaced with 0,5 x MS liquid-medium supplied with 100 mM sucrose and flg22/elf18 at the concentrations indicated and seedlings were grown for further 3 days. Seedlings were grown under continuous light and 23°C.

Anthocyanin isolation and measurement was performed as in Tneg et al. 2005. Anthocyanins were isolated by incubating seedling material from ca. 10 seedlings 1 % (v/v) hydrochloric acid in methanol for 12h. The mixture was centrifuged at 13.000 rpm for 5 minutes and the absorbance of the supernatant was measured at 530 and 657 nm. Relative anthocyanin concentrations were calculated with the formula $(A_{530}-A_{657}/4) / \text{g FW}$.

MAPK assay

For MAPK assays seedlings were grown on agar plates containing 0,5X MS and 25 mM sucrose for 10 days under 12h light/12h dark conditions.

Whole seedlings were treated with elf18 or flg22 at 1 μ M for the indicated times. Total proteins were extracted using lysis buffer 2 as described (Saijo et al., 2008) and separated by SDS-PAGE. MAPK activation was detected by immunoblot analysis using anti-phospho p44/p42 MAPK antibody.

ROS assay

For ROS assays, leaf discs (5 mm diameter) were excised from 4-week-old plants and were kept overnight on water before they were transferred to 50 μ l fresh water. Subsequently, ROS production was induced as described by Felix et al., 1999; by application of 100 nM elf18 or flg22, in a reaction mixture containing 50 μ l water, 20 μ M luminol (Fluka, Deisenhofen, Germany) and 1 μ g horseradish peroxidase (Sigma-Aldrich, Deisenhofen, Germany). Luminescence was measured by a luminometer (Centro LB 960 microplate luminometer, Berthold Technologies, Wildbach, Germany).

Callose assay

Seedlings were grown on agar plates containing 0,5X MS and 25 mM sucrose for 10 days under 12h light/12h dark conditions. Whole seedlings were treated with elf18 or flg22 at 1 μ M for 16-20h. Subsequently, seedlings were destained in 70 % EtOH and callose deposits stained with Aniline blue (described in Lipka et al. 2005) and cotyledons inspected under UV-light

Triple response assay

Surface-sterilized seeds were stratified for 3-5 days at 4°C, and then planted on half-strength MS agar plates with or without 10 μ M ACC (1-aminocyclopropane-1-carboxylate). Plates were placed vertically in dark at 22°C for 4-5 days, before taking pictures of representative seedlings.

Pathogen inoculation and growth assays

Pseudomonas syringae pv. *tomato* DC3000 bacteria were grown on NYG liquid media supplied with Rifampicin (Rif, 100 μ g/ml) over night at 28°C. Cultures were collected, washed once and resuspended in sterile 10 mM MgCl₂. Plants were sprayed with a bacterial suspension containing 10⁹ c.f.u. ml⁻¹ bacteria with 0,002% Silvet L-77.

Infected plants were kept in a covered container for 3 days, and representative leaves were harvested 4 days after inoculation. A total of 12 surface-sterilized leaf discs (5mm diameter, 30s in 70% ethanol, followed by 30s in sterile distilled water) excised from 2 leaves of 6 plants per genotype were randomly separated into 3 pools, and then subjected to quantification of leaf bacteria.

Leaf bacteria were quantified as follows: leaves were ground in 10 mM MgCl₂. After grinding the samples were thoroughly vortex-mixed and diluted 1:10 serially. Samples (10 µl out of 1 ml) were plated on NYGA + Rif (100 µg/ml) solid medium. Plates were placed at 28°C for 2 days and thereafter the colony-forming units counted. Bacterial infections were performed in three independent experiments for each condition.

Molecular biological methods

Genomic DNA extraction

Genomic DNA from *Arabidopsis* was isolated as described by Edwards et al. 1991. *Arabidopsis* leaf tissue was ground in Edwards buffer and centrifuged at 13,000 rpm for 5 min. The supernatant was collected and DNA was precipitated with isopropanol and centrifuged. The DNA pellet was washed with 70% ethanol, dried and resuspended in sterile water.

RNA extraction and cDNA synthesis

Total RNA from *Arabidopsis* seedlings was isolated using the RNeasy Plant Kit (QIAGEN, Hilden, Germany) according to the manual provided. cDNA was synthesized using 5 µg total RNA, oligo(dT) primers and the SuperScript II reverse transcriptase according to the manual provided (Invitrogen, Karlsruhe, Germany).

Semi-quantitative reverse transcriptase polymerase chain reaction (RT-PCR)

Seedlings were grown on agar plates containing 0,5X MS and 25 mM sucrose for 5-6 days under 12h light/12h dark conditions, then transferred to liquid media with 0,5X MS and 25 mM sucrose for additional 5-6 days.

Whole seedlings were treated with 1 µM elf18 or flg22 for the indicated time and RNA extraction and cDNA synthesis were performed as described above. PCR reactions were carried out in a Peltier Thermal Cycler PTC-225 (GMI Inc., Ramsey, USA). A typical PCR reaction mix and thermal profile is shown below using 10x PCR buffer.

Reaction mix		PCR programme		
cDNA (1:10)	2 µl	Initial	95 °C	5 min
PCR buffer (10x)	2,5	Denaturation	95 °C	30 sec
dNTPs (10 mM)	0.5	Annealing	55 °C	30 sec
Forward primer (10 µM)	1 µl	Extension	72 °C	1.5 min
Reverse primer (10 µM)	1 µl	Final extension	72 °C	3 min
Taq polymerase	0.5		16 °C	5 min
H ₂ O	ad 25 µl			

DNA fragments were subsequently separated by agarose gel electrophoresis. Gels were made of TAE buffer, containing 1-3 % (w/v) agarose (Bio-Budget Technologies, Krefeld, Germany) supplemented with ethidium bromide solution (1:40000). Gels were run in TAE buffer.

Quantitative RT-PCR

Seedlings were grown on agar plates containing 0,5X MS and 25 mM sucrose for 5-6 days under 12h light/12h dark conditions, then transferred to liquid media with 0,5X MS and 25 mM sucrose for additional 5-6 days.

Whole seedlings were treated with 1 µM elf18 or flg22 for the indicated time and RNA extraction and cDNA synthesis were performed as described above. Quantitative RT-PCR was performed on the IQ5 real-time PCR Thermocycler (Bio-Rad, Hercules, USA).

A typical PCR reaction mix and thermal profile is shown below. Expression of the genes of interest was normalized to the reference gene *At4g26410* encoding a methyltransferase and relative to the transcript abundance in Col or *gl1* wild-type control samples, unless indicated otherwise. Calculations were performed according to the comparative cycle threshold ($\Delta\Delta C_t$) method. The reference gene *At4g26410* was previously described to be stably expressed upon biotic stresses (Czechowski et al., 2005). Three technical replicates per sample were included and experiments were three times independently.

Reaction mix		PCR programme		
cDNA (1:10)	1 μ l	Initial	95 °C	2 min
PCR buffer (10 x)	2.5 μ l	Denaturation	95 °C	20 sec
dNTPs (10 mM)	0.5 μ l	Annealing	59 °C	30 sec
Forward primer (10 μ M)	1 μ l	Extension	72 °C	25 sec
Reverse primer (10 μ M)	1 μ l		95 °C	1 min
SYBR® Green (1:3000)	1.25 μ l		55 °C	1 min
Glycerol (50 %)	4 μ l	Melting curve	55 – 95 °C	10 sec; à 0.5 °C; 81
DMSO (100 %)	0.75 μ l			
Taq polymerase	0.5 μ l			
H ₂ O	ad 25 μ l			

DNA isolation

Quick DNA isolation protocol (used for rough-mapping)

Leaves from 2 week old seedlings were incubated in 50 μ l Buffer A at 96°C for 10 minutes. Thereafter, 50 μ l of Buffer B was added and 2 μ l of the resulting mixture was used as template in subsequent PCR to determine the genotype.

DNA isolation for fine-mapping

DNA isolation was performed using the DNA-isolation kit from SIGMA (SIGMA RED Extract-N-Amp plant PCR kit).

Designing DNA polymorphic sequence markers

Molecular markers have been designed and developed based on the sequence polymorphism information between the *Arabidopsis thaliana* accessions Columbia (Col) and Landsberg erecta (Ler) available at <http://www.arabidopsis.org> (Jander et al. 2002).

Primers were designed using the software Primer3.

SSLP and CAPS marker analysis

PCR has been performed under the following conditions unless otherwise stated:

PCR mixture (25µl)	
10X Buffer	2,5µl
dNTP 10µM	0,5µl
Primer1 10µM	0,5µl
Primer2 10µM	0,5µl
Taq polymerase	0,5µl
H2O	19µl
DNA	2µl

PCR program

94°	3 min	
94°	30 sec	x 45
55°	30 sec	
72°	1 min	
72°	10 min	
12°	10 min	

PCR-products were subjected to agarose gel-electrophoresis.

For CAPS marker analysis, PCR fragments were digested with the appropriate restriction enzyme and then subjected to agarose gel-electrophoresis.

Sequence Analysis

For sequence analysis, contiguous DNA fragments (contigs) covering the chromosomal regions with the size of approximately 2 kb each were amplified by PCR with the primers in table2. Purified PCR products were subjected to DNA sequence analysis. Polymorphism search was performed with the aid of the software SeqMan.

Microarray experiment and data analysis

Seedlings were grown on agar plates containing 0,5X MS and 25 mM sucrose for 5 days under 12h light/12h dark conditions, then transferred to liquid media with 0,5X MS and 25 mM sucrose for additional 5 days. Whole seedlings were treated with 1 μ M elf18 for 10 hours. Seedling material was harvested before treatment (0 hour timepoint) and 10 hours after elf18 treatment. For each replicate at least 10 seedlings were included. For each genotype and timepoint three replicates were collected. Total RNA was extracted as described above.

Following steps were performed at the Genome Centre at Max-Planck Institute for Plant Breeding Research:

Copy RNA (cRNA) was prepared following the manufacturer's instructions (www.affymetrix.com/support/technical/manual/expression_manual.affx).

Labeled cRNA transcripts were purified using the sample cleanup module (Affymetrix). Fragmentation of cRNA transcripts, hybridization, and scanning of the high-density oligonucleotide microarrays (Arabidopsis ATH1 genome array; Affymetrix) were performed according to the manufacturer's GeneChip Expression Analysis Technical Manual. Three replicates per time point and genotype were performed. The quality of the data was evaluated at probe level

by examining the arrays for spatial effects, distribution of absent and present calls, and the intensity of spike-in controls. The robust multiarray average procedure (Irizarry et al., 2003) was used to correct for background effects and chip effects and to summarize the probe values into probe set values, resulting in 22,811 normalized expression values per array. R/Bioconductor (Gentleman et al., 2004) was used to preprocess the raw microarray data. The ANOVA statistical test was applied in combination with the false discovery rate test method to correct for the P-values (Benjamini and Hochberg, 1995).

To identify candidate genes with potentially altered transcript accumulation in the *ein2* mutant upon elf18 elicitation genes were selected that showed a significant ($P \leq 0.05$) and at least 2-fold higher transcript accumulation after 10h elf18 treatment in comparison to transcript accumulation before treatment. Genes were selected that show at least 2-fold higher induction in WT than in the negative control *efr*. We focussed on genes that are 2-fold stronger elf18-induced in Col than in *ein2*. Genevestigator V3 (<https://www.genevestigator.com/gv/index.jsp>) was used for analysis of ET, ACC and SA-responsive genes.

Biochemical methods

Ligand-receptor binding assay

Chemical crosslinking studies were essentially performed as described in Zipfel et al. (2006) and Chinchilla et al. (2006). Seedlings were grown on agar plates containing 0,5X MS and 25 mM sucrose for 5-6 days under 12h light/12h dark conditions, then transferred to liquid media with 0,5X MS and 25 mM sucrose for additional 5-6 days. Seedling material from at least 20 seedlings was homogenized in liquid nitrogen and resuspended in binding buffer. Ca. 100 μ l seedling material was incubated with 60 fmol elf26-¹²⁵I-Tyr or ¹²⁵I-Tyr -flg22 for 15 minutes in the absence or presence of 10 μ M competitor peptides. Crosslinking was achieved by the addition of 10 μ l of 25 mM EGS and further incubation for 30 minutes. After washing with binding buffer samples were separated on SDS-PAGE and then visualized on a phosphoimager (Fuji FLA7000).

Immunoblot Analysis.

Total protein was extracted from whole seedlings in a lysis buffer containing 50 mM Tris-HCl pH 7.0, 2% SDS, 2 mM DTT, 1 mM 4-(2-aminoethyl) benzenesulfonyl fluoride hydrochloride and 1x Protease Inhibitor Mixture (Roche) and subjected to immunoblot analysis using anti-EFR or anti-FLS2 antibodies as described (Saijo et al. 2009). Anti-phospho p44/p42 MAPK antibody that specifically recognizes an active MAPK form was purchased from Cell Signaling Technology. The signal identity of active MPK3 and MPK6 forms has been verified (Saijo et al. 2009).

References

- Alonso *et al.*** (1999). EIN2, a bifunctional transducer of ethylene and stress responses in Arabidopsis. *Science*. 1999 Jun 25;284(5423):2148-52.
- An *et al.*** (2010). Ethylene-induced stabilization of ETHYLENE INSENSITIVE3 and EIN3-LIKE1 is mediated by proteasomal degradation of EIN3 binding F-box 1 and 2 that requires EIN2 in Arabidopsis. *Plant Cell*. 2010 Jul;22(7):2384-401.
- Anelli T, Sitia R** (2008) Protein quality control in the early secretory pathway. *EMBO J* 27: 315–327.
- Asai T. *et al.*** (2002). MAP kinase signaling cascade in Arabidopsis innate immunity. *Nature*. 415: 977-83.
- Bent AF *et al.*** (1992). Disease development in ethylene-insensitive Arabidopsis thaliana infected with virulent and avirulent Pseudomonas and Xanthomonas pathogens. *Mol Plant Microbe Interact*. 1992 Sep-Oct;5(5):372-8.
- Bent A.F. and Mackey D.** (2007). Elicitors, effectors and R genes: the new paradigm and a lifetime supply of questions. *Annu Rev Phytopathol*. 45: 399-436.
- Bisson M *et al.*** (2009). EIN2, the central regulator of ethylene signaling, is localized at the ER membrane where it interacts with the ethylene receptor ETR1. *Biochem J*. 2009 Oct 23;424(1):1-6.
- Block A. and Alfano JR.** (2011). Plant targets for Pseudomonas syringae type III effectors: virulence targets or guided decoys? *Curr Opin Microbiol*. 2011 Feb;14(1):39-46.
- Boisson M *et al.*** (2001). Arabidopsis glucosidase I mutants reveal a critical role of N-glycan trimming in seed development. *EMBO J*. 2001 Mar 1;20(5):1010-9.
- Boller** (2005) Peptide signaling in plant development and self/nonself perception. *Curr Opin Cell Biol*. 17:116-22
- Boller T, Felix G** (2009). A renaissance of elicitors: perception of microbe-associated molecular patterns and danger signals by pattern-recognition receptors. *Annu Rev Plant Biol*. 60: 379-406.
- Boudsocq *et al.*** (2010). Differential innate immune signaling via Ca(2+) sensor protein kinases. *Nature*. 2010 Mar 18;464(7287):418-22.
- Boutrot F *et al.*** (2010) Direct transcriptional control of the Arabidopsis immune receptor FLS2 by the ethylene-dependent transcription factors EIN3 and EIL1. *Proc Natl Acad Sci USA* 2010, 107:14502-14507

References

- Broekaert *et al.*** (2006). The role of ethylene in host-pathogen interactions. *Annu Rev Phytopathol.* 2006;44:393-416.
- Chao *et al.*** (1997). Activation of the ethylene gas response pathway in Arabidopsis by the nuclear protein ETHYLENE-INSENSITIVE3 and related proteins. *Cell.* 1997 Jun 27;89(7):1133-44.
- Chen *et al.*** (2009). ETHYLENE INSENSITIVE3 and ETHYLENE INSENSITIVE3-LIKE1 repress SALICYLIC ACID INDUCTION DEFICIENT2 expression to negatively regulate plant innate immunity in Arabidopsis. *Plant Cell.* 2009 Aug;21(8):2527-40.
- Chico *et al.*** (2008). JAZ repressors set the rhythm in jasmonate signaling. *Curr Opin Plant Biol.* 2008 Oct;11(5):486-94.
- Chinchilla D. *et al.*** (2007). A flagellin-induced complex of the receptor FLS2 and BAK1 initiates plant defence. *Nature.* 448: 497-500.
- Chisholm S.T. *et al.*** (2006). Host-microbe interactions: shaping the evolution of the plant immune response. *Cell* 124: 803-14.
- Clay NK *et al.*** (2009) Glucosinolate metabolites required for an Arabidopsis innate immune response. *Science* 323: 95–101
- Clarke *et al.*** (2001). Constitutive disease resistance requires EDS1 in the Arabidopsis mutants *cpr1* and *cpr6* and is partially EDS1-dependent in *cpr5*. *Plant J.* 2001 May;26(4):409-20.
- Dangl J.L. and Jones J.D.** (2001). Plant pathogens and integrated defense responses to infection. *Nature* 411: 826-33.
- Dodds and Rathjen** (2010) Plant immunity: towards an integrated view of plant-pathogen interactions. *Nat Rev Genet.* (8): 539-48
- Durrant WE, Dong X** (2004). Systemic acquired resistance. *Annu Rev Phytopathol.* 42: 185-209
- Dong X** (1998). SA, JA, ethylene, and disease resistance in plants. *Curr Opin Plant Biol.* 1998 Aug;1(4):316-23.
- Dong X** (2004) NPR1. All things considered. *Curr. Opin. Plant Biol* (7):547-552
- Felix G. *et al.*** (1999). Plants have a sensitive perception system for the most conserved domain of bacterial flagellin. *Plant J.* 18: 265-76.
- Ferrari S. *et al.*** (2007) Resistance to *Botrytis cinerea* induced in Arabidopsis by elicitors is independent of salicylic acid, ethylene or jasmonate signaling but requires PHYTOALEXIN DEFICIENT3. *Plant Physiol.* 144:367-79

References

- Forsyth A et al.** (2010) Genetic dissection of basal resistance to *Pseudomonas syringae* pv. *phaseolicola* in accessions of *Arabidopsis*. *Mol Plant Microbe Interact.* 23: 1545-1552
- Frye et al.** (2001). Negative regulation of defense responses in plants by a conserved MAPKK kinase. *Proc Natl Acad Sci U S A.* 2001 Jan 2;98(1):373-8.
- Furumizu et al.** (2008). A novel mutation in KNOF uncovers the role of alpha-glucosidase I during post-embryonic development in *Arabidopsis thaliana*. *FEBS Lett.* 2008 Jun 25;582(15):2237-41.
- Gigolashvili et al.** (2007). The transcription factor HIG1/MYB51 regulates indolic glucosinolate biosynthesis in *Arabidopsis thaliana*. *Plant J.* 2007 Jun;50(5):886-901.
- Gillmor et al.** (2002). Alpha-glucosidase I is required for cellulose biosynthesis and morphogenesis in *Arabidopsis*. *J Cell Biol.* 2002 Mar 18;156(6):1003-13.
- Glazebrook J et al.** (2003) Topology of the network integrating salicylate and jasmonate signal transduction derived from global expression phenotyping. *Plant J.* 34: 217-228
- Glazebrook J** (2005). Contrasting mechanisms of defense against biotrophic and necrotrophic pathogens. *Annu Rev Phytopathol.* 43: 205-27
- Gohre V et al.** (2008) Plant pattern-recognition receptor FLS2 is directed for degradation by the bacterial ubiquitin ligase AvrPtoB. *Curr Biol.* 18(23): 1824-32
- Gohre V, Robatzek S.** (2008) Breaking the barriers: microbial effector molecules subvert plant immunity. *Annu Rev Phytopathol.* 46: 189-215
- Gomez-Gomez L. and Boller T.** (2000). FLS2: an LRR receptor-like kinase involved in the perception of the bacterial elicitor flagellin in *Arabidopsis*. *Mol Cell.* 5: 1003-11.
- Greenberg JT et al.** (2000). Uncoupling salicylic acid-dependent cell death and defense-related responses from disease resistance in the *Arabidopsis* mutant *acd5*. *Genetics.* 2000 Sep;156(1):341-50.
- Haeweker et al.** (2010) Pattern recognition receptors require N-glycosylation to mediate plant immunity. *J Biol Chem* 285(7): 4629-36
- Halim et al.** (2009). PAMP-induced defense responses in potato require both salicylic acid and jasmonic acid. *Plant J.* 2009 Jan;57(2):230-42.
- Ham JH et al. (2007).** Layered basal defenses underlie non-host resistance of *Arabidopsis* to *Pseudomonas syringae* pv. *phaseolicola*. *Plant J* 2007, 51:604-616.

References

- Hann DR, Rathjen J** (2007) Early events in the pathogenicity of *Pseudomonas syringae* on *Nicotiana benthamiana*. *Plant J.* 49: 607-18
- Heidrich K et al.** (2011) Arabidopsis EDS1 Connects Pathogen Effector Recognition to Cell Compartment-Specific Immune Responses. *Science* 334: 1401-1404.
- Helenius A. and Aebi M.** (2004). Roles of N-linked glycans in the endoplasmatic reticulum. *Annu Rev Biochem.* 73: 1019-49.
- Huffaker A et al.** (2007). Endogenous peptide defense signals in Arabidopsis differentially amplify signaling for the innate immune response. *Proc Natl Acad Sci U S A.* 2007 Jun 19;104(25):10732-6.
- Jander G. et al.** (2002). Arabidopsis map-based cloning in the post-genome era. *Plant Physiol.* 129: 440-50.
- Jin H. et al.** (2007). Allele-specific suppression of a defective brassinosteroid receptor reveals a physiological role of UGGT in ER quality control. *Mol Cell.* 26: 821-30.
- Jin H. et al.** (2009). A plant-specific calreticulin is a key retention factor for a defective brassinosteroid receptor in the endoplasmic reticulum. *Proc Natl Acad Sci USA* 2009 Aug 11;106(32):13612-7
- Jones J.D. and Dangl J.L.** (2006). The plant immune system. *Nature* 444: 323-9.
- Kim MG et al.** (2005) Two *pseudomonas syringae* type III effectors inhibit RIN4-regulated basal defense in Arabidopsis. *Cell* 121: 749–759
- Kunze G. et al.** (2004). The N terminus of bacterial elongation factor Tu elicits innate immunity in Arabidopsis plants. *Plant Cell.* 16: 3496-507.
- Li J. et al.** (2002). BAK1, an Arabidopsis LRR receptor-like protein kinase, interacts with BRI1 and modulates brassinosteroid signaling. *Cell.* 110: 213-22.
- Li J et al.** (2009). Specific ER quality components required for biogenesis of the plant innate immune receptor EFR. *Proc Natl Acad Sci U S A.* 2009 Sep 15;106(37):15973-8.
- Li X. et al.** (2007) Flagellin induces innate immunity in nonhost interactions that is suppressed by *Pseudomonas syringae* effectors. *Proc Natl Acad Sci U S A.* 2005 Sep 6;102(36):12990-5.
- Liu J, Zhang S** (2004) Phosphorylation of 1-aminocyclopropane-1-carboxylic acid synthase by MPK6, a stress-responsive mitogen-activated protein kinase, induces ethylene biosynthesis in Arabidopsis. *Plant Cell.* 16:3386-3399

References

- Lo SC, Nicholson RL** (1998) Reduction of light-induced anthocyanin accumulation in inoculated sorghum mesocotyls. Implications for a compensatory role in the defense response. *Plant Physiol* 116: 979–989.
- Lu D et al.** (2010) A receptor-like cytoplasmic kinase, BIK1, associates with a flagellin receptor complex to initiate plant innate immunity *PNAS* 107: 496-502
- Lu D et al.** (2011) Direct ubiquitination of pattern recognition receptor FLS2 attenuates plant innate immunity. *Science*. 2011 Jun 17;332(6036):1439-42.
- Lu X et al.** (2009) Uncoupling of sustained MAMP receptor signaling from early outputs in an Arabidopsis endoplasmic reticulum glucosidase II allele. *Proc Natl Acad Sci U S A* 106(52):22522-7
- Lukowitz W. et al.** (2000). Positional cloning in Arabidopsis. Why it feels good to have a genome initiative working for you. *Plant Physiol*. 123: 795-805.
- McLusky SR et al.** (1999) Cell wall alterations and localized accumulation of feruloyl-30-methoxytyramine in onion epidermis at sites of attempted penetration by *Botrytis allii* are associated with actin polarisation, peroxydase activity and suppression of flavonoid biosynthesis. *Plant J* 17: 523–534
- Meier S et al.** (2008). Co-expression and promoter content analyses assign a role in biotic and abiotic stress responses to plant natriuretic peptides. *BMC Plant Biol*. 2008 Feb 29;8:24.
- Melotto M et al.** (2006). Plant stomata function in innate immunity against bacterial invasion. *Cell*. 2006 Sep 8;126(5):969-80.
- Mersmann S et al.** (2010) Ethylene signalling regulates accumulation of the FLS2 receptor and is required for the oxidative burst contributing to plant immunity. *Plant Physiol* 2010, 154:391-400.
- Mishina T and Zeier J** (2007) Pathogen-associated molecular pattern recognition rather than development of tissue necrosis contributes to bacterial induction of systemic acquired resistance in Arabidopsis. *Plant J*. 50(3): 500-13.
- Navarro L et al. (2004)** The transcriptional innate immune response to flg22. Interplay and overlap with Avr gene-dependent defense responses and bacterial pathogenesis. *Plant Physiol*. 135(2): 113-28.
- Nekrasov V et al.** (2009) Control of the pattern-recognition receptor EFR by an ER protein complex in plant immunity. *EMBO J* 28(21):3428-38.
- Nicaise V et al.** (2009) Recent advances in PAMP-triggered immunity against bacteria: pattern recognition receptors watch over and raise the alarm. *Plant Physiol* 150(4):1638-47

References

- Nürnberg T. et al.** (2004). Innate immunity in plants and animals: striking similarities and obvious differences. *Immunol. Rev.* 198: 249-66.
- Nürnberg T, Lipka V** (2005). Non-host resistance in plants: New insights into and old phenomenon. *Molecular Plant Pathology.* 6: 335-45
- Parodi A.J.** (2000). Protein glucosylation and its role in protein folding. *Annu Rev Biochem.* 69: 69-93.
- Pieterse CM et al.** (1998). A novel signaling pathway controlling induced systemic resistance in Arabidopsis. *Plant Cell.* 1998 Sep;10(9):1571-80.
- Pieterse CM and Van Loon** (2004) NPR1: The spider in the web of induced resistance signaling pathways. *Curr. Opin. Plant Biol.* (7): 456-464
- Pieterse CM et al.** (2009) Networking by small molecule hormones in plant immunity *Nat Chem Biol.* (5):308-316
- Qiu et al.** (2008) Arabidopsis mitogen-activated protein kinase kinases MKK1 and MKK2 have overlapping functions in defense signaling mediated by MEKK1, MPK4 and MKS1. *Plant Physiol.* 2008 Sep;148(1):212-22.
- Robatzek S et al.** (2006). Ligand-induced endocytosis of the pattern recognition receptor FLS2 in Arabidopsis. *Genes Dev.* 2006 Mar 1;20(5):537-42.
- Roux M et al.** (2011) The arabidopsis leucine-rich repeat receptor-like kinases BAK1/SERK3 and BKK1/SERK4 are required for innate immunity to Hemibiotrophic and Biotrophic pathogens. *Plant Cell* (6):2440-55
- Rowe and Bergmann** (2010). Complex signals for simple cells: the expanding ranks of signals and receptors guiding stomatal development. *Curr Opin Plant Biol.* 2010 Oct;13(5):548-55.
- Ryan CA et al.** (2007) New insights into innate immunity in Arabidopsis. *Cell Microbiol.* (8): 1902-8
- Saijo Y et al.** (2009) Receptor quality control in the endoplasmic reticulum for plant innate immunity. *EMBO J* 28(21):3439-49.
- Schulze B et al.** (2010) Rapid heteromerization and phosphorylation of ligand-activated plant transmembrane receptors and their associated kinase BAK1. *J Biol Chem,* 285:9444-9451.
- Segonzac C, Zipfel C** (2011). Activation of plant pattern-recognition receptors by bacteria. *Curr Opin Microbiol.* 4(1): 54-61.

- Shan L *et al.*** (2008) Bacterial effectors target the common signaling partner BAK1 to disrupt multiple MAMP receptor-signaling complexes and impede plant immunity. *Cell Host Microbe*. 4(1): 17-27.
- Shen QH *et al.*** (2006) Nuclear activity of MLA immune receptors links isolate-specific and basal disease-resistance responses. *Science* 315(5815):1098-103.
- Shirasu K** (2009). The HSP90-SGT1 chaperone complex for NLR immune sensors. *Annu Rev Plant Biol*. 2009;60:139-64.
- Slootweg E *et al.*** (2010) Nucleocytoplasmic distribution is required for activation of resistance by the potato NB-LRR receptor Rx1 and is balanced by its functional domains. *Plan Cell*. 12: 4195-215.
- Solano R *et al.*** (1998). Nuclear events in ethylene signaling: a transcriptional cascade mediated by ETHYLENE-INSENSITIVE3 and ETHYLENE-RESPONSE-FACTOR1. *Genes Dev*. 1998 Dec 1;12(23):3703-14.
- Solfanelli C. *et al.*** (2006). Sucrose-specific induction of the anthocyanin biosynthetic pathway in Arabidopsis. *Plant Physiol*. 140: 637-46.
- Stepanova AN and Alonso JM** (2009). Ethylene signaling and response: where different regulatory modules meet. *Curr Opin Plant Biol*. 2009 Oct;12(5):548-55.
- Suarez-Rodriguez *et al.*** (2007). MEKK1 is required for flg22-induced MPK4 activation in Arabidopsis plants. *Plant Physiol*. 2007 Feb;143(2):661-9.
- Sun W *et al.*** (2006) Within-species flagellin polymorphisms in *Xanthomonas campestris* and its impact on elicitation of Arabidopsis FLAGELLIN SENSING2-dependent defenses. *Plant Cell* 18(3) 764-79.
- Tatsuki and Mori** (2001). Phosphorylation of tomato 1-aminocyclopropane-1-carboxylic acid synthase, LE-ACS2 at the C-terminal region. *J Biol Chem*. 2001 Jul 27;276(30):28051-7.
- Teng S. *et al.*** (2005). Sucrose-specific induction of anthocyanin biosynthesis in Arabidopsis requires the MYB75/PAP1 gene. *Plant Physiol*. 139: 1840-52.
- Tessier DC *et al.*** (2000) Cloning and characterization of mammalian UDP-glucose glycoprotein: glucosyltransferase and the development of a specific substrate for this enzyme. *Glycobiology* (4): 403-12.
- Tsuchisaka A and Theologis A** (2004). Unique and overlapping expression patterns among the Arabidopsis 1-amino-cyclopropane-1-carboxylate synthase gene family members. *Plant Physiol*. 2004 Oct;136(2):2982-3000.
- Tsuda K *et al.*** (2008). Interplay between MAMP-triggered and SA-mediated defense responses. *Plant J*. 2008 Mar;53(5):763-75.

References

- Tsuda, K et al.** (2009) Network properties of robust immunity in plants. *PLoS Genet.* 5, e1000772 (2009).
- Tsuda K, Katagiri F** (2010). Comparing signaling mechanisms engaged in pattern-triggered and effector-triggered immunity. *Curr Opin Plant Biol.* 13(4): 459-65.
- Van Loon LC et al.** (2006) Ethylene as a modulator of disease resistance in plants. *Trends Plant Sci.* 11: 184-191
- Vance RE et al.** (2009) Patterns of pathogenesis: discrimination of pathogenic and nonpathogenic microbes by the innate immune system. *Cell Host Microbe* 6(1): 10-21
- Wang K et al.** (2002). Ethylene biosynthesis and signaling networks. *Plant Cell.* 2002;14 Suppl:S131-51.
- Wiermer M et al.** (2005). Plant immunity: The EDS1 regulatory node. *Curr Opin Plant Biol.* 2005 Aug;8(4):383-9.
- Wildermuth MC et al.** (2002). Isochorismate synthase is required to synthesize salicylic acid for plant defence. *Nature.* 2001 Nov 29;414(6863):562-5.
- Williams D.B.** (2006). Beyond lectins: the calnexin/calreticulin chaperone system of the endoplasmatic reticulum. *J Cell Sci.* 119: 615-23.
- Xiang T et al.** (2008) *Pseudomonas syringae* effector AvrPto blocks innate immunity by targeting receptor kinases. *Curr Biol* 18(1): 74-80.
- Yasuda M et al.** (2008). Antagonistic interaction between systemic acquired resistance and the abscisic acid-mediated abiotic stress response in *Arabidopsis*. *Plant Cell.* 2008 Jun;20(6):1678-92.
- Yoo et al.** (2008). Dual control of nuclear EIN3 by bifurcate MAPK cascades in C2H4 signaling. *Nature.* 2008 Feb 14;451(7180):789-95.
- Yoo et al.** (2009). Emerging connections in the ethylene signaling network. *Trends Plant Sci.* 2009 May;14(5):270-9.
- Zhang J et al.** (2007) A *Pseudomonas syringae* effector inactivates MAPKs to suppress PAMP-induced immunity in plants. *Cell Host Microbe* 1: 175–185.
- Zipfel C. et al.** (2004). Bacterial disease resistance in *Arabidopsis* through flagellin perception. *Nature.* 428: 764-7.
- Zipfel C. et al.** (2006). Perception of the bacterial PAMP EF-Tu by the receptor EFR restricts *Agrobacterium*-mediated transformation. *Cell.* 125: 749-60.
- Zipfel C.** (2008) Pattern-recognition receptors in plant innate immunity. *Curr Opin Immunol.* 20(1) 10-6.

Acknowledgements

I would like to thank my supervisor Dr. Yusuke Saijo and Prof. Paul Schulze-Lefert for the possibility to do my PhD-thesis here at the Max-Planck Institute and for all what I could learn from them.

I also would like to thank Prof. Ute Höcker and Dr. Cyril Zipfel for evaluating my thesis, and I'm especially grateful to Cyril that he comes to Cologne to participate in my thesis committee.

Most importantly, I would like to thank my colleagues and friends Anne, Kazue, Eva, Kohji and Xunli for their help and contribution and motivation.

To my 'office-colleagues' Katharina, Johannes, Servane, Justine, Nora, Ralf and Stephane I would like to thank for many good ideas, nice discussions and a nice atmosphere.

Last but not least, I would like to thank my family and especially Lotje. Without you I wouldn't have made it.

Erklärung

Ich versichere, dass ich die von mir vorgelegte Dissertation selbständig angefertigt, die benutzten Quellen und Hilfsmittel vollständig angegeben und die Stellen der Arbeit - einschließlich Tabellen, Karten und Abbildungen -, die anderen Werken im Wortlaut oder dem Sinn nach entnommen sind, in jedem Einzelfall als Entlehnung kenntlich gemacht habe; dass diese Dissertation noch keiner anderen Fakultät oder Universität zur Prüfung vorgelegen hat; dass sie – abgesehen von auf Seite I angegebene Teilpublikationen - noch nicht veröffentlicht worden ist sowie, dass ich eine solche Veröffentlichung vor Abschluss des Promotionsverfahrens nicht vornehmen werde. Die Bestimmungen dieser Promotionsordnung sind mir bekannt. Die von mir vorgelegte Dissertation ist von Prof. Dr. Paul Schulze-Lefert betreut worden.

Köln, 12 December 2011

Nico Tintor